

O

AR-009-345

DSTO-TR-0217

T

A Robust 2-70MHz Linear  
Power Amplifier

W. Martinsen

S

APPROVED FOR PUBLIC RELEASE

© Commonwealth of Australia

19960212 225

D

# **A ROBUST 2 - 70MHz LINEAR POWER AMPLIFIER**

*W. Martinsen*

**Communications Division  
Electronics and Surveillance Research Laboratory**

DSTO-TR-0217

## **ABSTRACT**

### **Technical Report**

Spatial Processing Group DSTOS currently has oblique ionosonde transmitters deployed in a variety of remote, often unmanned, locations in tropical, arid inland, and polar regions, and equipment reliability is of the utmost importance. The commercial H.F. power amplifiers initially installed proved unreliable in the field, and motivated the development of a more robust unit. 10 Watt and 50 Watt designs are presented with their measured characteristics, and a detailed discussion of important design criteria.

**DTIC QUALITY INSPECTED 4**

### **RELEASE LIMITATION**

*Approved for public release*

**DEPARTMENT OF DEFENCE**

**DEFENCE SCIENCE AND TECHNOLOGY ORGANISATION**

*Published by*

*DSTO Electronics and Surveillance Research Laboratory  
GPO 1500  
Salisbury, South Australia, Australia*

*Telephone: (08) 259-5077  
Fax: (08) 259-7110*

*© Commonwealth of Australia 1995  
AR No. 009-345  
July 1995*

**APPROVED FOR PUBLIC RELEASE**

# ***A ROBUST 2 - 70MHz LINEAR POWER AMPLIFIER***

## **EXECUTIVE SUMMARY**

Spatial Processing Group (SPG) operates and maintains several High Frequency (HF) transmitters as a part of the Low Latitude Ionospheric Sounding Program (LLISP). These transmitters are located in remote sites both in Australia and overseas, with the majority being in the tropics. Originally, commercial power amplifiers were used in the transmitters. These amplifiers proved unreliable in the field and at times costly to repair. The majority of amplifier failures occurred in tropical regions and have been attributed to the effects of lightning.

This report describes the DSTO design of a robust 10 Watt and 50 Watt HF Power Amplifier. A key design feature is the ability of the power output stage to withstand extremes of Standing Wave Ratio (SWR) and the direct induction of energy into the antenna driven element arising from a nearby cloud to ground lightning strike.

The design, construction, and subsequent implementation of the amplifiers described in this report has made a significant contribution to the reliability of the LLISP network.

**THIS PAGE IS INTENTIONALLY BLANK**

## Author

### **Wayne M. Martinsen** Communications Division

*Wayne Martinsen was indentured as an apprentice Communications Technician in 1972 with Transport Communications Pty. Ltd.(Buranda, Qld.). He attended Yeronga Technical College (Brisbane, Qld.) where he received honours in the majority of his subjects. In 1975 his apprenticeship indentures were transferred to The Radio Centre (Archerfield Aerodrome, Qld.) where he was employed as an Air Maintenance Engineer, Category Radio. He was involved in all aspects of repair and maintenance of avionics systems associated with the light aircraft industry. Upon completing his training as an apprentice he sat for and passed various Dept. of Transport Licensed Air Maintenance Engineer (L.A.M.E.) exams. In 1977 he joined the R.A.A.F. and after graduating from their School of Radio, where he received training in military systems, he worked on a wide variety of airborne communications, navigation and anti-submarine warfare systems. In 1987 he was discharged from the R.A.A.F. and applied for a position with D.S.T.O. at Salisbury, and was accepted as a Technical Officer (Engineering) with SPG Group. Here he was tasked with the design and development of R.F. circuits required for tropospheric and ionospheric research.*

**THIS PAGE IS INTENTIONALLY BLANK**

## Contents

1.	INTRODUCTION	1
2.	AMPLIFIER DESIGN	2
2.1	<i>Class AB bias</i>	4
2.1.1	<i>Summarising class AB</i>	7
2.2	<i>Class A bias</i>	8
2.3	<i>Lightning Protection</i>	9
3.	10 WATT POWER AMPLIFIER	11
3.1	<i>Tailoring the output impedance</i>	13
3.2	<i>Output matching network</i>	17
3.3	<i>Input matching network</i>	18
3.4	<i>Biasing</i>	19
3.5	<i>Transistor matching</i>	19
3.6	<i>Termination resistors</i>	20
3.6.1	<i>Summarising <math>R_T</math></i>	24
3.7	<i>Performance testing 10 watt module</i>	25
3.8	<i>Complete 10 watt amplifier</i>	26
4.	50 WATT POWER AMPLIFIER	26
4.1	<i>Performance testing 50 watt amplifier</i>	30
4.2	<i>Near lightning strike test</i>	31
5.	CONCLUSION	31
6.	ACKNOWLEDGMENTS	32
7.	REFERENCES	33
8.	FIGURES	35
8.1	<i>list of figures</i>	35

APPENDIX Motorola Semiconductor Data Sheets MRF136

Distribution list



## TABLES

<b>I</b>	Peak drain/source voltage for class AB push/pull amplifier when producing 10 watts into an open circuit at the output port.	<b>5</b>
<b>II</b>	Peak drain/source voltage for class AB push/pull amplifier when producing 10 watts into an unterminated 1.5m coax cable.	<b>5</b>
<b>III</b>	OPI <sub>p</sub> <sup>3</sup> versus input drive level for class AB.	<b>6</b>
<b>IV</b>	Variation in OPI <sub>p</sub> <sup>3</sup> for class A and AB with 4:1 and 1:4 impedance mismatch.	<b>12</b>
<b>V</b>	Variation in Z <sub>in</sub> and Z <sub>out</sub> of the circuit in Fig.1 with changes in I <sub>d</sub> .	<b>16</b>
<b>VI</b>	r <sub>dcom</sub> versus frequency.	<b>23</b>

# **1. Introduction**

The use of solid state devices, as opposed to thermionic valves, in small to medium class radio frequency (R.F.) power amplifiers, has resulted in a marked increase in the occurrence of catastrophic damage to the output stage devices when connected to antennas in the field. The two main causes are:

1. Extremes in standing wave ratio (S.W.R.).
2. High voltages and currents induced into the antenna system by near and direct lightning strikes.

Spatial Processing Group (S.P.G.) operates and maintains several high frequency (H.F.) transmitters as part of its commitment to ionospheric research. Most of these transmitters are located in remote sites both in Australia and overseas with the majority being in the tropics. The cost and logistic difficulties associated with having these units returned for repair is quite daunting. Commercial units originally deployed have proved unreliable and at times very costly to repair. The units installed in the tropics experience the highest failure rates, some due to over-heating, but most because of the effects of lightning. The urgent need to keep S.P.G.'S ionosonde network fully operational prompted the decision to produce a more reliable amplifier specifically designed to operate under the following conditions.

- (a) **Extremes in S.W.R. at all power levels without derating.**  
Some broadband H.F. antennas currently in use have impedances that are outside the 3:1 S.W.R. circle for the majority of their designed frequency range. With sweep rates as high as 1MHz per second over the range 2 to 70 MHz, automatic tuning of the antenna is deemed impractical. It was considered essential therefore that the power amplifier be designed to withstand extremes of standing waves without having to reduce forward power.
- (b) **Energy induced into the antenna by lightning strikes in close proximity.**  
The majority of failures at S.P.G.'s remote transmitter sites located in the tropics have been caused by the effects of lightning. Correlating the time of failure with the local weather reports has indicated a direct link to thunderstorm activity. Examination of the units returned for repair showed no signs of arcing, missing or vaporised circuit board tracks or components. The consistent fault was a complete failure of the solid state active output devices, but with no external appearance of damage. The lack of obvious damage indicated the unlikelihood of a direct lightning strike being the cause. Once repaired the units were installed and operated in one of S.P.G.'s local transmitter sites near Adelaide. They were soak tested for periods ranging from several weeks to several months before being sent back into service. Units which performed faultlessly during their soak test sometimes failed within days of being installed

at remote tropical sites. All sites are airconditioned so the failure could not be attributed to ambient air temperatures. All equipment is fitted with power line conditioning, therefore failures are unlikely to be caused by fluctuations or spikes on the AC supply. Computing and other digital and analogue equipment, used for timing and the generation of the swept R.F. signal fed to the input of the power amplifier, were unaffected and still functioned as designed. It was therefore deduced that the power amplifier failures were most likely to be caused by the direct induction of energy from a near lightning strike into the antenna, generating large differential voltages between the inner and outer conductors of the coaxial feedline.

(c) **A wide range of climatic conditions.**

S.P.G. currently operates ten transmitter sites for its ionosonde network. These sites range from Antarctica, to central Australia, to the tropics and some are unmanned and remote, inspected only periodically by maintenance personnel. Although the units operate in air conditioned buildings, consideration must be given to the possible effects upon the system should the air conditioning unit fail.

All S.P.G.'s remote sites have a 10 watt power amplifier as a backup unit which is brought into service should the main 50 watt amplifier fail. This report initially describes the development of a solid state 10 watt 2-70MHz R.F. amplifier module suitable for service in the backup role, and functioning to the new standard. The report continues with the design of a complete 50 watt power amplifier to replace the commercial units currently in use. The complete power amplifier was required to produce its rated output power with 0dBm input, and provision was to be made to disable the R.F. output as the input signal swept through emergency and other forbidden frequencies.

It was felt that the results of an investigation into the points of comparison between different classes of operation and output configurations of R.F. power amplifiers with respect to the conditions highlighted in (a) and (b) above would reveal the best choice of design. Only the design of the power output stage will be covered in detail.

## ***2. Amplifier Design***

The 2-70MHz frequency range covers just over five octaves, and a total of 6 sub-octave filters would be required to ensure adequate attenuation of the harmonic output. Such a configuration would require 12 changeover relays, each with a 100 watt R.F. rating to switch between the different filters. Typical contact electrical life of this type of mechanical relay is 100,000 operations. With one operation per relay per sweep and up to 12 sweeps per hour, this amounts to 105,120 operations per year per relay. The mean time between failures for the

twelve relays would be approximately one month., which is clearly unacceptable, and another solution to the harmonic problem had to be found.

The current standard for the harmonic output of a 10 watt R.F. transmitter is -40dBc or better - i.e. with an output level of +40dBm, the individual harmonic tones must be less than 0dBm. Using these figures to calculate the minimum required intercept points (ref.12) gives an output second order intercept point ( $OIP^2$ ) of +74dBm and an output third order intercept point ( $OIP^3$ ) of +55.25dBm. An amplifier operating in a linear mode produces the least amount of internally generated distortion products at its output. By making the output transistor configuration a push/pull pair it is possible to suppress the internally generated even order products. Provided proper attention is paid to matching the active devices and keeping the input/output matching circuits balanced, the  $OIP^2$  of +74dBm was considered achievable.

An  $OIP^3$  of +55.25dBm proved difficult to realise, and a closer examination of the potential interference caused by the third harmonic was undertaken. Considering a sweep rate of 250KHz per second to be typical for frequency modulated continuous wave (FMCW) soundings, the third harmonic will sweep at 750KHz/sec. Since the average bandwidth for H.F. communications receivers is around 3KHz, this 3rd harmonic component, as an interferer, will only last for approximately 0.004 seconds and therefore does not constitute a serious interference problem. The higher odd order products will have velocities proportionally higher and pose even less of a problem. However, every effort was made in the design to keep the magnitude of all harmonic products to reasonable levels.

A 70MHz low pass (L.P.) 5th order Chebyshev filter will be installed in the power amplifier output to limit the upper frequency response.

Amplifiers and antennas used for FMCW ionosondes are normally broadband, spanning several octaves, and the level of broadband noise generated by the amplifier and subsequently radiated by the antenna is a cause for concern. Most modern active devices have excellent noise characteristics so the radiated noise power will be the noise generated by the transmitter's first pre-amplifier, amplified by successive stages plus their noise contribution. The first pre-amplifier should therefore have a low noise figure, such that the noise floor of the signal source predominates.

Having decided to take advantage of the suppression of the even order harmonics offered by the push/pull configuration, consideration was then given to the class of bias to be used in the design of the linear amplifier; a crucial element in the choice of bias was an understanding of what might happen at the amplifier's output port when a reflected wave and energy induced into the antenna from a near lightning strike are present.

The most common form of bias for push/pull circuits is class AB, and this configuration will be discussed first. Although this form of bias was finally rejected for this particular application, the design philosophy pursued, the tests done and the reasons for rejection are considered to be worth documenting in detail.

## 2.1 *Class AB Bias*

Impedance matching of the active devices to a 50 Ohm transmission line is usually done at the rated output power of the amplifier. This ensures maximum power transfer from the output of the active devices to the transmission line. However, the output impedance of a class AB final in its quiescent state is very much dependent upon its quiescent current ( $I_Q$ ). The lower the  $I_Q$  relative to the current drawn by the final push/pull pair at its rated output power, the higher and more removed from 50 Ohms this quiescent impedance will be. Operating the amplifier at a power level below its rated output alters the active devices' dynamic output impedance from the point where matching has been provided. Because the matching network is fixed, the output impedance of the amplifier is no longer 50 Ohms, and will be somewhere between 50 Ohms and the impedance at its quiescent state, varying in sympathy with changing input drive levels.

There is another point to consider. No matter what the input drive level is, there are two points on the input sine wave where the output impedance rises to its quiescent state, i.e.  $0^\circ$  and  $180^\circ$ . Also, it is not uncommon for a class AB power amplifier to have a quiescent current  $1/10$  that of its final operating current when producing its rated R.F. output.

To demonstrate and measure the effects of the impedance variations on the peak voltage appearing at the output terminal of the active devices, a series of measurements was carried out on the completed 10 watt power amplifier module described later in this text. The bias was adjusted to give an  $I_Q$  of  $1/10$  that of its operating current when producing 10 watts R.F. output into a dummy load. To emphasise the effect, a second measurement was made with the bias set to 0V where the  $I_Q$  was 0mA. A gate threshold voltage of approximately 3V made this equivalent to operating the amplifier in class C push/pull. A length of RG-58 coax cable 1.5m long was used to connect the amplifier to the dummy load. With the aid of a network analyser, the velocity factor of this cable was calculated to be 0.63. A test frequency of 46MHz was chosen for reasons which will become clear later. One of the drains of the push/pull pair was directly monitored with a 100MHz oscilloscope via a X10 probe. The impedance of this probe at 46MHz is 510 Ohms, approximately seven times the drain impedance at a drain current ( $I_D$ ) of 50mA (see table V). Table I shows the peak voltages measured at the transistor's drain using an oscilloscope when the output of the amplifier was delivering 10 watts into a 50 Ohm dummy load and also when the

dummy load was isolated from the amplifier by disconnecting the coax cable at the amplifier's output terminal - i.e. the open circuit condition, with reflected and incident waves in phase.

**Table I:** Peak drain/source voltage for class AB push/pull amplifier when producing 10 watts into an open circuit at the output port.

I <sub>Q</sub>	TERMINATION CONDITIONS	
	50 Ohms	O/c at P.A.
0 mA	47 V <sub>p</sub>	67 V <sub>p</sub>
100 mA	44 V <sub>p</sub>	62 V <sub>p</sub>

The coaxial cable was reconnected to the output terminal of the amplifier and then disconnected from the dummy load at the dummy load end. The coaxial cable had a velocity factor of 0.63, and was 1.5m long. At the test frequency of 46Mhz, the reflected wave arriving back at the drains was therefore 270° displaced from the forward wave. The peak of the reflected wave arrived at the drain when the drain impedance was at its highest or quiescent state. Table II shows the measured peak voltages at the transistor's drain when the coaxial cable was both terminated and unterminated at the dummy load end.

**Table II:** Peak drain/source voltage for class AB push/pull amplifier when producing 10 watts into an unterminated 1.5m coax cable.

I <sub>Q</sub>	TERMINATION CONDITIONS	
	50 Ohms	O/c at DUMMY LOAD
0 mA	47 V <sub>p</sub>	89 V <sub>p</sub>
100 mA	44 V <sub>p</sub>	77 V <sub>p</sub>

Clearly these peak voltages exceeded the manufacturer's specification of 65V maximum for the active devices employed. This impedance variation, which caused excessively high voltages to be developed from the delayed return wave, was obviously unacceptable, even more so when it was considered that the amplifier under test was capable of producing an output 6dB higher.

There is another reason why class AB bias is undesirable. Variations in output impedance of the active devices, especially at low current levels, create distortion products that effectively degrade the output third order intercept (OIP<sub>3</sub>) performance. To understand why this occurs, the test circuit shown in Fig.1a was constructed to measure the variation of drain impedance with drain current. A network analyser was connected to the drain via the D.C. blocking capacitor and a quick sweep was made from 1 to 100MHz to ensure there were no parasitic resonances. A test frequency of 7MHz was chosen so that the impedance vector fell on the R line on the Smith chart and simplified the

calculations. The slight variation away from the R line over the range of the measurements was considered small enough to be ignored. Table V shows the results obtained. In the previous examples an operating current of 1A flowed when the amplifier delivered 10 watts to the dummy load. With the  $I_Q$  set to 100mA, each field effect transistor (F.E.T.) drew 50mA. Table V shows that with a quiescent current of 50mA the output impedance was 70 Ohms. In the push/pull configuration this equated to an output impedance of approximately 140 Ohms. The output impedance would therefore change, with increasing drive level, from 140 Ohms at the quiescent state to 50 Ohms at its rated power output.

The effect this impedance change has on the  $OPI_p^3$  was measured. A two-tone test signal was injected at the input and varied to produce several different output levels from the class AB amplifier. The  $OPI_p^3$  was recorded. Table III lists the results obtained.

*Table III:  $OPI_p^3$  versus input drive level for class AB.*

OP dBm/Tone	$OPI_p^3$ dBm	$I_Q = 100\text{mA}$  $f_1 = 7\text{MHz}$  $f_2 = 7.01\text{MHz}$
+10	+31	
+15	+33	
+20	+36	
+25	+42	
+30	+48	
+35	+54	

Note the  $OPI_p^3$  was proportional to the output power level instead of being constant as is usually assumed in a standard non-linear analysis. Also it was at its worst when the amplitude range of the output signal was predominantly in the region where there was the greatest drain impedance variation. To confirm that the variation in drain impedance was causing the non-linearity, the input signal was adjusted to give +20dBm per tone at the output. This corresponded to an  $OPI_p^3$  of +36dBm. The frequencies of the two tones were 7MHz and 7.01MHz. A non-harmonically related third tone of 61.4MHz was then injected into the input and its level increased to minimise the original two-tone signal's 3rd order products. This was achieved when the output level of the 61.4MHz signal was at +40dBm. The  $OPI_p^3$  of the amplifier using the original two tones then measured +51dBm. This was an improvement of 15dB. The small two-tone test signal was now riding on the back of the larger 10 watt tone. It was being carried into, and spending most of its time in, the region where the drain impedance was the most constant. Only when the 10 watt tone went through  $0^\circ$  and  $180^\circ$  was the two tone test signal subjected to the effects of the varying drain impedance.

It can happen in a field situation that a transmitter can cause interference to a local service, and the offending signal must be reduced in power. In such a

situation, there is a need to know the relationship between the harmonic output and the actual output power level of the fundamental. An accepted rule of thumb is for every 1dB decrease in the fundamental, the second harmonic will decrease by 2dB, the third by 3dB etc.. Class AB amplifiers do not follow this simple rule. Table III clearly shows the transfer function is more non-linear at low power levels than it is at higher power levels. Figure 3 shows the test set up employed to measure the harmonic output of the test amplifier when its bias was adjusted for both class A and AB. A 10.5MHz L.P. filter was used to attenuate the harmonics of the signal source. To demonstrate the change in linearity of the transfer function with output power for class AB, the output was reduced from 10 watts to 5 watts and comparisons made. Note the effect this 3dB reduction in output power had on the harmonic output when compared to the same amplifier in class A mode (refer figs. 5 to 8).

A class AB push/pull amplifier can be used as a high power single balanced mixer, the alternate switching off and on of the power devices providing the non-linear action required for mixing. Any A.C. ripple that may be on the power supply rail has the ability to modulate the input R.F., especially if there is poor regulation in the bias circuitry, and this ripple will be fed to the input of the active devices in common mode. The ability of the power output stage to function as a mixer can also be a source of radio frequency interference (R.F.I.). Take for example a transmitter site where there are two antennas erected adjacent to one another. If one of these antennas is broadband with a broadband class AB amplifier connected to it, the energy induced into it from the adjacent antenna would see the variation of drain impedance of the driven class AB amplifier as a non-linear element and create cross products with the amplifier's input driving signal. These cross products, provided they are within the systems bandwidth, will then be radiated by the broadband antenna and have the potential to cause R.F.I..

### 2.1.1 *Summarising Class AB*

The varying output impedance of a driven class AB amplifier can be the source of many problems. It has been shown that:-

1. The output impedance varies with signal level.
2. As a direct result of the above, the  $OPI_p^3$  varies with signal level.
3. Reflected waves have the ability to generate peak voltages across the outputs of active devices which can exceed the manufacturer's recommended maximum specifications. These voltages maximise when the peak of a reflected wave generated by an infinite S.W.R. arrives at the transistor drains as the input signal is traversing  $0^\circ$  or  $180^\circ$ .
4. Energy induced into the antenna system from a near lightning strike can be analysed in a similar manner to that of a reflected wave. The greatest voltages are produced across the outputs of the active devices when they



are either in their quiescent state or traversing  $0^\circ$  or  $180^\circ$ . This is examined in more detail under the heading of *Lightning Protection*.

5. The non-linearity or the switching action of a driven output stage has the ability to produce spurious products which can be radiated causing R.F.I. when R.F. energy radiating from an adjacent antenna is coupled to the broadband antenna driven by a broadband class AB amplifier.

For reasons highlighted above, class AB power amplifiers are not the best option for broadband work covering several octaves of bandwidth. They are more suited to spot frequency or narrowband work where tighter control of antenna S.W.R. is available through the use of an appropriate matching network. Also, by inserting a spot frequency or narrowband filter between the output port of a class AB amplifier and the antenna:-

- a. The generation of unwanted cross products caused by the coupling of energy from an adjacent radiating antenna to the driven output port of a class AB amplifier can be controlled.
- b. Energy induced into the antenna from a near lightning strike will be band limited upon its arrival at the outputs of the semiconductors and hence minimise the risk of damage.

## 2.2 Class A Bias

With a conduction angle of  $360^\circ$ , the output impedance of a single-ended class A amplifier swings about a point dictated by the device characteristics and quiescent current. The larger the output voltage, the greater will be the output impedance swing, which will reach its limits at cut-off and saturation. The application of negative feedback can greatly reduce the swing in output impedance. The output impedance, which is set by feedback, only becomes affected under conditions which alter the loop gain. The output impedance can be held relatively constant over a very large dynamic range during the full  $360^\circ$  of input drive by using two class A active devices to form a push/pull circuit. If the impedance matching to the output of the active devices is correct, a reflected wave returning to the transmitter will not be re-reflected upon its arrival. Instead it will be absorbed by the active devices and dissipated as heat. This will suppress the generation of high peak voltages as explained in the previous class AB discussion. This relatively constant output impedance also holds the  $OPI_p^3$  constant regardless of input drive level until distortion of the output envelope occurs through saturation or cut off. Also, by operating the output active devices in class A the switching action and its associated non-linearity are removed, the device no longer acting like a mixer. A commensurate reduction in the R.F.I. associated with the coupling of energy from an adjacent antenna is therefore achieved.

## 2.3 Lightning Protection

It is assumed that no output stage can suffer a direct strike by lightning and remain functional. This discussion on lightning protection will therefore be limited to ground strikes that are in close proximity to the antenna and to the direct induction of energy from such a strike into the antenna driven element.

Most of the ionosonde transmitters operated by S.P.G. are deployed in the tropics between 20°S and 20°N to the north of Australia. Within this region the number of thunderstorm days per year varies from 20 to 140. Converting these figures into the expected number of ground flashes (ref.4) gives 3 to 21 cloud to ground lightning flashes per square kilometre per year. The area within a 10km radius of an antenna installation can experience between 900 to over 6000 ground strikes annually.

Broadband H.F. antennas can have large voltages and currents induced into them from the electro-magnetic fields generated by close proximity lightning strikes. The magnitude of these voltages and currents at the power amplifier output terminal depends on:-

1. The field strength surrounding the antenna (ie. strength and proximity of strike),
2. antenna aperture (frequency dependent),
3. degree of matching between the antenna and feedline,
4. feedline losses,
5. any lightning protection measures taken, and
6. bandwidth of filters and impedance matching networks used.

Energy induced into the antenna system from a near lightning strike can be analysed in a similar manner to that of a reflected wave when it arrives at the output port of a solid state power amplifier, however the energy arriving at the output of the active devices is impulsive in shape and can be larger in magnitude than a reflected wave. The field intensity distribution of a cloud to ground lightning strike peaks at approximately 9KHz with an  $f^{-1}$  frequency dependence from 100KHz to 2MHz,  $f^{-2}$  between 2MHz and 10MHz, and  $f^{-5}$  above 10MHz (ref.1). ( $f^{-1} = 3\text{dB/oct}$ ;  $f^{-2} = 6\text{dB/oct}$ ; .....  $f^{-5} = 15\text{dB/oct}$ ).

From this it can be seen that the majority of the energy radiated from a ground strike lies below 2MHz. It is a simple matter to isolate this energy from the amplifier by installing a 2MHz high pass (H.P.) filter between the amplifier's output port and the antenna. It is important to consider what impedance this filter should present to the out-of-passband energy arriving from the antenna.

Presenting this energy to a high impedance encourages the development of high voltages and risks damage by exceeding the voltage ratings of the filter circuit components. A gas type lightning arrester could be used to limit this voltage, but this takes a finite amount of time in which to operate, during which the filter circuit is subjected to the high voltage, perhaps causing breakdown and an alternative path to be formed. This is not acceptable. Presenting this energy to a low impedance prevents the development of high voltages, but does produce high currents. The magnitude of these currents is inversely proportional to the impedance of the source, which in this case is the impedance of the antenna. Travelling wave antennas such as rhombics and deltas have termination resistors which become the source impedance. Other broadband H.F. antennas, e.g. log periodics and elevated feed monopoles, have impedances that are complex and frequency dependent when analysed outside of their designed frequency range. The 2MHz H.P. filter should also provide a D.C. path to ground to prevent any build up of static charge in the antenna system. From this it can be seen that the first element in the filter must be a shunt inductor to ground. Figure 9 shows a 7th order 0.1dB Chebyshev filter developed for this purpose. A lightning arrester was installed in parallel with the first shunt inductor to limit the peak in-band A.C. voltage. The striking voltage of the arrester should be at least twice the maximum peak R.F. voltage the amplifier can generate at its output in the forward direction when terminated into a 50 Ohm dummy load. This ensures that at full R.F. output the arrester will not strike under extreme S.W.R. conditions. With a 2MHz H.P. and a 70MHz L.P. filter installed in the amplifier output, the only energy from a near lightning strike that can reach the drains of the active devices is that which lies within the combined passbands of the filters. The effects this energy can have upon its arrival at the drains will now be examined.

Solid state active devices can be damaged by exposing them to voltages or currents in excess of the manufacturer's safe operating conditions. In the case of power F.E.T.s, if the drain to gate breakdown voltage ( $V_{DGR}$ ) is reached, the resulting damage is usually instantaneous and permanent. When the oxide insulating layer between the gate and semi-conductor substrate has been punched through, the resulting current heats the conduction path. Often there is enough heat produced to melt some of the metallisation and spew it along the surface of the breakdown channel thus causing a gate to semi-conductor substrate short. Exceeding the  $V_{DGR}$  is the main cause of damage to R.F. power devices from lightning strikes. If the drain/source current limits are exceeded, the resulting damage is usually caused by excessive heating of the silicon junction resulting in thermal breakdown then permanent damage.

Excess voltage causes instantaneous and permanent damage but excess current takes time to heat the junction. The amount of time required to thermally damage the junction is inversely proportional to the input power applied. The more power that is dissipated by the junction the faster it will heat to the point where damage occurs. A feature of a lightning strike is that it produces a lot of energy discharged within a short period of time. If this energy were to arrive at the drains of a class AB amplifier with the active devices in their quiescent state, the higher impedance presented would encourage the development of high

voltages and risk drain/gate voltage breakdown. Even if the amplifier is driven to its full rated output, there are still two points on the input driving wave where the output impedance is at its quiescent state,  $0^\circ$  and  $180^\circ$ . Only class A bias with its full  $360^\circ$  conduction angle provides the constant drain impedance required to suppress the generation of high voltages from a reverse wave and energy induced into the antenna from a lightning strike in close proximity.

It was mentioned earlier that high voltages at the drain of an active device should be avoided, but high instantaneous currents could be tolerated. Energy induced into the antenna from a lightning strike is delivered to the amplifier via a coaxial transmission line, generally with a nominal impedance of 50 Ohms. Reducing this impedance by a factor of four, using a transmission line transformer, effectively halves the voltage and doubles the current. This makes the induced energy more palatable from the active devices' point of view, especially if the current can be shared by devices connected in parallel. If the gas discharge tube fires at 200V, the very low impedance presented to out-of-band signals by the 2MHz H.P. filter indicates the energy which caused the discharge has to be R.F. in nature (ie. 2MHz and above) and delivered at the impedance of the transmission line, i.e. 50 Ohms. Applying Ohms law gives a current of 4A. Passing this through the 1:4 transmission line transformer in the reverse direction gives a voltage of 100V at a current of 8A. This then becomes the maximum voltage and current that the P.A. module will have to withstand for the duration of the strike if it is to have immunity from this kind of damage. Typical times for a ground to cloud strike are 0.1 to 5uS rise and 20 to 300uS overall duration (ref.2). The instantaneous 8A is acceptable for this duration, however the 100V still exceeds the manufacturer's specification of 65 volts maximum, typical for TMOS transistors. It was intended to install this 1:4 transmission line transformer into the 50 watt design, therefore a way of presenting this voltage to the drains must be incorporated into the design of the output impedance matching network of the power amplifier.

### ***3. 10 Watt Power Amplifier***

The choice of a particular R.F. power transistor for a broadband linear amplifier design, is greatly dependent on the non-linearity of the transistor's transfer function, since this dictates the maximum  $OIP_3$  that can be achieved without using specialised techniques such as "Feed Forward", or the parallelling of active devices. The maximum  $OIP_3$  is achieved when the output of the active device is matched to the transmission line with minimum losses. For example, if the output coupling circuit had a 1dB insertion loss, the active devices would need to be driven 1dB harder to overcome this loss in order to generate the same output power. By increasing the active devices drive by 1dB, the third order products are raised by 3dB, effectively reducing the amplifier's  $OIP_3$  by 1.5dB. If the insertion loss is in the form of an impedance mismatch and not dissipative, the resultant reflected wave can degrade the  $OIP_3$  even further.

To demonstrate this effect, a broadband 4:1 impedance ratio transformer was constructed from 50 Ohm coax and inserted directly at the output port of the 10 watt power amplifier module when biased in both class A and AB. This simulated a poorly designed output matching network. The amplifier was first biased in class A and connected directly to the dummy load. An input two-tone signal was applied and its level increased to achieve an output level of +30dBm/tone.  $OPI_p^3$  was then measured. Holding the input level constant, the 4:1 transformer was then inserted directly at the output port of the amplifier to reduce the amplifier's output impedance by a factor of four. The deviation in dB from +30dBm/tone was measured together with the new  $OPI_p^3$ . The transformer was then reversed, increasing the output impedance of the amplifier by a factor of four. Again the deviation in dB of the two tones from +30dBm and  $OPI_p^3$  was measured. This procedure was then repeated for class AB. The output level was then increased to +35dBm/tone and the measurements repeated for both classes of operation. Table IV lists the results. It is interesting to note a 2dB improvement in  $OPI_p^3$  for class AB +30dBm/tone when the transformer was used to decrease the output impedance. This highlights the variation of output impedance of class AB with input drive level. The 4:1 transformer provided a better impedance match at the +30dBm/tone level and hence an improvement in  $OPI_p^3$ . Also note that only when the class AB amplifier was driven close to its rated output power did its overall performance with respect to the  $OPI_p^3$  under mismatched conditions approach that of the class A amplifier. The number in the lower right of each box indicates the deviation in dB of the power contained in each tone from the straight through connection.

**Table IV:** Variation in  $OPI_p^3$  for class A and AB with 4:1 and 1:4 impedance mismatch.

	CLASS A +30 dBm/Tone	CLASS AB +30 dBm/Tone	CLASS A +35 dBm/Tone	CLASS AB +35 dBm/Tone
STRAIGHT THROUGH CONNECTION TO 50 OHM LOAD	+56.5 dBm 0dB	+48 dBm 0dB	+55.3 dBm 0dB	+53.7 dBm 0dB
OUTPUT IMPEDANCE DECREASED BY A FACTOR OF 4	+52.6 dBm -2.4dB	+50 dBm 0dB	+46.2 dBm -3dB	+45.3 dBm -1.7dB
OUTPUT IMPEDANCE INCREASED BY A FACTOR OF 4	+52.2 dBm -2.8dB	+42.8 dBm -3.7dB	+50 dBm -2.7dB	+49.1 dBm -2dB

The 1.2dB reduction in  $OPI_p^3$  for the straight through connection of class A at +35dBm/tone from that at +30dBm was produced by the peak of the two-tone envelope entering the 1dB<sub>comp</sub> point.

To achieve the five octaves of bandwidth required, the output transformer had to be in the form of a transmission line. This restricted the number of possible impedance transformation ratio combinations. Maximum transfer of power for a given class of operation is achieved when the output impedance of the active device is matched to the transmission line with minimum losses. Therefore, the dynamic output impedance ( $r_d$ ) of the active devices needed to be tailored to match that offered by the transformer used for impedance matching. The objective then was not to try and match a given output impedance to a transmission line, but to tailor the output impedance to match that offered by the matching transformer, with its fixed turns ratio, as it transforms the impedance of the transmission line or dummy load.

### 3.1 Tailoring The Output Impedance

The manufacturer's data on the MRF136 transistor quotes an output power rating of 15 watts at a  $V_{cc}$  of 28V. When two are used as a push/pull pair they should be capable of delivering 30 watts. This meets the 10 watt specification and allows approximately 5dB of headroom. The derating of the transistors from the manufacturer's rated output of 30 watts for a push/pull pair to 10 watts is required to ensure the harmonic output meets with the current standards. The following formula was used to calculate the output impedance of each of the push/pull transistors :-

$$r_d = \frac{(V_{DS} - V_{DS(ON)})^2}{2P} \quad (1)$$

where,  $r_d$  = the active devices dynamic output impedance.  
 $V_{DS}$  = potential difference between drain and source.  
 $V_{DS(ON)}$  = drain-source on voltage.  
 $P$  = power.

$V_{DS(ON)}$  was not listed in the manufacturer's data and therefore a measurement was made with a gate-source voltage of 10 volts and a drain current of 1A.  $V_{DS(ON)}$  was found to be 1.3V. Substituting  $P=15W$ ,  $V_{DS} = 28V$  and  $V_{DS(ON)} = 1.3V$  then solving for  $r_d$  gives 24 Ohms. This calculation was done to obtain the active devices' dynamic output impedance required to produce the required power. Resistive feedback was used between the drain and gate to stabilise the gain, and the output impedance was tailored using Miller's theorem to provide an impedance match to the transmission line transformer.

It is possible to effectively tailor, within reasonable bounds, the dynamic output impedance to be any chosen value. However, lowering this dynamic impedance through the Miller effect from the required 24 Ohms to say six Ohms,

holding  $V_{cc}$  constant and re-arranging equation (1) to solve for power, does not mean it is possible to extract more power out of the active device. The maximum power that can be obtained is very much dependent upon the active devices' internal physical construction. Provided the match to the six Ohms is correct, it should still be possible to obtain the 15 watts the device is capable of delivering minus the increase in losses due to the lower impedance, especially at the higher frequencies. These losses are usually in the form of skin effect resistance and stray circuit inductance. To highlight these losses, two lengths of tinned copper wire were soldered 15mm apart onto a piece of tinned half ounce copper P.C.B. material. This simulated the coupling between two discrete components, say two bypass capacitors, via a P.C.B. ground plane. The free ends of the wires were then connected to an H.P.-4191 R.F. impedance analyser and the circuit parameters at 2MHz and 70MHz measured. The P.C.B. material was then removed without disturbing the connection of the wires at the analyser, and the ends that were attached to the P.C.B. material were soldered together. A second set of measurements was taken at 2MHz and 70MHz and subtracted from their respective first. The skin effect resistance of the 15mm path of P.C.B. ground plane increased from a few milliohms at 2MHz to 0.26 Ohm at 70MHz. The slight variation of the measured 5.5nH inductance of the ground plane between the two frequencies was considered small enough to be ignored. At 2MHz there was an inductive reactance of 0.1 Ohm, at 70MHz this reactance rose to 2.4 Ohms. Although this was just one of many possible circuit paths on a P.C.B. layout, it served to show that series distributed circuit inductance would limit the upper frequency response. Designing a broadband amplifier to cover this frequency range with an  $r_d$  of six Ohms requires careful consideration of component placement on a P.C.B. layout. The  $OPI_p^3$  of the device should be unaffected throughout its dynamic range when operating at this low  $r_d$ .

By increasing the dynamic output impedance to 96 Ohms, again holding  $V_{cc}$  constant and providing the appropriate matching circuit, it was found that the amplifier's  $OPI_p^3$  was the same as for the previous example for peak output powers up to but not exceeding approximately 3.7 watts. This is the figure that is returned when equation (1) is re-arranged to solve for power. In pursuing peak powers greater than this, the  $OPI_p^3$  will degrade and the harmonic content will increase beyond what would be intuitively expected for a 15 watt device. The problems associated with an  $r_d$  of six Ohms with respect to the distributed circuit inductance and skin effect would hardly be noticed at this higher  $r_d$  of 96 Ohms. The amplifier is however sensitive to circuit capacitance and it is this which affects the upper frequency response.

One final configuration will be discussed. It has already been shown that to deliver 15 watts of R.F. from a 28V rail requires an output impedance or an  $r_d$  of 24 Ohms. A matching network was designed to match the 24 Ohms to 50 Ohms and was attached to the output of the active device. Next, by consulting the manufacturer's data sheets the active devices' input impedance was calculated and the appropriate matching circuit provided. With the gate impedance known, the feedback resistor ( $R_f$ ) value was readily calculated and installed

between gate and drain to give the required gain. The circuit was now complete and tests were carried out to check its performance.

The output impedance required to deliver the 15 watts from a 28V supply was calculated and a suitable matching circuit provided. However, the results were disappointing. Proper consideration had not been given to the effects of the feedback resistor upon the input ( $Z_{11}$ ) and output ( $Z_{22}$ ) impedances once it was placed in circuit. The manufacturer's data handbook specified  $Z_{11}$  and  $Z_{22}$  for the  $V_{cc}$  and output power required, but only in the absence of any feedback. Once feedback is added to the device its characteristics change, and the more feedback that is applied the greater is the change. In the current case, feedback had altered the devices' output impedance to some value other than 24 Ohms, and the matching circuit therefore was no longer optimum, resulting in a degradation in the amplifier's performance.

A design method to ensure the correct value of  $r_d$  is achieved is now presented. This method sacrifices the ability to choose gain in preference to being able to dictate a value for  $r_d$ . An  $r_d$  of approximately 24 Ohms in a push/pull configuration gives a drain to drain impedance of 48 Ohms. The closest transformer ratio to match this to a transmission line impedance of 50 Ohms is 1:1. Working backwards now from the 50 Ohm transmission line through the 1:1 transformer gives a drain to drain impedance of 50 Ohms or an  $r_d$  of 25 Ohms. This value of  $r_d$  will be achieved by tailoring the circuit elements contributing to the Miller effect.

Before the value of  $R_f$  could be derived the input impedance or shunt Miller resistance to ground needed to be chosen. It had to be low in order to swamp out the input capacitance at the gate at 70MHz. By making the input and output impedances 50 Ohms the push/pull amplifier could be a stand alone module, making designing and testing easier. A transmission line transformer with a ratio of 1:1 has the widest frequency response (measured in octaves) when compared to transformers with ratios other than 1:1. Its upper frequency response is not limited by the transmission line length (ref.3). With a frequency range of 2MHz to 70MHz or just over 5 octaves the 1:1 ratio transformer became the logical choice. Inserting this at the input would give a gate to gate impedance of 50 Ohms or a gate to ground impedance of 25 Ohms. The 3dB point of the input circuit to one of the gates can be approximated by,

$$f_{3dB} = \frac{1}{2\pi RC} \quad (2)$$

$$= 265\text{MHz}$$

where,  $C = 24\text{pF}$  ( gate to source capacitance of MRF136 ).  
 $R = 25\text{ Ohms}$  the impedance of the signal source.



This was sufficiently removed from the maximum frequency of 70MHz to not be a limiting factor. Although an input Miller impedance of 25 Ohms was aimed for, priority was given to tailoring the output Miller impedance to 25 Ohms in order to maximise the transfer of power from the output of the active device to the load. This ensured that the degradation of  $OPI_p^3$  through an impedance mismatch was minimal.

The value of  $R_f$  was chosen using the following empirical method. The circuit of fig.1a was built and the bias adjusted for class A. A network analyser was used to monitor  $r_d$ .  $R_f$  was initially a 500 Ohm variable resistor. Its value was adjusted until  $r_d$  equalled 25 Ohms. The variable  $R_f$  was then removed, measured with an Ohmmeter, and replaced with a fixed resistor.

A value of 270 Ohms for  $R_f$  was found to satisfy the requirements for an  $r_d$  of 25 Ohms. Table V shows the output impedance ( $Z_{OUT}$ ) or the  $r_d$  measured using a network analyser at 7MHz for various values of  $I_D$  with an  $R_f$  of 270 Ohms.

**Table V:** Variation in  $Z_{in}$  and  $Z_{out}$  of the circuit in fig.1 with changes in  $I_D$ .

$I_D$ (mA)	$Z_{OUT}$ (Ohms)	$Z_{IN}$ (Ohms)
0	290	300
50	70	55
100	45	43
200	35	34
300	30	30
400	27.5	30
500	26.5	30
600	25	30
700	25	30
800	25	30
900	25	30
1000	25	30
1250	25	30
1500	25	30

The 25 Ohm resistor marked  $R_{IN}$  in fig.1a was removed and placed between the drain and ground via the decoupling capacitor. The network analyser was then used to measure the value of input impedance ( $Z_{IN}$ ) or shunt Miller resistance to ground, (see fig.1b). This is also shown in Table V. Figure 2 is the Smith chart showing both input and output impedances at an  $I_D$  of 1A with  $R_f$  in and out of circuit to highlight its effect over the frequency range of 2 to 70MHz. The voltage gain at 7MHz was also measured using an oscilloscope with a X10 probe and found to be 7.7. This closely agreed with Miller's theory which states,

$$A_g = \frac{R_f}{Z_{IN}} - 1 = 8 \quad (3)$$

where  $A_g$  = voltage gain.  
 $R_f$  = feedback resistor (270 Ohms).  
 $Z_{IN}$  = input Miller resistance (30 Ohms).

and therefore indicated that all was well. The circuit was used as the starting point for the push/pull design.

### 3.2 Output Matching Network

The circuit shown in fig.11 was built to demonstrate the shortcomings of the output transformer configuration. The second harmonic varied between -45dBc to -15dBc over the frequency range of 2 to 30MHz when producing +40dBm output. The area where this method of transformer coupling can be improved is in the suppression of even order harmonics, which leave the drains as common mode currents, pass straight through to the centre tap of the output transformer un-attenuated, and are then dumped into the ground plane. It will be shown later that the common mode dynamic output impedance ( $r_{dcom}$ ) of the push/pull pair is in the order of a few Ohms; connecting this directly to ground, via a decoupling capacitor, will drive the even order distortion products from a very low impedance into the ground plane where they can modulate the circulating ground currents and hence appear at the output. The centre-tapped output transformer provided a convenient means of isolating the common mode currents from the wanted R.F.. A circuit based on a 180° hybrid combiner using transmission line transformers was developed to better manage the even order distortion products (see fig.12a). A more detailed description is given under the heading of *Termination Resistors*.

To obtain the maximum bandwidth possible the 1:1 output balun needed to be constructed from 50 Ohm transmission line. 50 Ohm transmission line was made by twisting two lengths of 23 S.W.G. enamel covered wire together at nine twists per inch. A piece 1m long had the following distributed parameters.

Distributed L = 257nH

Distributed C = 113pF

$$Z_o = \sqrt{\frac{L}{C}} = 47.7 \text{ Ohms} \quad (4)$$

Under ideal conditions a 1:1 transmission line balun does not have its upper frequency response limited by the transmission line length. However in the real world the output impedance of the active devices becomes more reactive as the frequency is increased. The greater the deviation from the ideal resistive termination the more dependent the upper frequency response becomes on the transmission line length. Because of the capacitive loading on the output transformer by the active devices at the higher frequencies, it was decided to ensure that the transmission line length adhered to the same design rules as transformers with impedance ratios other than 1:1. That is, the line length did not exceed  $1/8 \lambda$  at the highest frequency to be used (ref.11). With the aid of a network analyser the velocity factor of this twisted pair was measured and found to be 0.63. At 70MHz, the highest frequency of interest, the full wavelength in this transmission line is approximately 2.7m. Applying the  $1/8 \lambda$  rule gives a maximum line length of 337mm.

Amidon material 43 was chosen for the toroidal balun for its high permeability (850) and its inherent ability to absorb R.F. above approximately 70MHz. This ability to absorb R.F. offers two advantages:-

1. Helps to attenuate the harmonic output of the amplifier above 70MHz by absorbing some of this energy into the core material.
2. Suppresses any VHF/UHF parasitic oscillations by lowering the Q of the magnetic circuits at these frequencies.

Six turns of this transmission line were wound on an Amidon FT-50A-43 toroid to form the 1:1 balun. The inductance of one winding was  $10\mu\text{H}$ . At 2MHz, the lowest frequency, it had a reactance of approximately 125 Ohms. This was five times  $r_d$  and followed the "at least 5 times at the lowest frequency" rule for broadband transformers (ref.11). The length of transmission line required for six turns was 140mm. This satisfied the less than  $1/8 \lambda$  for the upper frequency response. For simplicity in manufacture the centre-tapped R.F. choke was the same as the 1:1 balun, the only difference being the way it was connected in the circuit.

### 3.3 *Input Matching Network*

Table V shows a gate to source spot frequency impedance of 30 Ohms. The gate to gate input impedance of the push/pull amplifier was therefore 60 Ohms. The input matching network was designed along the same lines as the output network. The input transmission line 1:1 balun consists of 10 turns of 0.4mm enamel covered wire bifilar wound at 11 twists/inch on an Amidon FT-37-43 toroid. The inductance of one winding was  $36\mu\text{H}$  and the distributed impedance was measured and found to be 53 Ohms. For simplicity the centre tapped R.F. choke was constructed the same as the input balun.

The input/output matching was now complete, but variation of both input and output S.W.R. with frequency over the five octaves was expected. Optimisation of the output S.W.R. and best compromise of the input through the manipulation of  $R_f$  and the insertion of a resistor between the gates was carried out on the final assembly.

### 3.4 *Biasing*

MOSFETs have a negative temperature coefficient, on the gate threshold voltage ( $V_{GS(th)}$ ) at low current levels, which turns positive at higher currents. This means that the gate threshold voltage at high current levels increases with temperature, trying to turn the device off (ref.6). Biasing the power F.E.T.s into class A places them in this positive  $V_{GS(th)}$  temperature coefficient region and therefore simplifies the design of the bias circuit. Had class AB been chosen, the  $V_{GS(th)}$  temperature coefficient would swing from negative at its quiescent state to positive when R.F. drive was applied. This would require a complex bias circuit to properly address.

It was found experimentally that the best compromise between device dissipation (drain/source voltage ( $V_{DS}$ ) versus drain current ( $I_D$ )) and  $OIP_3$  for the operating point of the MRF136 transistor biased in class A was for a  $V_{DS}$  of 28V at an  $I_D$  of 1A. This operating point returned consistent results for the manufacturer's different batch numbers. The 28 watts of heat generated per device is a manageable level. The gate voltage ( $V_{GS}$ ) required to set the  $I_D$  to 1A varied between 4 to 6 volts for the devices tried. An 8.2V zener diode was chosen to provide a reference voltage from which the bias is derived. This diode has a slight positive temperature coefficient which helps to offset the positive shift in the transistors'  $V_{GS(th)}$  at high current levels as the temperature rises. The zener also prevents any A.C. ripple that could be present on the power rail from being coupled to the gates as a common mode voltage and thus modulating the R.F. output. A bypass capacitor, fitted at the wiper of the bias adjusting trim pot, filters out the noise generated by the avalanche action of the reference diode.

### 3.5 *Transistor Matching*

The MRF136 transistors are available as a matched pair in a common package. The cost of the matched pair is approximately four times that of a single transistor. Because it was intended to bias the transistors in class A, any subtle differences in the A.C. characteristics between the devices would be swamped out by the effects the feedback resistor ( $R_f$ ) has upon the gain and input and output impedances. It was therefore not considered cost effective to purchase the matched pairs, since matching the D.C. characteristics was all that was

required. The transistors' D.C. characteristics were matched by comparing the  $I_D$  holding  $V_{GS}$  constant. A maximum deviation in  $I_D$  of 2% was the limit for matching pairs. A full A.C. and D.C. matching would have been required had class AB been chosen. The higher impedance of  $r_d$  in its quiescent state and on each alternate half cycle of the input driving signal when the active device is cut off would not swamp out these variations in the devices' A.C. characteristics. 60 percent of the first batch of 100 transistors purchased in March 92 formed matched pairs. The increase to 80 percent of a second batch of 100 purchased 14 months later was attributed to improved manufacturing techniques. This second batch also consistently returned an  $OPI_p$  1dB higher than the first.

### 3.6 Termination Resistors

A closer examination of the output impedance presented by the transistor drains for both differential and common mode operations was required in order to choose the value of termination resistors ( $R_T$ ) required for the  $180^\circ$  hybrid splitter/combiners. Differential mode will be covered first.

Odd order distortion products generated within the transistors appear at the drains as differential voltages and currents and are therefore analysed in a similar manner to the fundamental. The basic circuit of the output matching network is shown in fig.12a. This has been re-drawn in fig.12b to better emphasise the magnetic coupling of the 1:1 balun. The -E appearing across the lower winding of the balun undergoes a  $180^\circ$  phase change, through transformer action, to E into the top winding, and is in series and in phase with the top voltage generator. The net magnetic flux in the 1:1 balun is zero and the circuit is further simplified in fig.12c. The centre-tapped R.F. choke shown in fig.12a has across its ends the differential voltages E and -E. The construction of this choke was the same as for the 1:1 balun. The inductance of the centre tap to either end is  $10\mu H$ . At 2MHz the inductive reactance ( $X_L$ ) is approximately 125 Ohms. This is where the reactance is the lowest for the frequency range being used. As the frequency is increased  $X_L$  also increases. Provided the phase difference between the two voltage generators is  $180^\circ$  and their magnitude are equal, the centre tap of the R.F. choke will be at earth potential and no power will be dissipated in  $R_T$ . It should also be noted that under the same conditions the net lines of flux in the 1:1 balun is zero and there is no inductive reactance associated with it.

If however the magnitudes of the two generators are unequal, the centre-tapped choke appears as a wideband 4:1 impedance ratio transformer to the summation of the two voltages. The voltage across the resistor  $R_T$  is equal to:-

$$E_T = \frac{E + (-E)}{2} \quad (5)$$

where,  $E_T$  = voltage across resistor  $R_T$   
 $E$  = voltage from one side of R.F. choke to ground  
 $-E$  = voltage from the other side of R.F. choke to ground and  $180^\circ$  displaced from  $E$ .

From this it can be seen if the R.F. choke functions as a 4:1 transformer, the value of  $R_T$  required to provide a match at the center tap for unbalanced amplitudes is:-

$$R_T = \frac{r_d + r_d}{4} \quad (6)$$

where;  $r_d + r_d$  = the summation of the two dynamic drain impedances of the push/pull pair, usually but not necessarily of equal value.

The 1:1 balun is also affected by an imbalance in amplitude. The sum of the magnetic flux within its core no longer cancels and the residual makes the balun appear as an inductor whose inductance increases with increasing amplitude imbalance. This inductance, which appears in series with the load, could be unnoticed at 2MHz but adversely affect the frequency response at 70MHz.

When the proper attention is paid to design and circuit construction, the amount of power dissipated in  $R_T$  through unequal amplitudes is very small. Voltages developed across the ends of the centre-tapped R.F. choke from a reflected wave generated by extremes of S.W.R. will be differential, of equal amplitude, and  $180^\circ$  displaced with respect to ground. Again very little power will be dissipated in  $R_T$ . It is only when the summation of  $E$  and  $-E$  is not zero or they are not  $180^\circ$  displaced that the power in  $R_T$  will be of concern. This is most likely to happen when a fault in the push/pull pair has occurred. Under such conditions, gain, upper frequency response and output power will be noticeably affected and the amplifier would be removed from service for repair.

Common mode voltages will now be considered. Internally generated even order distortion products appear at the drains as common mode voltages and currents. Provided the common mode sources are of equal amplitude and are in phase, the magnetic field produced in the 1:1 balun by its two windings will have the same sense and hence reinforce each other. The balun now functions as an R.F. choke isolating the load from the common mode sources. The magnetic fields generated in the centre tapped R.F. choke will be equal but of opposite

sense and hence cancel each other. The net inductance is zero. This R.F. choke now appears as a short circuit connecting the two drains and the termination resistor together forming a parallel circuit. It is tempting to think that the output impedance for this common mode operation, and hence the value of  $R_T$ , would be the two  $r_d$  impedances in parallel.  $R_T$  would then have the same value as that for an imbalance in the differential mode. This however is not the case. The value of  $r_{dcom}$  in this common mode of operation is not the same as the  $r_d$  in differential mode. Ignoring the bias and D.C. power, fig.13 is the basic circuit of the power amplifier. The input/output 1:1 baluns now appear as R.F. chokes isolating the input signal source and the load from the active devices. The input/output centre-tapped R.F. chokes appear as a short circuit connecting the gates and input  $R_T$  together and likewise with the drains and output  $R_T$ . The two feedback resistors ( $R_f$ ) are now in parallel and can be replaced with one resistor. The circuit has been redrawn in fig.14 highlighting these changes. The voltage generator for the even order distortion products can now be seen. The value of  $r_{dcom}$  is still unknown and is dependent upon the input  $R_T$  and its relationship to  $R_f$ . This is the Miller effect. The forward gain of the paralleled active devices to the voltages appearing at the drains and coupled to the gates via  $R_f$  is:-

$$-A_g = \frac{Z_{Rf}}{Z_{Rf} + Z_T} - 1 \quad (7)$$

where;  $-A_g$  = forward voltage gain (less than 1 and inverting).

$Z_{Rf}$  = parallel combination of the feedback resistor as depicted in fig.14 and combined gate/drain capacitance.

$Z_T$  = parallel combination of the input  $R_T$  and the combined gate/source capacitance.

If the input  $R_T$  was made extremely small, the forward voltage gain would be approaching zero and very little negative feedback could be applied. The effect on the common mode voltage at the drains would be minimal. If however the input  $R_T$  was made very high, the forward gain would approach unity and maximum benefit could be obtained from the negative feedback. It should be noted that any value of input  $R_T$  will form a voltage divider with  $Z_{Rf}$  and reduce the amount of feedback applied. Also, the gate to source capacitance forms a frequency dependent voltage divider network with  $Z_{Rf}$ . This decreases the feedback as the frequency is raised resulting in an increase in even order harmonic output. At this stage the input  $R_T$  was given some arbitrarily high value while an output  $R_T$  was chosen.

If the output  $R_T$  was made zero Ohms, all the even order distortion products could be dumped into the ground plane. This is undesirable for two reasons.

1. The path from the drains through the centre tapped choke to ground then finally to the transistor source tabs has distributed inductance

associated with it. At some V.H.F./U.H.F. frequency there will be enough inductive reactance in the drain circuit to provide a  $90^\circ$  phase shift between the drain voltage and current. A further  $90^\circ$  phase shift is provided by the internal drain/gate capacitance. The feedback applied to the gate would then be positive and oscillation would occur. Isolating the source and load impedances gives rise to the neutralisation problem normally associated with thermionic valves. With the input/output baluns acting as R.F. chokes, there is very little resistive loading placed on this power oscillator and damage to the active devices may result.

2. The  $r_{dcom}$  of just a few Ohms could modulate the ground plane with the even order distortion products. This would be very noticeable at the higher frequencies where the reactance of the distributed inductance and skin effect in the ground plane combine to form the working load.

It should be noted that the even-order harmonics delivered to the load resistor ( $R_L$ ) are primarily due to imbalances between the active devices and subtle differences in their associated circuits. These imbalances create differences in amplitude, with respect to ground, in the common mode voltages. These differences appear as differential voltages to the 1:1 balun and hence are coupled to  $R_L$ . If the output  $R_T$  was made very large, there would be no working load for the common mode generators and their output would increase to the open circuit voltage. The magnitude of their differential is also proportionally increased and this is reflected in the even order harmonic output delivered to  $R_L$ . From the above it can be seen that a low value of output  $R_T$  is preferred. However, too low a value will risk common mode parasitic oscillations.

The common mode output impedance ( $r_{dcom}$ ) was then measured with the input  $R_T$  open circuit and also with an arbitrary value of 240 Ohms. A network analyser was connected where the output  $R_T$  would normally reside. Measurements were made at four frequencies and Table VI lists the results.

**Table VI:**  *$r_{dcom}$  versus frequency.*

FREQUENCY	VALUE OF $r_{dCOM}$ WHEN INPUT $R_T = \infty$	VALUE OF $r_{dCOM}$ WHEN INPUT $R_T = 240\Omega$
7MHz	$1.9\Omega - j1.0\Omega$	$2.7\Omega - j1.0\Omega$
14MHz	$2.0\Omega - j3.17\Omega$	$2.8\Omega - j3.0\Omega$
30MHz	$3.2\Omega - j7.7\Omega$	$3.9\Omega - j7.3\Omega$
60MHz	$6.0\Omega - j13.84\Omega$	$6.6\Omega - j13.1\Omega$

Note the difference in output impedance between differential mode (nominally 50 Ohms; fig.16) to that of the common mode in table VI. The input  $R_T$  of 240 Ohms was chosen purely as a starting point. It appeared as a 960 Ohm load ( $240 \times 4$ ) to the imbalance in amplitude of the common mode voltages applied to the gates. Most of the imbalances would have been caused by differences in stray



inductance and capacitance between the two halves of the push/pull circuit and therefore were more noticeable at the higher frequencies. Table VI shows that there are no dramatic changes to  $r_{dcom}$  at 60MHz when the 240 Ohm input termination is added. This is the area where the strays were most noticeable and indicated the 240 Ohms for the input  $R_T$  was suitable. Inserting this resistor had minimal effect on the second harmonic of a 30MHz input signal, indicating that the effects of the combined shunt gate/source capacitance predominated. Harmonics appearing higher than 70MHz would be attenuated by a L.P. filter fitted at the transmitter's output port. The common mode output impedance at 60MHz with the 240 Ohm resistor for the input  $R_T$  is:-

$$|Z| = \sqrt{R^2 + X^2} \quad (8)$$

$$Z = 14.6 \text{ Ohms } \angle 63^\circ$$

where;  $Z$  = common mode output impedance.

$R$  = 6.6 Ohms from table VI.

$X$  =  $j13.1$  Ohms from table VI.

A 250 Ohm variable resistor was installed for the output  $R_T$  and an input signal of 3MHz applied. The output  $R_T$  was adjusted and the harmonic output examined. The even order harmonics were progressively suppressed when the output  $R_T$  was adjusted from 250 Ohms down to approximately four Ohms. This is where the amplifier became unstable in the common mode. Altering the input signal to 30MHz and carrying out the same tests showed that very little increase in the suppression of the even-order harmonics could be achieved with an output  $R_T$  below approximately 20 Ohms. This indicated that below 20 Ohms the distributed inductance of the ground plane predominated. A value of 15 Ohms for the output  $R_T$  was chosen, sufficiently removed from the "four Ohms or less" instability point to ensure stable operation and below 20 Ohms where very little increase in suppression could be obtained.

### 3.6.1 Summarising $R_T$

It has been shown that there is a difference in the output impedance of the drains as they produce differential and common mode voltages and currents for the push/pull circuit presented. It was also shown that if the proper attention is paid to balancing the two sides of a push/pull amplifier, very little could be gained by matching the output  $R_T$  to an imbalance in amplitude of the differential voltages. Under normal operating conditions the difference in amplitude would be very small and hence the power dissipated in the output  $R_T$  would also be small. There are however gains to be made in the suppression of internally generated even-order products through the manipulation of both input and output  $R_T$ . A high value of input  $R_T$  (240 Ohms was chosen) has minimal effect upon the negative feedback's ability to suppress the even order products. The gate/source capacitance however degrades this feedback

resulting in an increase in the even order products as the frequency is raised. A very low value of output  $R_T$  is preferred, but this can cause instability at V.H.F./U.H.F. frequencies. An output  $R_T$  of 15 Ohms was empirically found to be a reasonable compromise between amplifier stability and the even order harmonic output.

### 3.7 Performance Testing 10 Watt Module

Figure 15 shows the final design of the 10 watt output module. The 200 Ohm resistor between the gates together with the 340 Ohm resistor for  $R_f$  were values derived during optimisation. Quiescent current was set at 2A total for class A operation. Figure 16 is the Smith chart showing the  $Z_{IN}$  and  $Z_{OUT}$  of the module. The following performance figures were measured.

Frequency Range	: 2MHz to 70MHz
Power Gain	: 17dB
Gain Variation	: less than +/- 1dB (fig.22)
$OPI_p^3$	: +57dBm at 8MHz (fig.23) : +52dBm at 65MHz (fig.24)
$OPI_p^2$	: +102dBm at 5MHz (fig.17,ref.12) : +99dBm at 8MHz (fig.18,ref.12) : +81dBm at 30MHz (fig.19,ref.12) : +81dBm at 60MHz
$OP1dB_{comp}$	: +43dBm
OP Impedance	: 50 Ohms nominal
OPVSWR	: 1.4:1 maximum (fig.16)
IP Impedance	: 50 Ohms nominal
IPVSWR	: 1.8:1 maximum (fig.16)
D.C. input power	: 28V at 2A

Figures 17 to 19 show the harmonic output of the module when delivering 10 watts into a dummy load. Figure 3 is the test set-up used to measure the harmonic output.

The following procedure was carried out to test the durability of the amplifier module under extremes of S.W.R.. The module was driven hard into compression producing +46dBm at the output. Keeping the input drive level constant, the coax cable connecting the module to the dummy load was disconnected from the output port to create an open circuit. An R.F. "sniffer" made of a one turn loop 5cm. in diameter connected to a spectrum analyser was placed over the active devices and used to monitor the amplifier. The input signal frequency was swept from 2MHz to 70MHz then back to 2MHz in 100KHz increments with a 0.1 second dwell time. A short circuit was then placed at the output port and the input again swept. This test was done to ascertain the presence of any destructive parasitic resonances within the output coupling network under open and short circuit conditions. A length of foam dielectric low loss coax cable 1.5m long was connected to the output port and the short and open circuit transferred to the far end of the coax cable. The test was then repeated to determine the response of the module to differences in phase between the forward and reflected waves. The module, when pushed 3dB beyond the  $OP1dB_{comp}$ , was consistently free of parasitic oscillations and suffered no discernible degradation in measured performance.

### 3.8 Complete 10 Watt Amplifier

The design of the pre-amp and driver stages for this standby transmitter was considered to be straightforward and is therefore not covered in detail. A CA2818 hybrid was chosen for the R.F. pre-amp. The manufacturer specifies a noise figure of 5.5dB which should keep the broadband noise appearing at the transmitter output port to acceptable levels. The driver stage is an MRF136 TMOS transistor operating in class A and has a gain of 14dB. The R.F. pre-amp, driver and 10 watt power amplifier were mounted on a common heatsink. This complete assembly was then suspended in a wind tunnel built around a standard 120mm muffin fan and forced air cooled. All the components of the 28V power supply were also contained within the wind tunnel. This was done to ensure adequate cooling should the airconditioning unit at the installation site fail. A 2MHz to 70MHz bandpass filter (fig.21) designed around the concepts highlighted under *Lightning Protection* was installed at the transmitter output port. The complete R.F. circuit appears as figs. 15, 20 and 21. The gain variation and  $OPI_p^3$  of the 10 watt standby transmitter are shown in figs. 22, 23 and 24.

## 4. 50 Watt Power Amplifier

The earlier discussion on lightning protection introduced the concept of stepping down the 50 Ohms of the transmission line using a 1:4 transformer to 12.5 Ohms in order to reduce the impact of the energy induced into the antenna from a near lightning strike before offering it to the transistor drains. The impedance of the coaxial transmission line required to make this transformer is 25 Ohms, the

geometric mean of the two terminating impedances. 25 Ohm coax was made by replacing the inner conductor of RG-174/U coax cable with 20AWG PTFE wire whose overall outside diameter is 1.5mm and inner conductor diameter is 1mm. A 1m length of this modified coax had the following distributed parameters.

$$\text{Distributed } L = 125\text{nH}$$

$$\text{Distributed } C = 207\text{pF}$$

$$Z_0 = \sqrt{\frac{L}{C}} = 24.6 \text{ Ohms} \quad (9)$$

The velocity factor was measured and found to be 0.63.

Tests were carried out on various toroidal cores to find one which could be used for this 1:4 transformer. Ferrite materials designed for broadband R.F. transformers produce inductors that have a low Q when analysed within this area of operation. The low Q indicates power is absorbed within the core material. At low power levels the amount of energy absorbed and dissipated as heat within the material is not sufficient to cause any adverse effects. At high power levels, the heat generated within the toroidal material can exceed its ability to dissipate it to the surrounding environment. This eventually leads to thermal breakdown of the materials permeability. It was intended that this 50 watt amplifier would survive the same abuse tests as the standby unit, particularly when driven hard into compression and a short circuit placed at the output port. None of the ferrites tried survived a simulation of this test. They all over-heated to the point of thermal breakdown. To overcome this problem it was necessary to measure the Q, over the frequency range of interest, of an inductor wound on a various types of toroidal former. The higher the Q, the lower the power absorbed by the toroid and hence the less internally generated heat. Only powdered iron seemed to have a high Q across the 2MHz to 70MHz frequency range. It should be noted however, that once this material has been used to make a broadband transformer, and this transformer has been loaded down with source and load impedances, its ability to produce high Q inductors becomes meaningless. Two materials in particular, Amidon material 2 and 6, looked promising. Of these two, material 6 was chosen for its slightly higher permeability. It also exhibited the least amount of heat and had a flatter response across the required frequency range. Eleven turns of 25 Ohm coax was wound on an Amidon T-80-6 toroid and wired as a 1:4 auto-transformer. The inductance of the 50 Ohm winding at 2MHz was 2.5uH and the line length was 300mm. Accepted design rules for broadband transformers were broken, and a compromise reached between core heating, line length and inductive reactance at the lowest frequency. More work needs to be carried out to find a core material with a higher permeability and low internal losses. This transformer was used to step the 50 Ohm transmission line impedance down to 12.5 Ohms and provide the working load for the 50 watt power amplifier.

A 50 watt push/pull power amplifier module using a matched pair of MRF171 MOSFET transistors was constructed using the same design method as presented for the 10 watt module. The best compromise between device dissipation and  $OIP_3$  was reached at a  $V_{cc}$  of 28V and a total  $I_Q$  of 5.8A. The  $OIP_3$  was +59dBm,  $OP1dB_{comp}$  +50dBm and the gain variation at 50 watts output was +/-1dB from 2MHz to 70MHz. The amplifier did not survive the abuse test when it was driven into compression and a short circuit placed at the output port. It was also felt that the total heat being dissipated by the active devices when operating in class A was excessive. The active devices had to be physically as close as possible in order to keep the inductive path between their source tabs low. This ensured that reduction of gain at the higher frequencies through degenerative feedback was kept to a minimum. The thermal conductivity of aluminium ( $2.18W/cm^{\circ}C$ ) was not ideal and the close proximity of the two transistors operating in class A concentrated the heat produced in a small area of the heat sink. This localised concentration of heat was minimised by mounting the transistors on a copper plate ( $3.94W/cm^{\circ}C$ ) which in turn was attached to the heatsink. This ensured a more rapid dispersion of the 162 watts of heat produced. Each transistor dissipated 81 watts of heat into the heatsink. Calculating the junction temperature of the active device (ref.7) indicated an operating temperature in the vicinity of  $180^{\circ}C$ . This was too close to the maximum temperature of  $200^{\circ}C$  and quite possibly is the reason for the failure of the amplifier to survive the short circuit abuse test. To lower the  $I_Q$  in an attempt to drop the junction temperature also meant lowering the  $OIP_3$ . This was not acceptable. The thermal problems associated with operating only two active devices in class A to generate 50 watts of output power was deemed impractical to solve. A new approach was required.

The 10 watt module that had already been developed had proved very rugged. Its  $OP1dB_{comp}$  of 20 watts indicated four modules could be placed in parallel to deliver the 50 watts with 2dB of headroom. Power from a reflected wave and energy induced into the antenna from a near lightning strike would be shared by eight active devices. The thermal problem of localised heating of the heatsink associated with operating only two active devices would also be solved. The physical size of the individual modules would ensure a more even distribution of the generated heat. The calculated junction temperature of the active devices of the 10 watt module was approximately  $125^{\circ}C$ . Placing the four modules in parallel would also lower the overall output impedance to 12.5 Ohms. The output of the combining network could then be connected directly to the 1:4 output transformer. The block diagram of the proposed complete 50 watt power amplifier is shown in fig.25.

Figure 27 is the circuit diagram for the four power amplifiers used in the 50 watt design. Four modules were built and their outputs paralleled via a combining network which was in turn connected to the 1:4 output transformer. The four inputs were also paralleled with a combining network and returned an input impedance of approximately 18 Ohms. Care had to be taken when installing the input/output 1:1 baluns onto the circuit card to ensure the correct phase of R.F. was delivered to the output combiners. A driver stage (fig.26) with

nominal input and output impedances of 60 Ohms and 25 Ohms respectively was built and installed. The preamplifier (fig.26) used both lossless and resistive feedback and had a gain of 15dB with a noise figure of 3dB. All of the above components were installed on a pair of heatsinks obtained from R.S. Components (cat No.658-025). These heatsinks are designed to be joined together and forced air cooled by a standard 120mm square axial flow fan. All power supply components except for the transformer and main electrolytic filter capacitors were also mounted on the heatsinks. The heatsinks are thermally monitored and a cutout provided should their temperature exceed 65°C. It was found the temperature of the heatsinks rose 22°C above ambient when the amplifier was operating with no R.F. input drive.

Initial testing revealed a 0.5dB premature roll off of the upper frequency response when compared to the frequency response of a single module. This was attributed to slight variations in group delay of the output combining network as it coupled the outputs of the four modules to the 1:4 output transformer. These variations were caused by the subtle differences in winding capacitance between the two halves of the individual combiners. The difference in capacitance could be reduced by swamping it with a larger capacitor of known value. Too large a capacitor however, will degrade the upper frequency response. A value of 18pF was empirically chosen. This capacitor needed to have a minimum 100V rating for reasons described earlier in *Lightning Protection* and also must withstand the peak R.F. output voltage when the module is driven hard into compression and connected to an open circuit. Placing this capacitor at the end of the 85mm long piece of 50 Ohm coax used to connect the output of the modules to the input of the combiners had the same effect, when examined on a network analyser, as using the same length of 25 Ohm coax without the capacitor. Measuring the distributed L and C of this modified 85mm 50 Ohm coax with the 18pF capacitor connected and calculating the apparent distributed impedance, returned a figure of 26 Ohms. This confirmed the 85mm length of 25 Ohm coax could be used here. Whether 50 Ohm or 25 Ohm coax was used, care had to be taken to ensure that the lengths of coax line connecting the outputs of the four power amplifier modules to the inputs of the combiners were equal to prevent variations in group delay affecting the upper frequency response. The 25 Ohm coax was chosen because its breakdown voltage far exceeded that of the readily available 18pf high Q capacitors and it meant four fewer components in the combining network. The four 50 Ohm coax leads from the combining network to the inputs of the modules had also to be of equal lengths.

Provision was made on the driver and power amplifiers to disable their outputs by removing their bias either manually or under computer control. This was done to conserve the integrity of emergency frequencies by disabling the transmitter for relevant portions of the sweep and also to minimise the mains power consumed between sweeps.

#### 4.1 Performance Testing 50 Watt Amplifier

The following performance figures were measured on this complete assembly.

Frequency Range	: 2MHz to 70MHz
Power Gain	: 49dB
Gain Variation	: less than +/- 1dB (fig.36)
OPI <sub>p</sub> <sup>3</sup>	: +62dBm at 8MHz (fig.32) : +59dBm at 65MHz (fig.33)
OP1dB <sub>comp</sub>	: +49dBm
OP Impedance	: 50 Ohms nominal
OPVSWR	: 3:1 maximum (fig.29)
IP Impedance	: 50 Ohms nominal
IPVSWR	: 2:1 maximum (fig.28)
Noise Figure	: 5dB
D.C. input power	: 28V at 9A

The poor OPVSWR is to be expected. This highlights the compromises made in the design of the 1:4 output transformer and is an area where improvements can be made. Figures 28 and 29 are the Smith charts showing  $Z_{IN}$  and  $Z_{OUT}$  respectively of the complete amplifier from 2 to 70MHz. Figures 34 and 35 shows the third order products when producing an output of 10 watts/ tone. The slight decrease in OPI<sub>p</sub><sup>3</sup> (compared with that shown in figs. 32-33) is due to the peaks of the two tone envelope entering the OP1dB<sub>comp</sub> point. The assembly was driven hard into compression delivering 120 watts of R.F. output into a dummy load. The abuse tests as described earlier for the 10 watt design were then carried out, and this had no impact on the above performance figures. The 2MHz high pass and 70MHz low pass filters were installed and the abuse tests repeated. Apart from the effects of the insertion loss of the filters there was no other measurable deviation in the above performance figures or any sign of parasitic oscillations or breakdown in the gas discharge tube installed in the 2MHz high pass filter. A 2dB pad installed at the amplifier input in order to reduce the gain so that a 0dBm input signal produced +47dBm output, caused no change in the broad band noise generated by the amplifier, however the overall noise figure increased to 7dB. Input S.W.R. was improved to less than 1.4:1 by the inclusion of this 2dB pad.

## 4.2 *Near Lightning Strike Test*

Figure 37 shows the test set up to simulate large differential voltages generated between the inner and outer conductors of a coaxial transmission line by an antenna that is in close proximity to a lightning strike. A high voltage, high energy 0.5mfd capacitor was used to store the charge from a 30KV generator. The earthed outer braid of RG-213 coax was connected to one terminal of this capacitor. A needle point spark gap of 10mm was set between the inner conductor of the coax and the capacitors other terminal. The breakdown voltage of the spark gap was in the vicinity of 15KV (ref.8). The input drive level to the amplifier was adjusted to produce 50 watts of R.F. output into a dummy load at a frequency of 20MHz. Without altering the R.F. input drive level, the dummy load was disconnected from the amplifier's output port and the coax cable with the high voltage spark gap was connected in its place. The amplifier's forward and reflected power was 50 watts. The high voltage generator was turned on and the high voltage capacitor allowed to slowly charge to the spark gap breakdown voltage. After breakdown of the gap had occurred, the dummy load was reconnected to the amplifier's output port and the output power re-measured. There was no discernible change in output power. This test was carried out several times with the same results.

## 5. *Conclusions*

The design of a robust 2MHz to 70MHz linear power amplifier has been presented. It was shown that if the junction temperature of the output active devices is kept low, a conduction angle of  $360^\circ$  provides the best immunity to damage caused by extremes of S.W.R. and energy induced into the antenna from near lightning strikes. It was also shown that an appropriately designed 2MHz high pass filter with a low out-of-passband impedance, fitted at the output port of a power amplifier, will shunt to ground the majority of the energy induced into an antenna from a near lightning strike; this action greatly increases the output active devices' chances of survival. The 10 and 50 Watt versions of the amplifiers described can operate continually into any load, at any phase angle, and any power level up to and including their OP1dB<sub>comp</sub>. Since March 1992, the amplifiers have been progressively deployed in many hostile and often unmanned field sites with excellent results.



## ***6. Acknowledgments***

This author wishes to acknowledge the contributions made by the following people during the development of this document:-

**Angus Massie (Jr)**, for his suggestions on both the content and presentation of technical details.

**Peter Wilinski**, for proof reading the manuscript through its development.

## 7. References

1. J.E. Nanevich, E.F. Vance, and J.M. Hamm, " Observation of lightning in the frequency and time domains ". SRI International, Electromagnetic Sciences Laboratory, Menlo Park, California 94025, USA.
2. Critec Pty. Ltd. "The control of lightning and power transients" publication number CR PN 01 B.
3. Jerry Sevick, " Transmission line transformers " ARRL publication.
4. Martin A. Uman, " The lightning discharge " International Geophysics Series, volume 39.
5. Marlin E Greer. " Negative Feedback Amplifiers " Murray State University, Murray, Kentucky 42071. R.F. Design May/ June 1984.
6. Heige O. Granberg, " Power MOSFETs versus bipolar transistors " Motorola application note AN-860.
7. Lou Danley, " Mounting Stripline-Opposed-Emitter (SOE) Transistors " Motorola application note AN-555.
8. Howard W. Sams & Co.,Inc. " Reference Data For Radio Engineers " Indianapolis, Indiana 46268. ISBN-0-672-21218-8.
9. A. H. Morton, " Advanced Electrical Engineering " ISBN-0-273-40172-6.
10. Octavius Pitzalis Jr and Thomas P. Couse, " Broadband Transformer Design For R.F. Transistor Power Amplifiers." Technical Report ECOM-2989 July 1968 U.S. Army Electronics Command, Fort Monmouth, New Jersey.
11. David N. Haupt, " Broadband Impedance-Matching Transformers as Applied to High Frequency Power Amplifiers. " Erbttec Engineering, Inc. 760 29th street, Boulder, Colorado 80301.

12. Steve Winder, "Single Tone Intermodulation Testing," R.F. Design, Dec. 1993.
13. James R. Huntsman, "Proper Shielding Protects ICs From Electrostatic Damage." Electronics/14 July 1982.

## 8. Figures.

### 8.1. List of figures.

1. Test circuits used to measure  $r_a$  and input shunt Miller resistance.
2. Smith chart highlighting the effects of  $R_i$ .
3. Test set up employed to measure harmonic output.
4. Test set up employed to measure  $OPI_p^3$ .
5. Harmonic output class A 8MHz 10 watts.
6. Harmonic output class AB 8MHz 10 watts.
7. Harmonic output class A 8MHz 5 watts.
8. Harmonic output class AB 8MHz 5 watts.
9. 2MHz 7th order 0.1dB H.P. Chebyshev filter.
10. 70MHz 5th order 0.1dB L.P. Chebyshev filter.
11. Standard push/pull amplifier.
12. Basic output matching network.
13. Basic circuit of power amplifier.
14. Basic circuit common mode operation.
15. Final design of 10 watt module.
16. Smith chart showing  $Z_{in}$  and  $Z_{out}$  of 10 watt module.
17. 5Mhz harmonic content at 10 watts output.
18. 30MHz harmonic content at 10 watts output.
19. 60MHz harmonic content at 10 watts output.
20. R.F. pre-amp and driver circuit.
21. 2-70MHz bandpass filter.
22.  $\Delta$ Gain/frequency for complete 10 watt amplifier.
23. 8MHz  $OPI_p^3$  at +30dBm/ tone.

24. 65MHz OIP<sub>3</sub> at +30dBm/ tone.
25. Block diagram of 50 watt amplifier.
26. R.F. pre-amp, driver and splitter/combiner 50 watt amplifier.
27. 2-70MHz power amplifier 50 watt amplifier.
28. Smith chart of Z<sub>in</sub> from 2-70MHZ 50 watt amplifier.
29. Smith chart of Z<sub>out</sub> from 2-70MHz 50 watt amplifier.
30. 50 watt amplifier 8MHz 10 watt output harmonics.
31. 50 watt amplifier 8MHz 50 watt output harmonics.
32. 50 watt amplifier 8MHz OIP<sub>3</sub> at +30dBm/ tone.
33. 50 watt amplifier 60MHz OIP<sub>3</sub> at +30dBm/ tone.
34. 50 watt amplifier 8MHz OIP<sub>3</sub> at +40dBm/ tone.
35. 50 watt amplifier 60MHz OIP<sub>3</sub> at +40dBm/ tone.
36. 50 watt amplifier gain variation 2-70MHz at +47dBm.
37. Test set up to simulate large induced differential voltages.

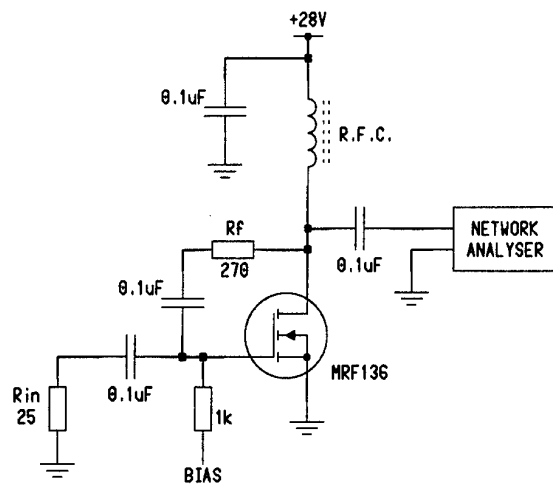


Fig 1A

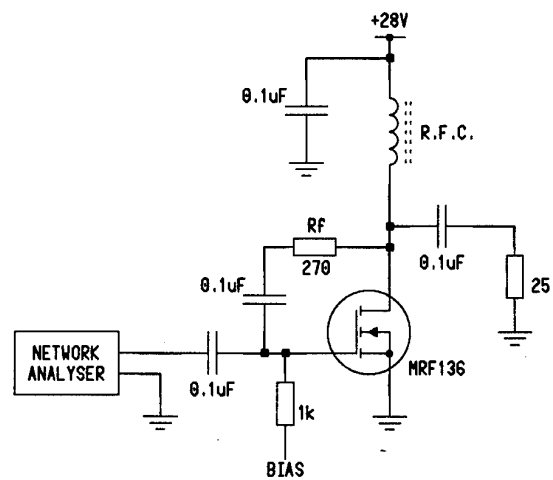
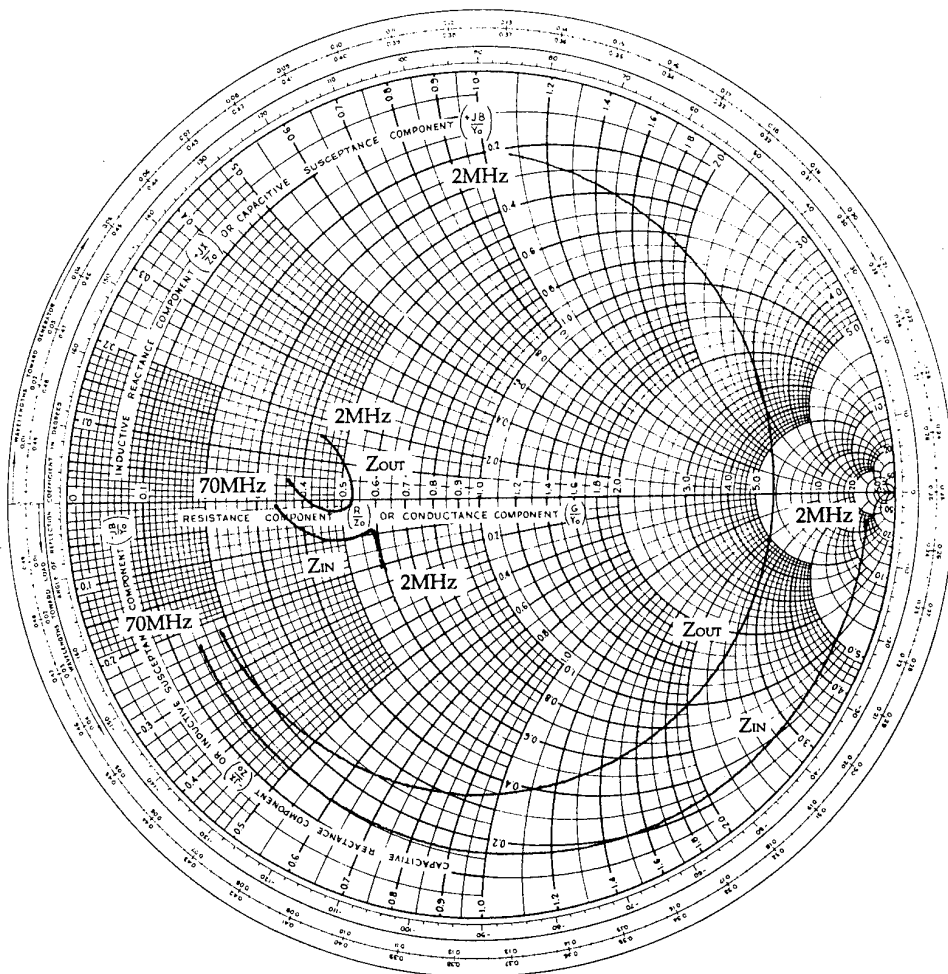
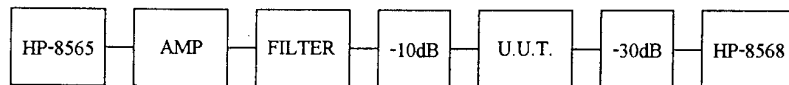


Fig 1B

Test circuits used to measure  $r_d$  and  
input shunt Miller resistance



**Fig.2** Smith chart highlighting the effects of  $R_f$ .



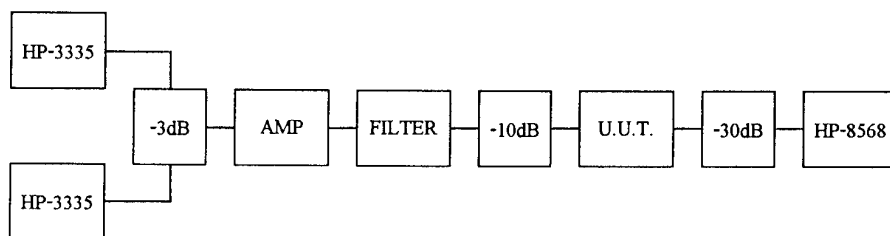
HP-8565 = R.F. SIG. GEN  
 HP-8568 = SPECTRUM ANALYSER  
 FILTER = LOW PASS  $F_c$  AS REQUIRED

U.U.T. = UNIT UNDER TEST

AMP = +40dB GAIN  
 $OPIp^3$  +60dBm  
 $OPIp^2$  +95dBm

### HARMONIC TEST CONFIGURATION

FIG. 3



HP-3335 = R.F. SIG. GEN  
 HP-8568 = SPECTRUM ANALYSER  
 FILTER = LOW PASS  $F_c$  AS REQUIRED

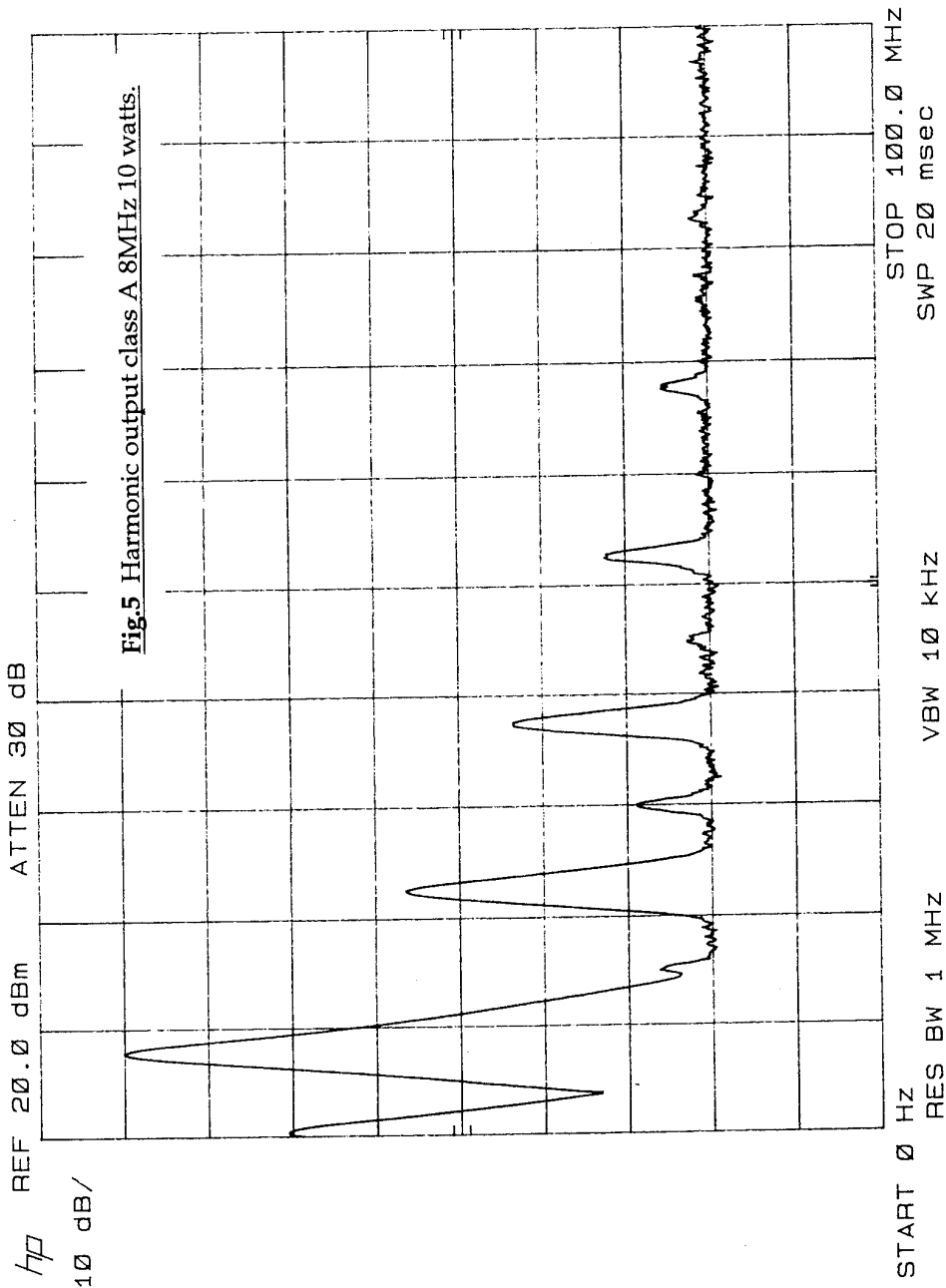
U.U.T. = UNIT UNDER TEST

AMP = +40dB GAIN  
 $OPIp^3$  +60dBm  
 $OPIp^2$  +95dBm

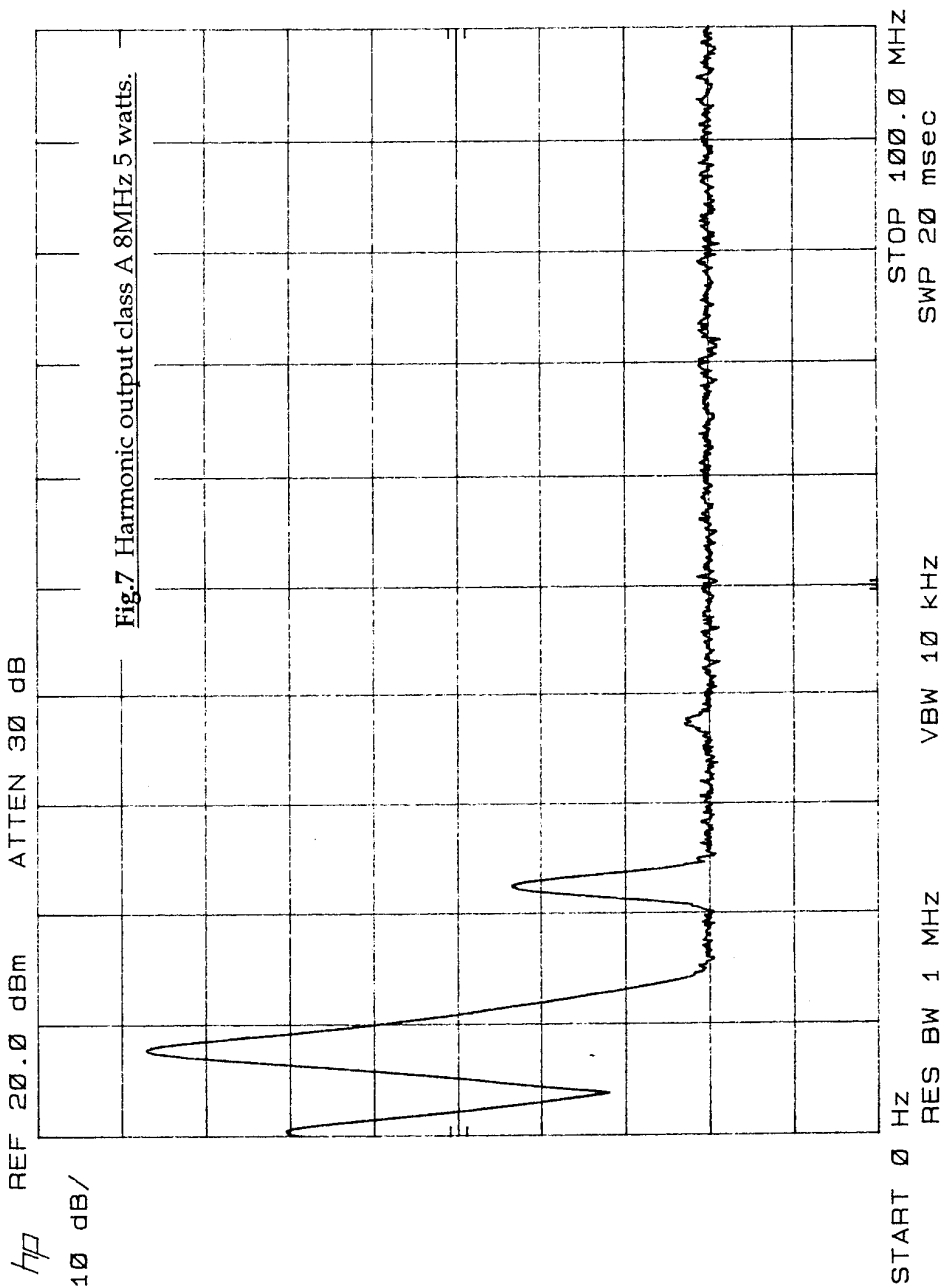
### OPIp<sup>3</sup> TEST CONFIGURATION

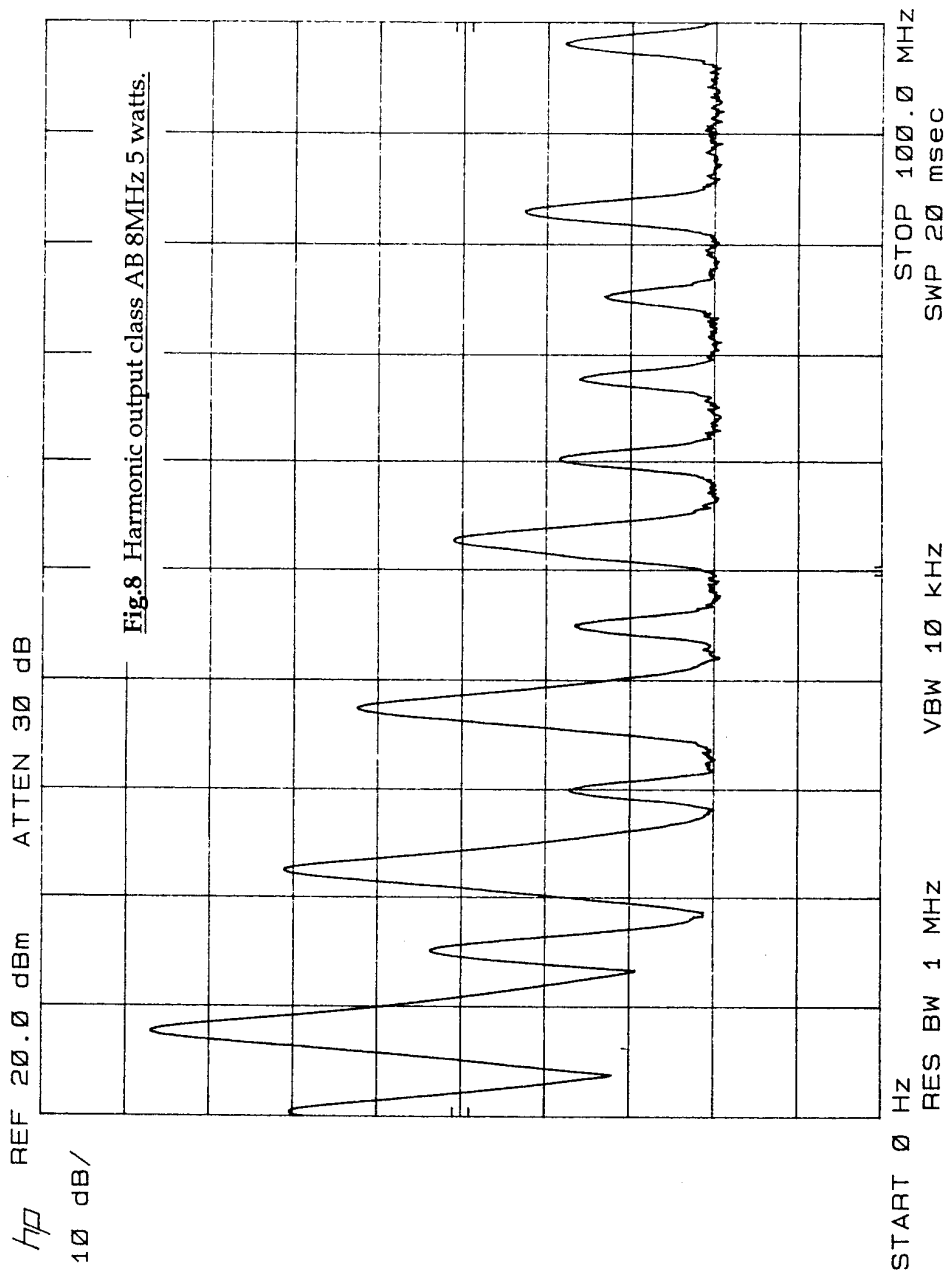
FIG. 4











Filter Order	:	=	7
3dB Frequency (KHz)	:	=	1800.000
Source Resistance (Ohms)	:	=	50
Load Resistance (Ohms)	:	=	50
Series C Values (uF)	:	C2 =	0.001164
	:	C4 =	0.001052
	:	C6 =	0.001164
Shunt L Values (mH)	:	L1 =	0.003505
	:	L3 =	0.001974
	:	L5 =	0.001974
	:	L7 =	0.003505

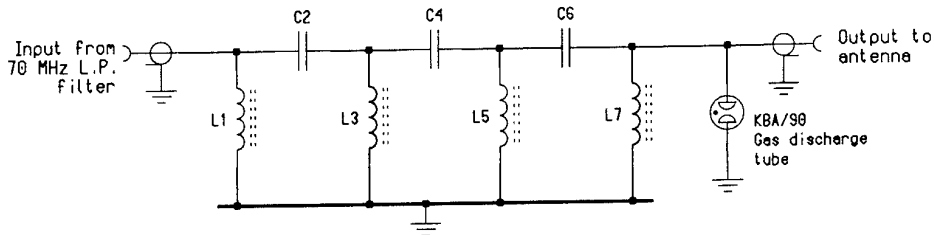


Fig 9

2MHz 7th order 0.1dB H.P. chebyshev filter

Filter Order	:	=	5
3dB Frequency (KHz)	:	=	75000.000
Source Resistance (Ohms)	:	=	50
Load Resistance (Ohms)	:	=	50
Series L Values (mH)	:	L1 =	0.00165
	:	L2 =	0.00165
Shunt C Values (uF)	:	C1 =	0.000055
	:	C3 =	0.000095
	:	C5 =	0.000055

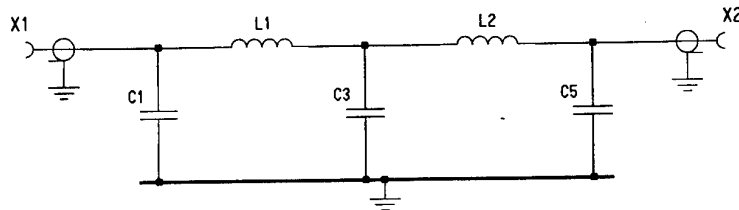


Fig 10

70MHz 5th order 0.1dB L.P. chebyshev filter

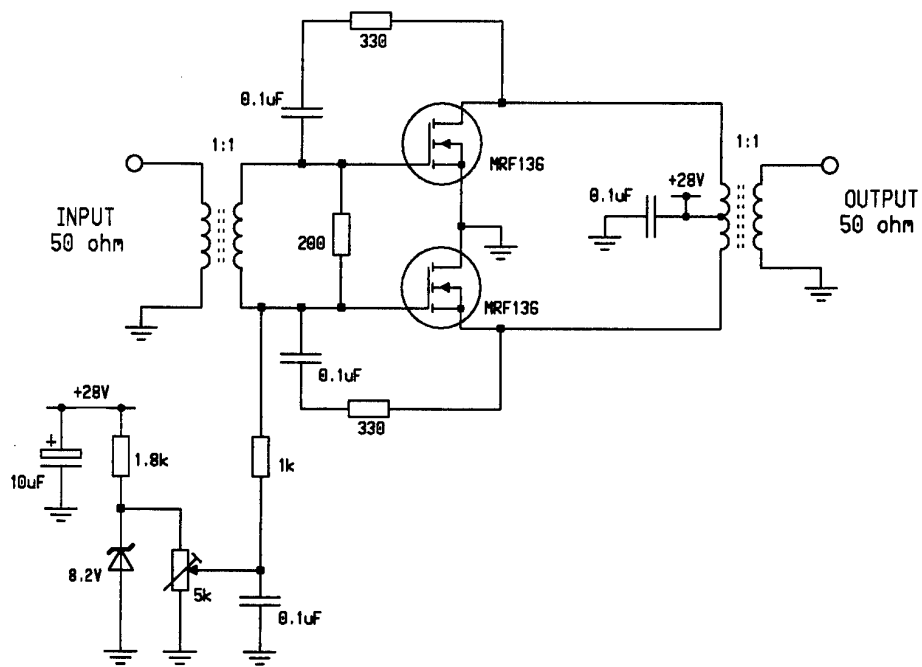


Fig 11

Standard push/pull amplifier

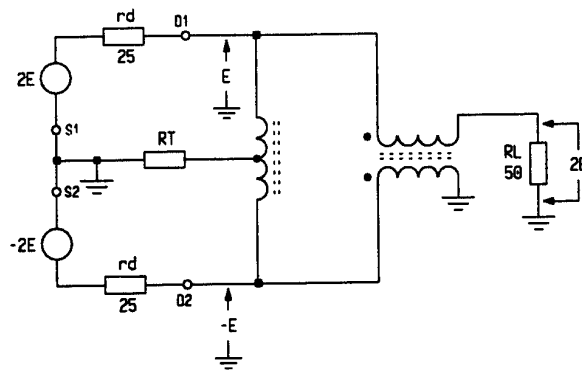


Fig 12a

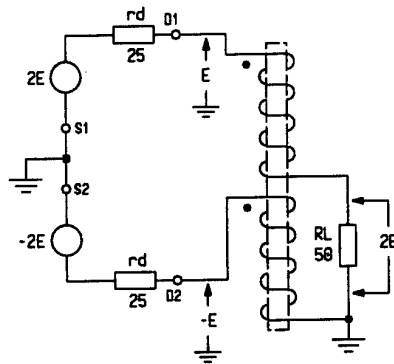


Fig 12b

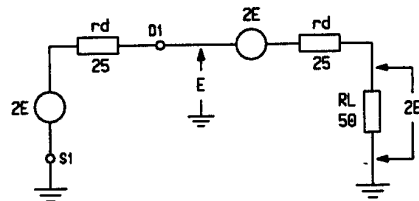


Fig 12c

Basic output matching network

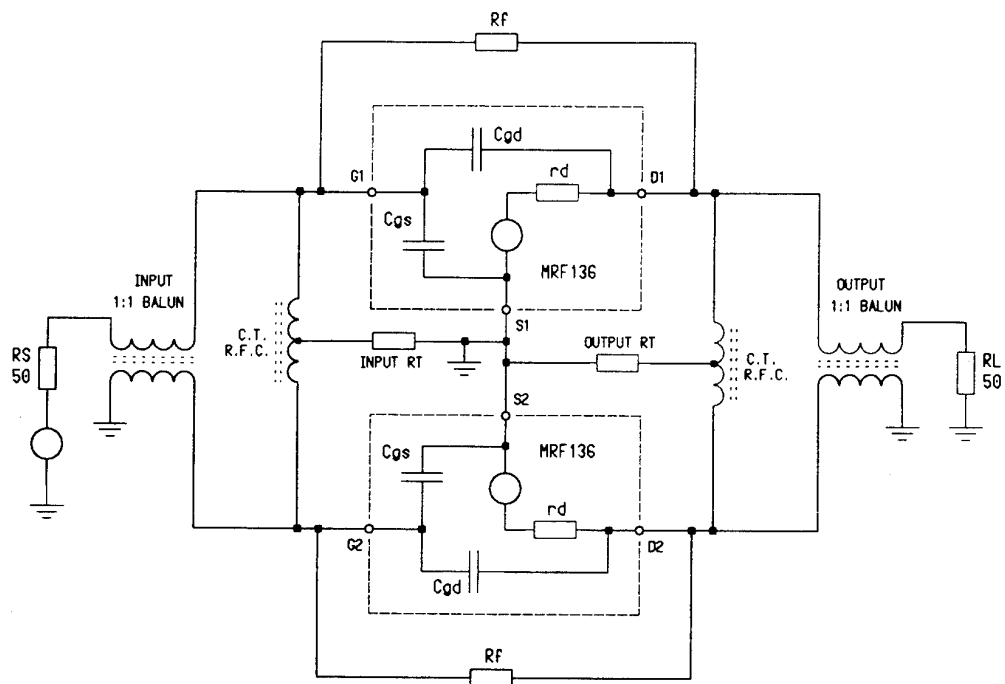


Fig 13

Basic circuit of power amplifier



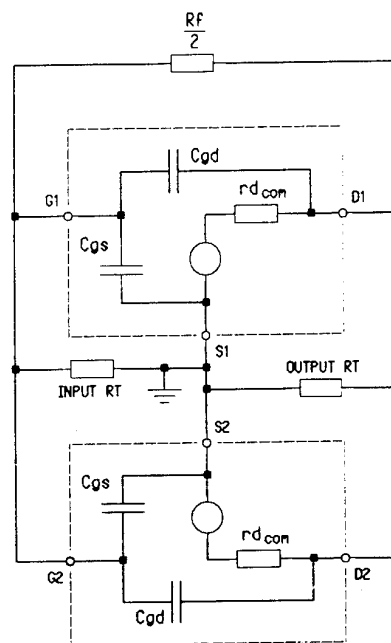
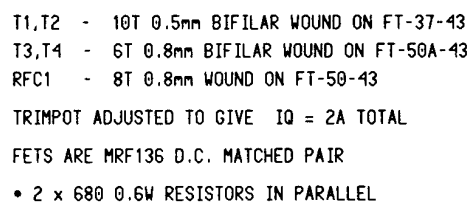


Fig 14

Basic circuit common mode operation



### Final design of 10 watt module

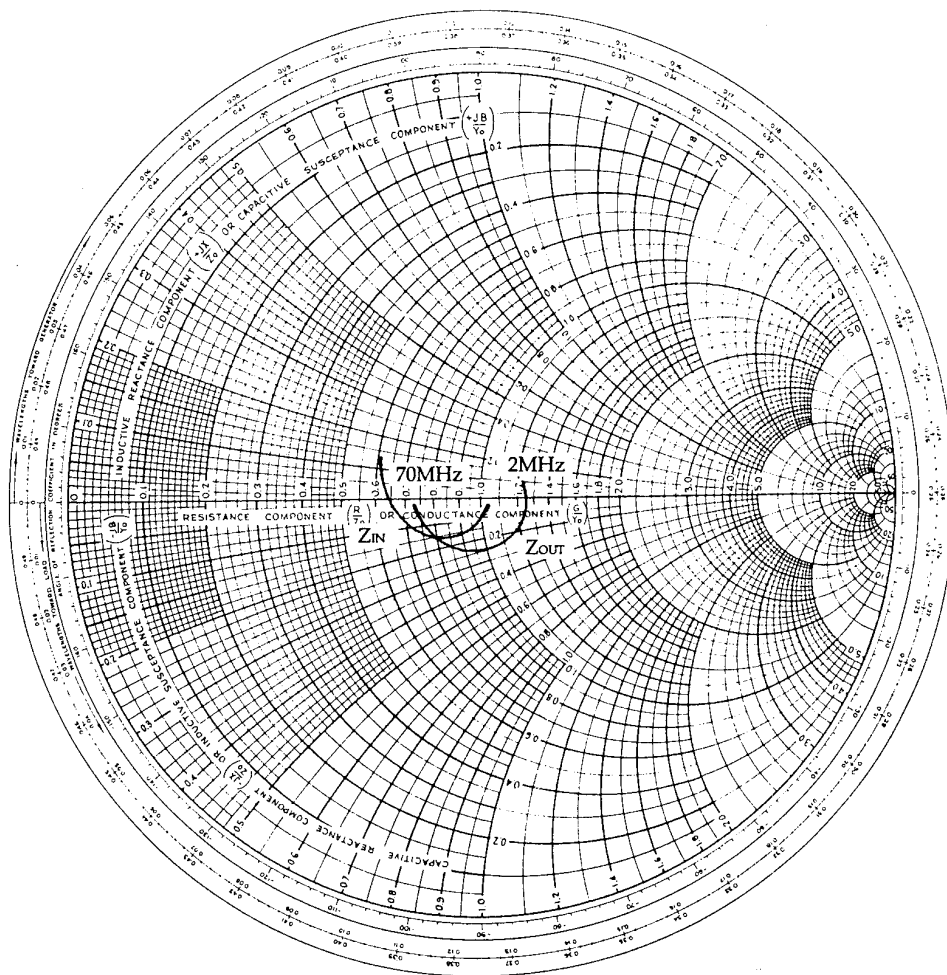
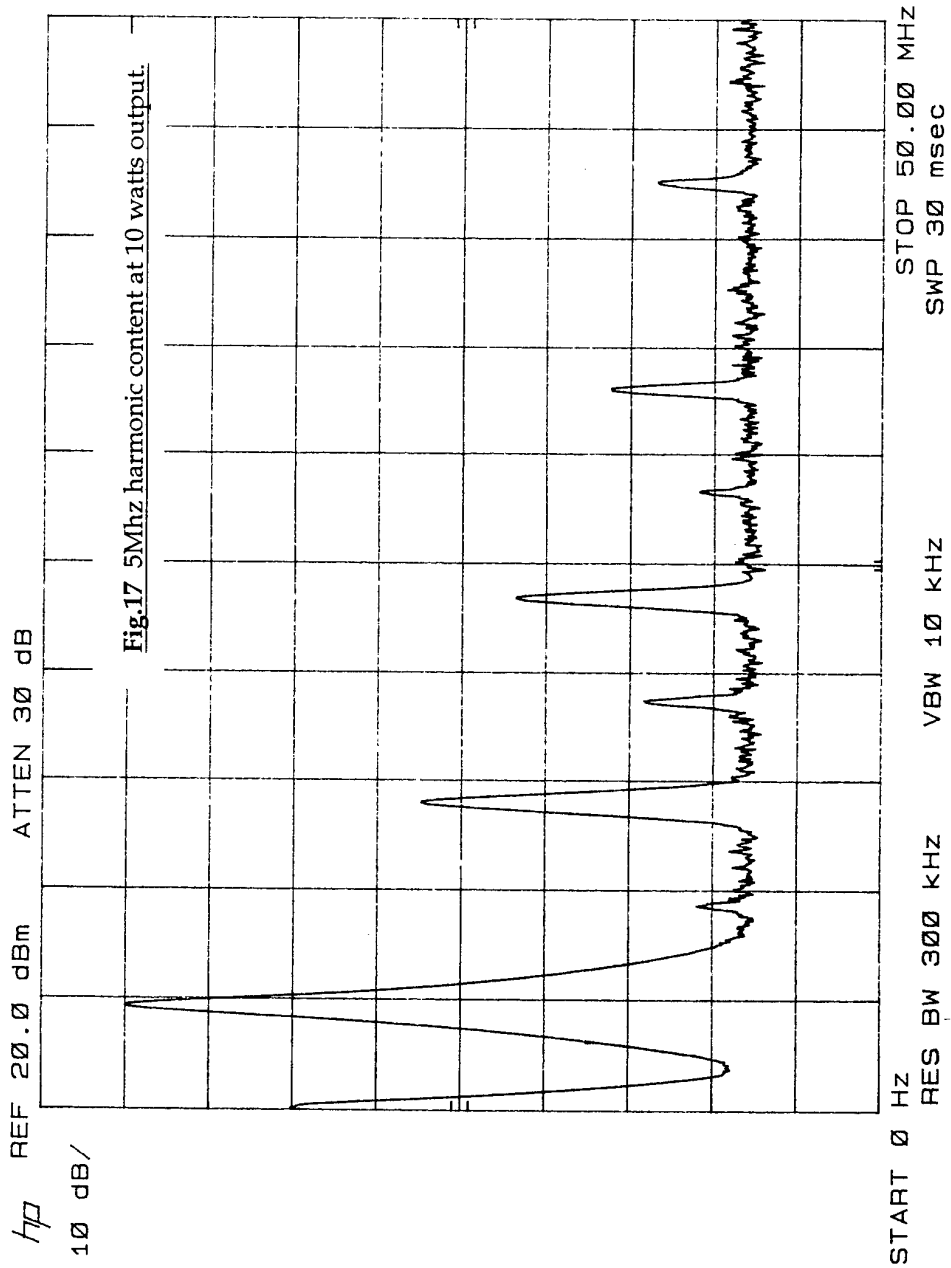
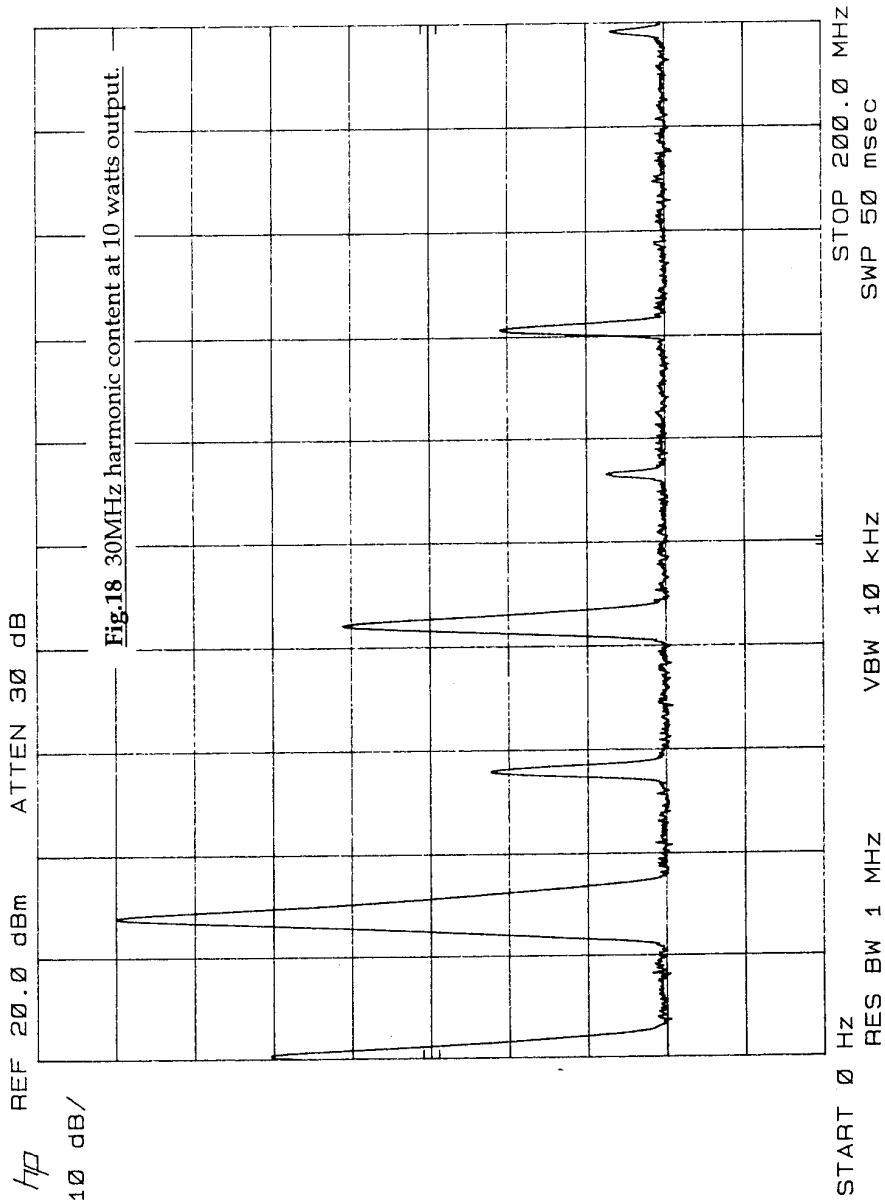


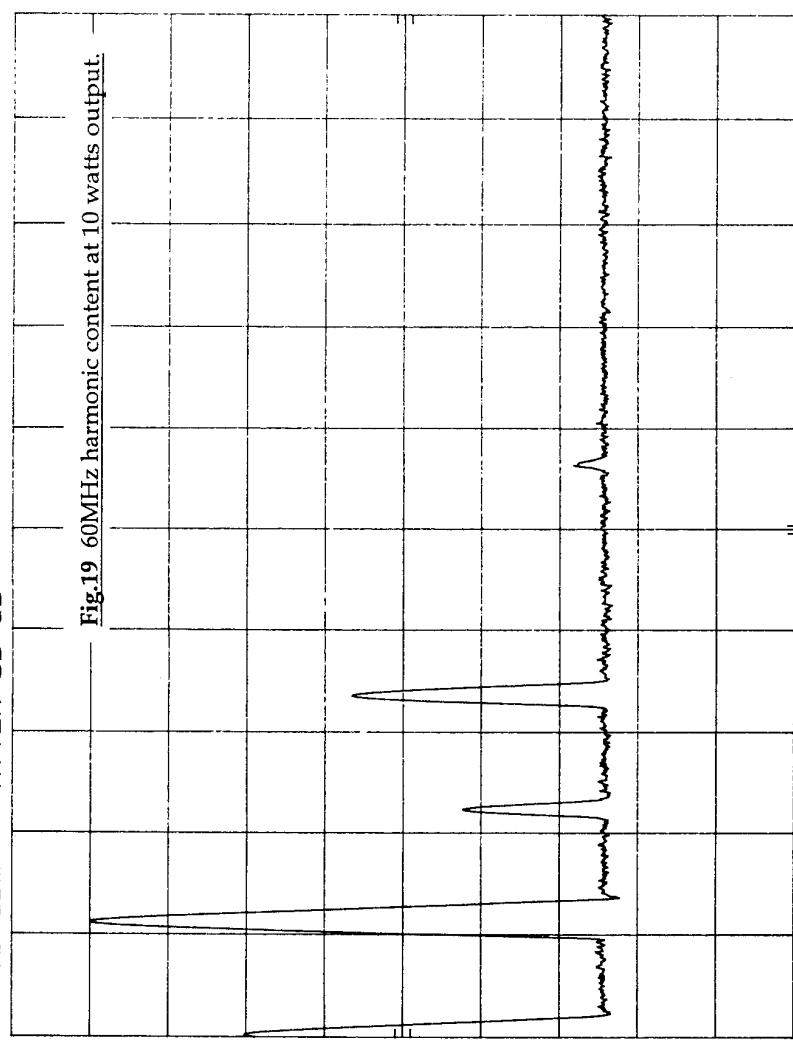
Fig.16 Smith chart showing  $Z_{in}$  and  $Z_{out}$  of 10 watt module.





hp REF 20.0 dBm ATTEN 30 dB

10 dB/



START 0 HZ RES BW 3 MHz VBW 10 KHZ STOP 500.0 MHz SWP 30 msec



3.16uH - 25T 0.8mm on T-80-6  
 1.8uH - 18T 0.8mm on T-80-6  
 172nH - 7T 1.0mm on 7mm Dia AIRCORE

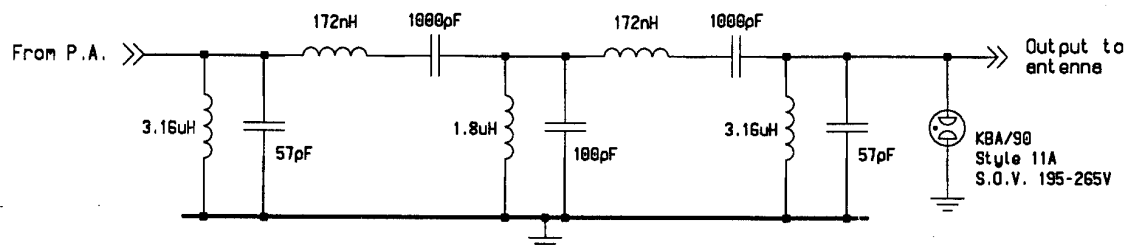


Fig 21

2-70MHz bandpass filter



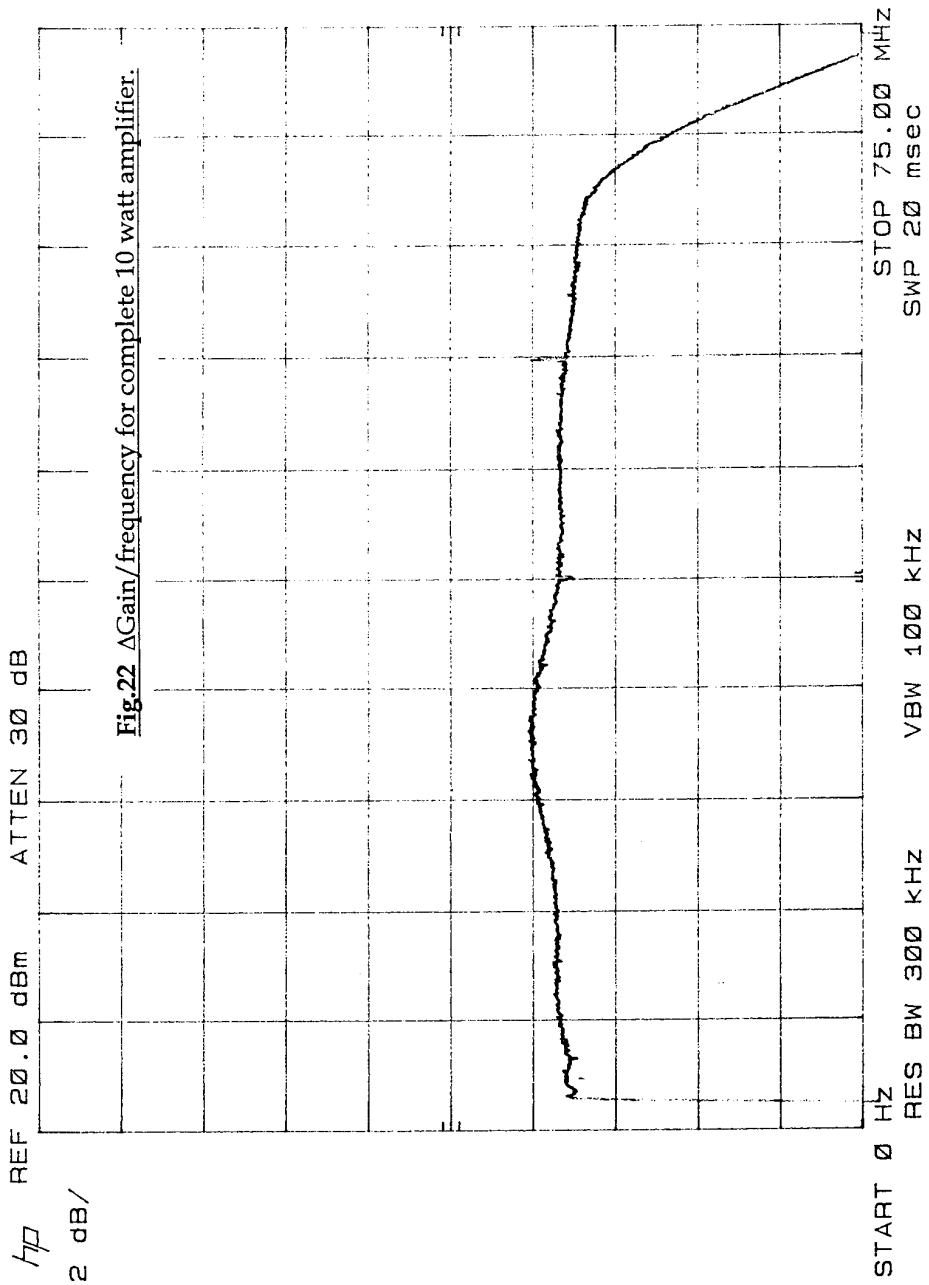
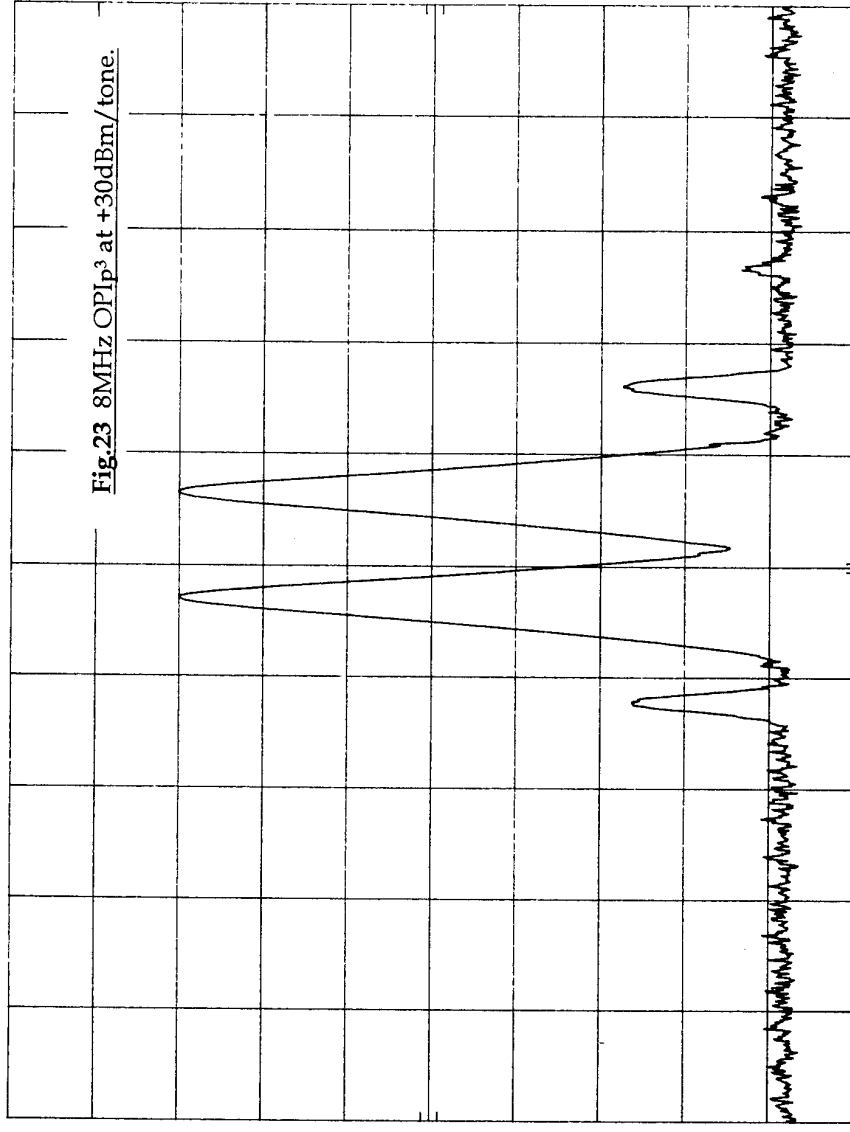
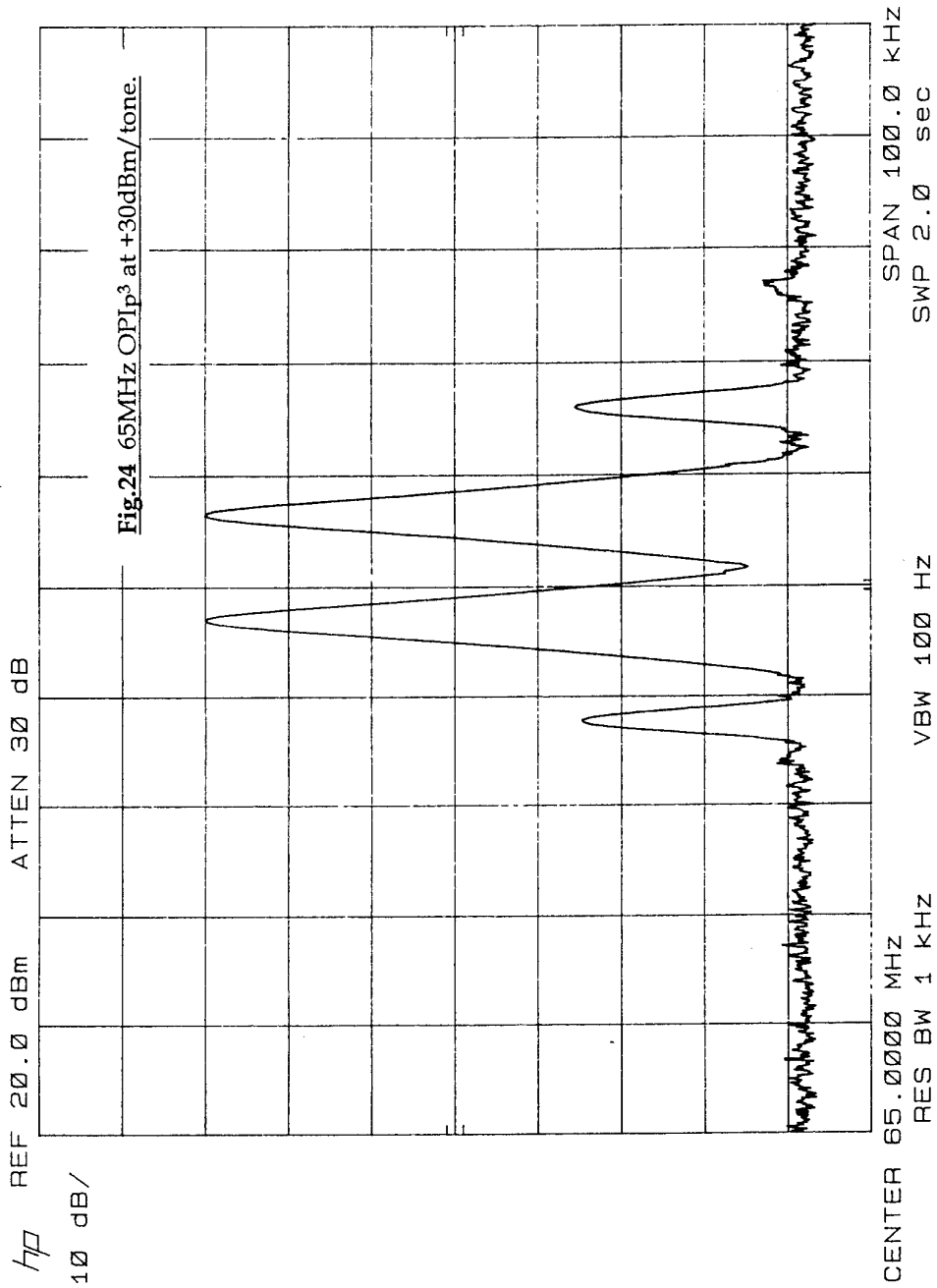


Fig.22  $\Delta$ Gain/frequency for complete 10 watt amplifier.

hp REF 20.0 dBm ATTEN 30 dB  
10 dB/



CENTER 8.0000 MHz  
RES BW 1 kHz  
SPAN 100.0 kHz  
SWP 2.0 sec  
VBW 100 Hz



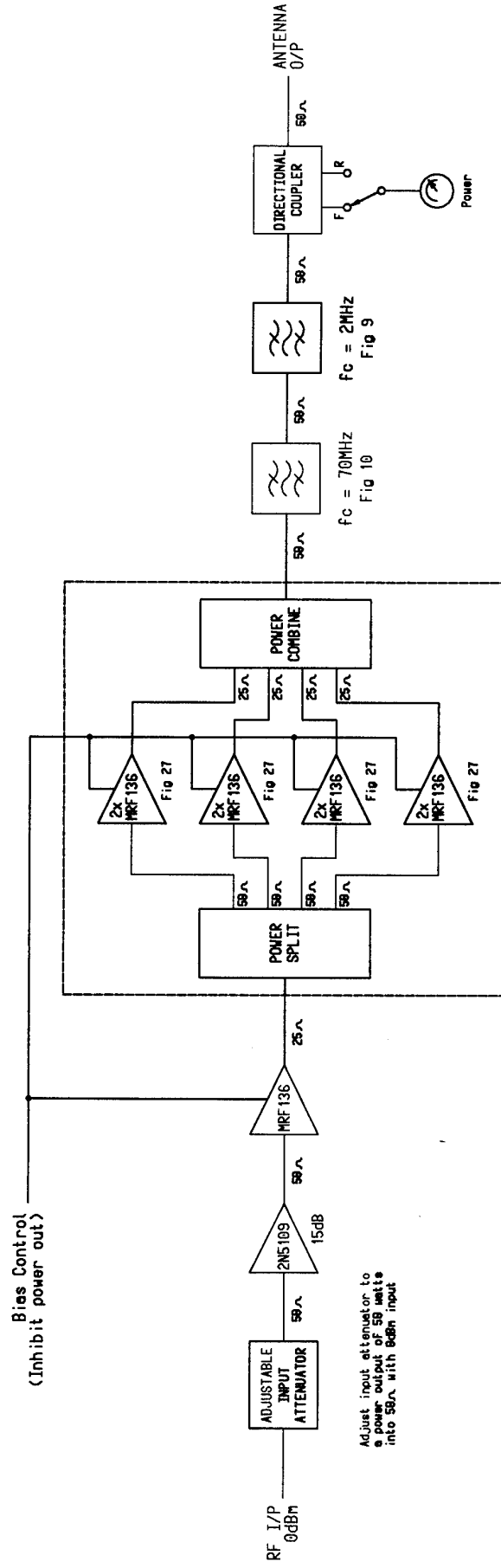


Fig 25

Block diagram of 50 watt transmitter

- T1, T2 - 24T 39 SWG ECH BIFILAR WOUND ON FT-23-43 TOROIDAL CORE, SECONDARY 2T  
 T3 - 14T 0.4mm ECH BIFILAR WOUND ON FT-37-61 TOROIDAL CORE  
 RFC1 - 4T 0.4mm ECH WOUND ON Fx2249 FERRITE CORE  
 RFC2 - 28T 0.4mm ECH WOUND ON FT-37-61 TOROIDAL CORE

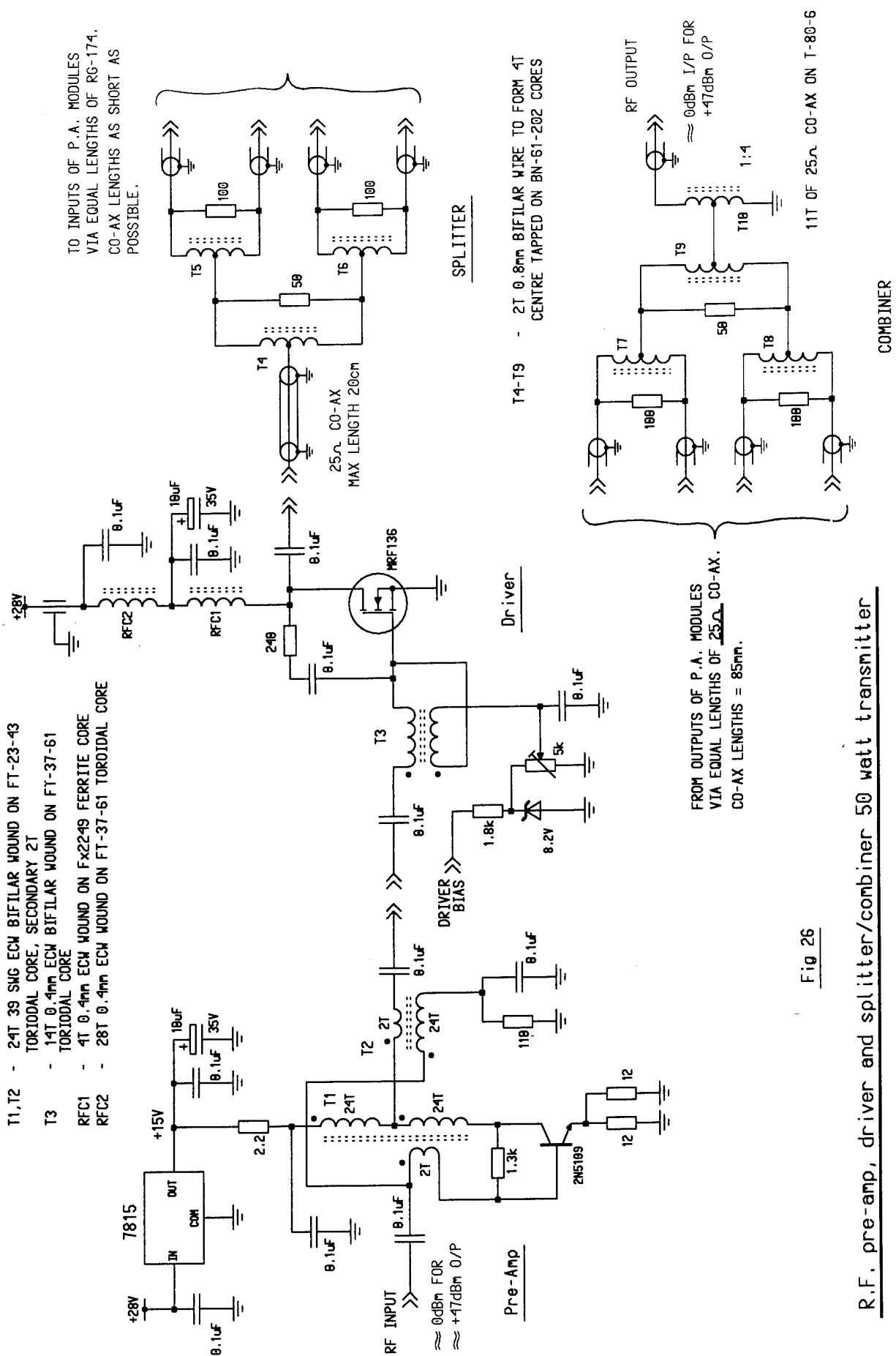
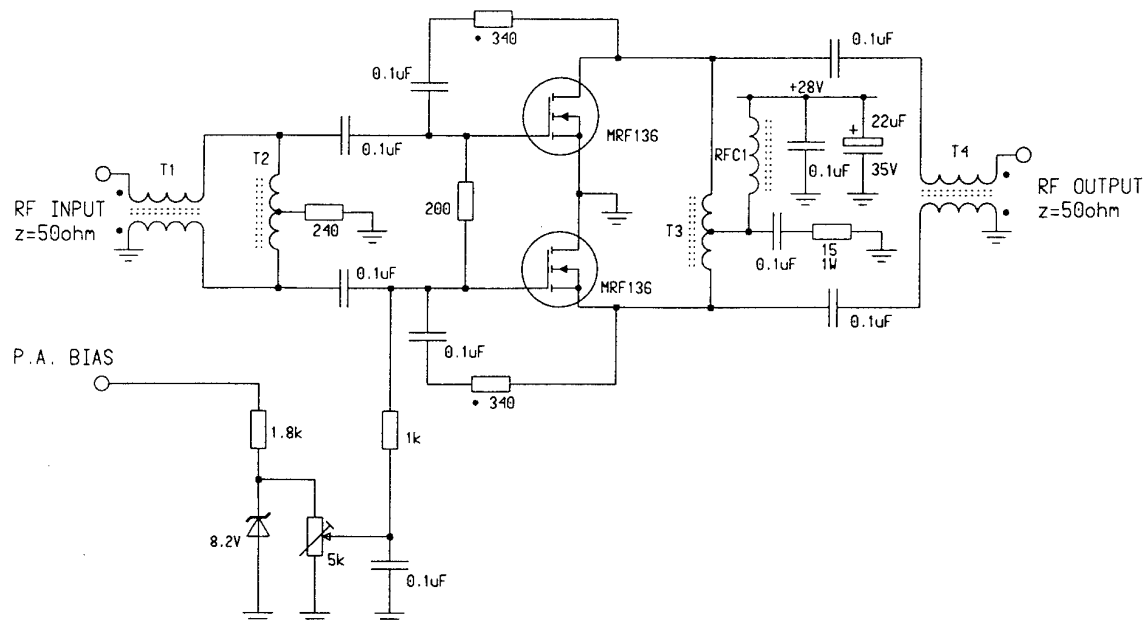


Fig 26

R.F. pre-amp, driver and splitter/combiner 50 watt transmitter



T1,T2 - 10T 0.5mm BIFILAR WOUND ON FT-37-43  
 T3,T4 - 6T 0.8mm BIFILAR WOUND ON FT-50A-43  
 RFC1 - 8T 0.8mm WOUND ON FT-50-43

TRIMPOT ADJUSTED TO GIVE TOTAL  $I_Q = 2A$

FETS ARE MRF136 D.C. MATCHED PAIR

• 2 x 680 0.6W RESISTORS IN PARALLEL

Fig 27

2-70MHz power amplifier 50 watt transmitter

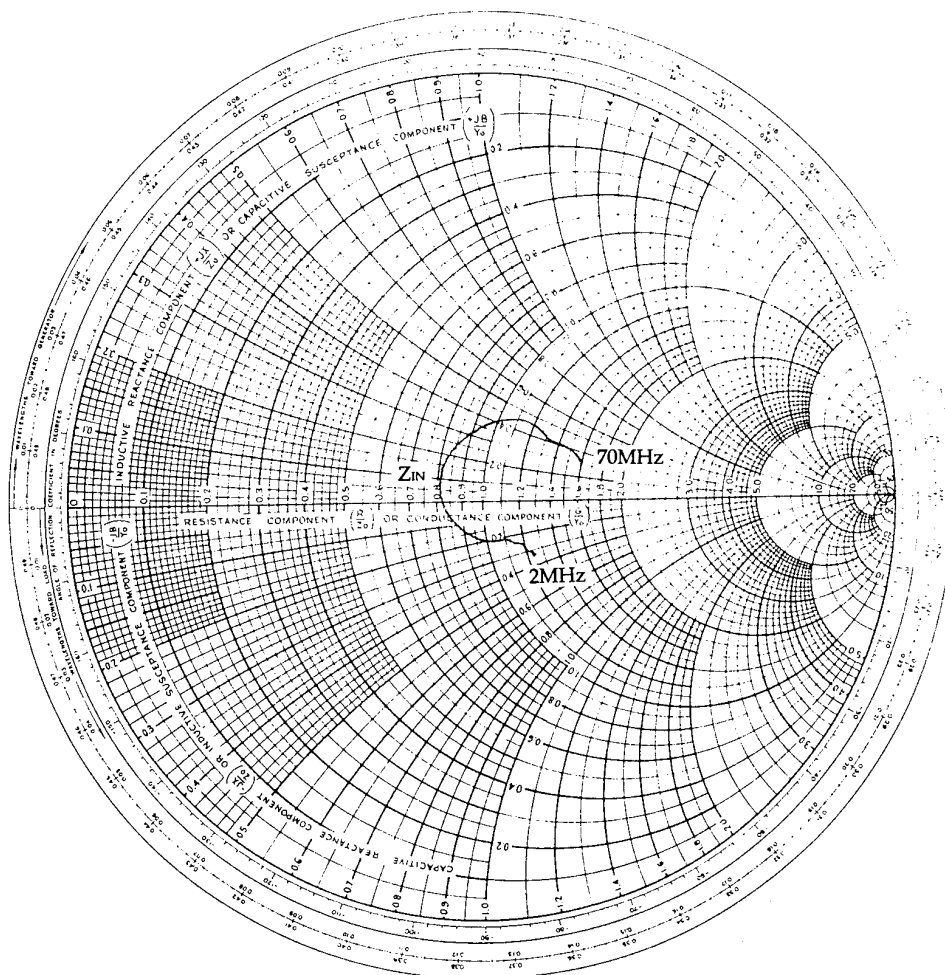


**Fig.28** Smith chart of  $Z_{in}$  from 2-70MHZ 50 watt amplifier.

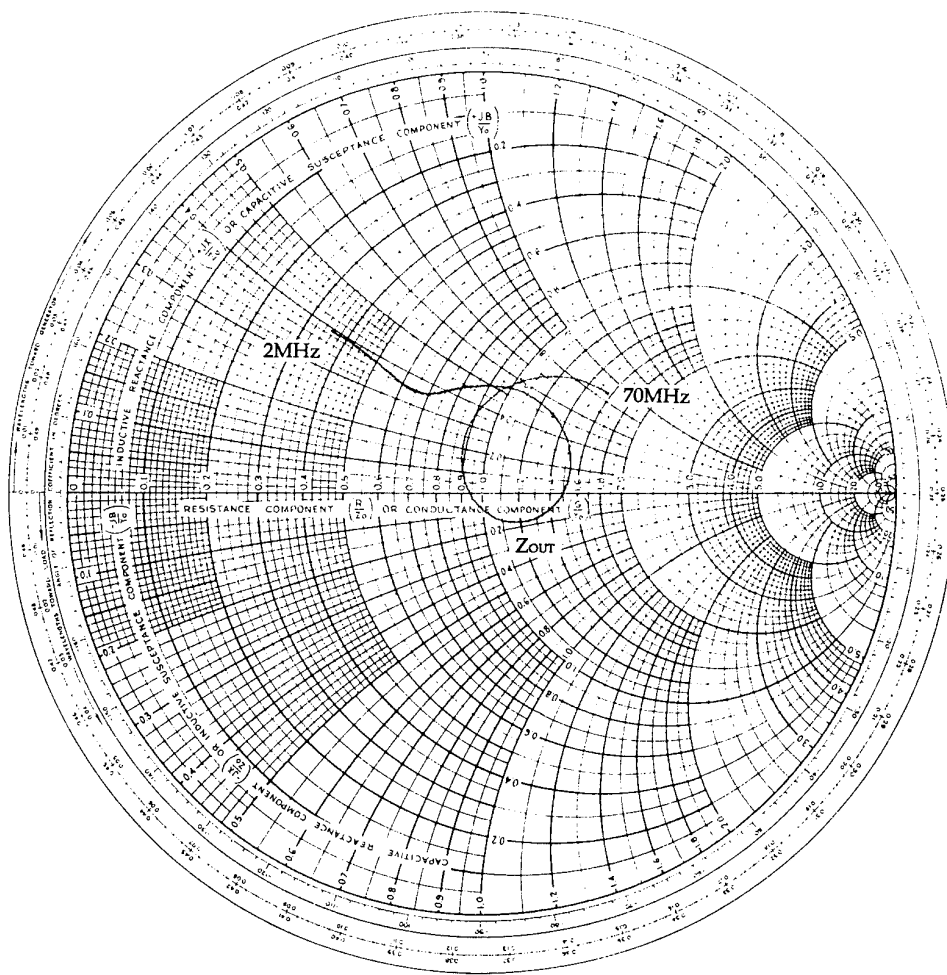
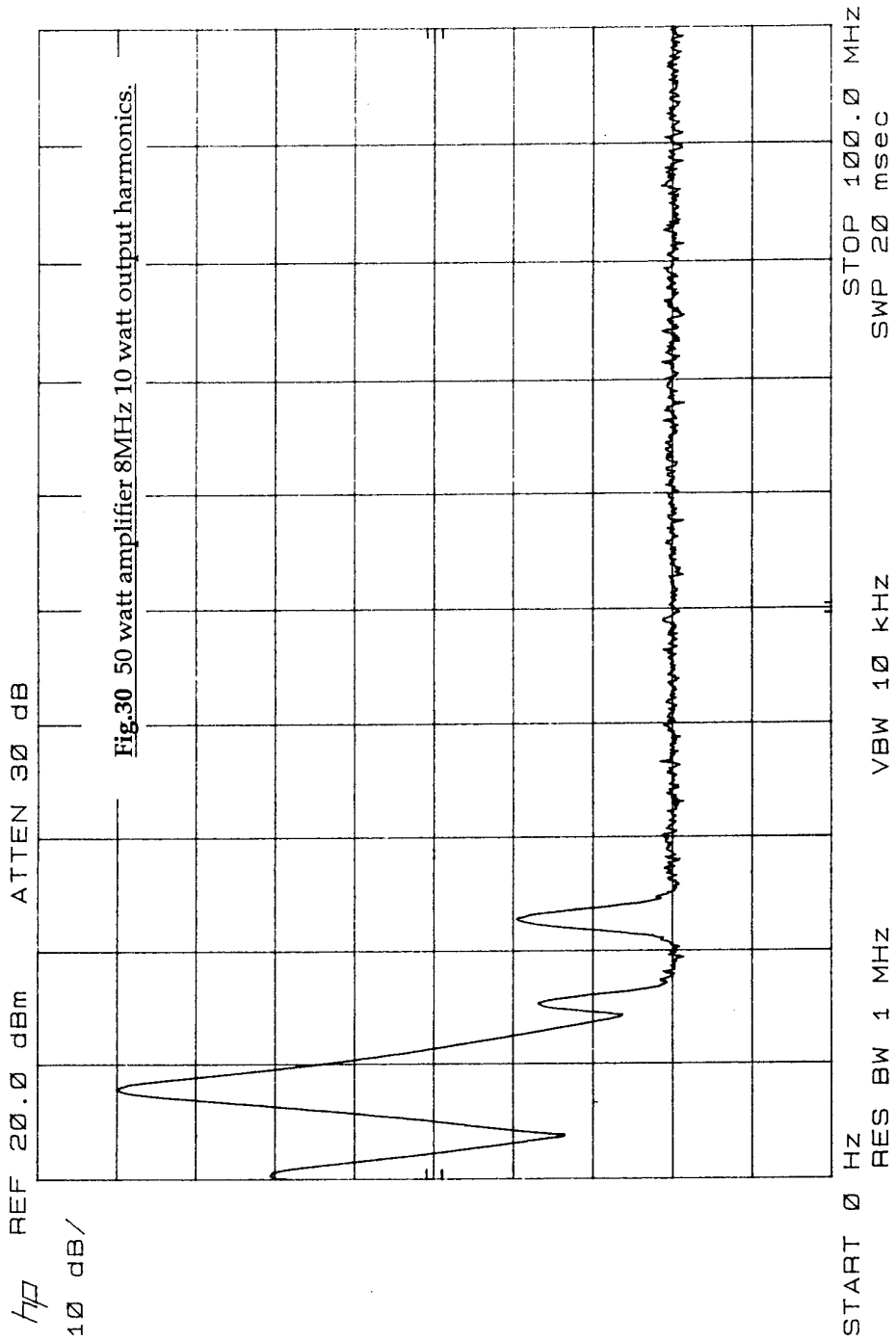
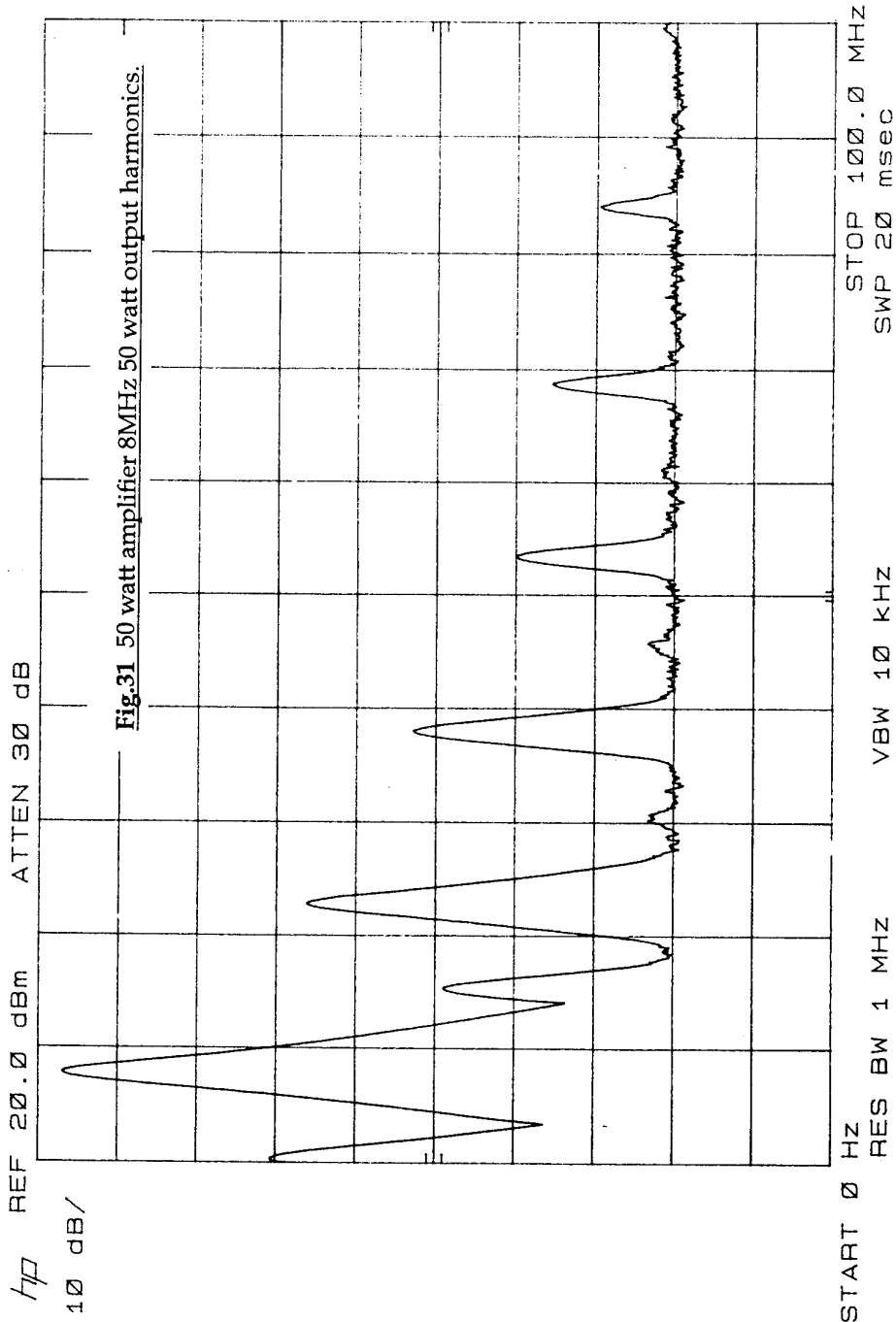
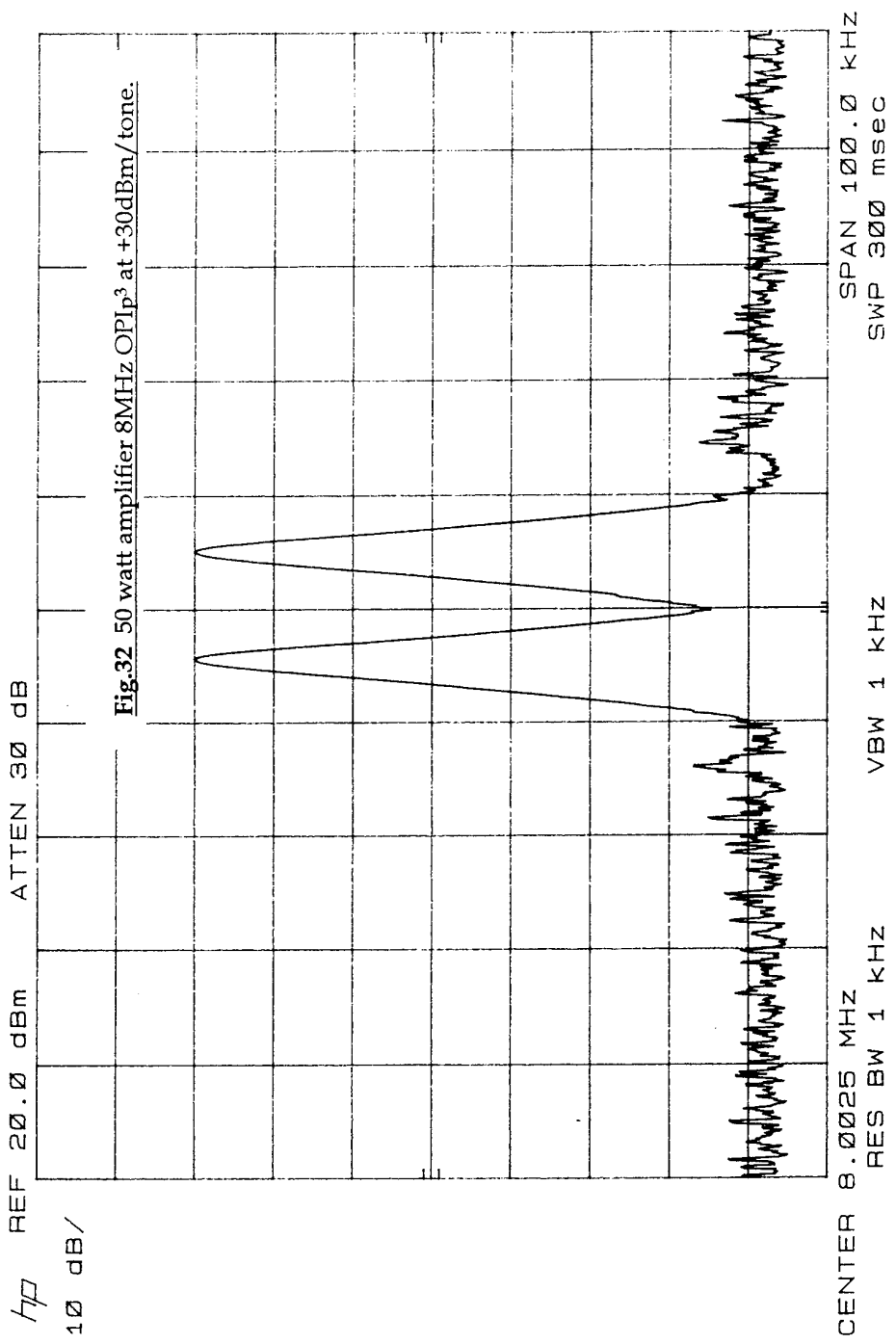


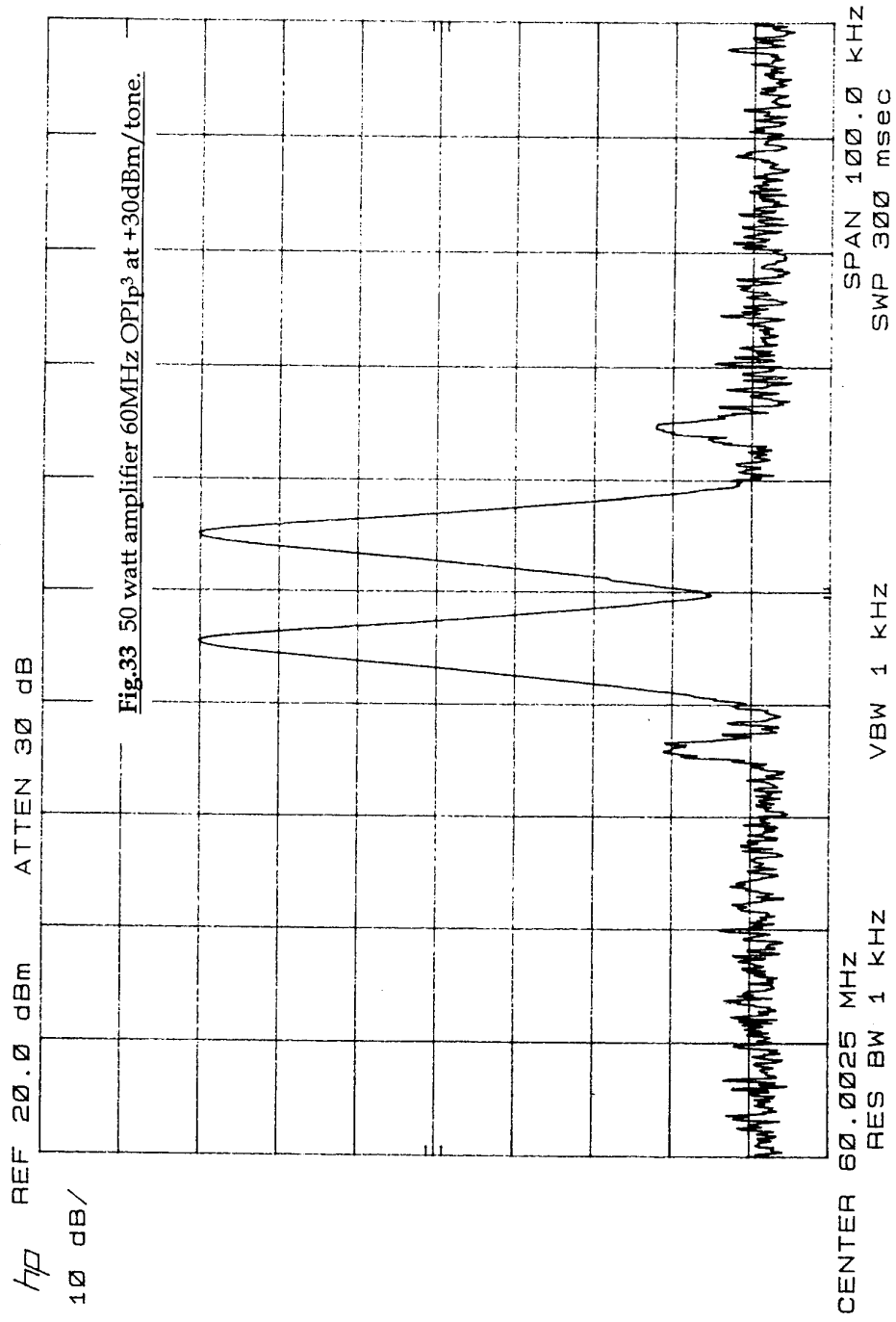
Fig.29 Smith chart of  $Z_{out}$  from 2-70MHz 50 watt amplifier.

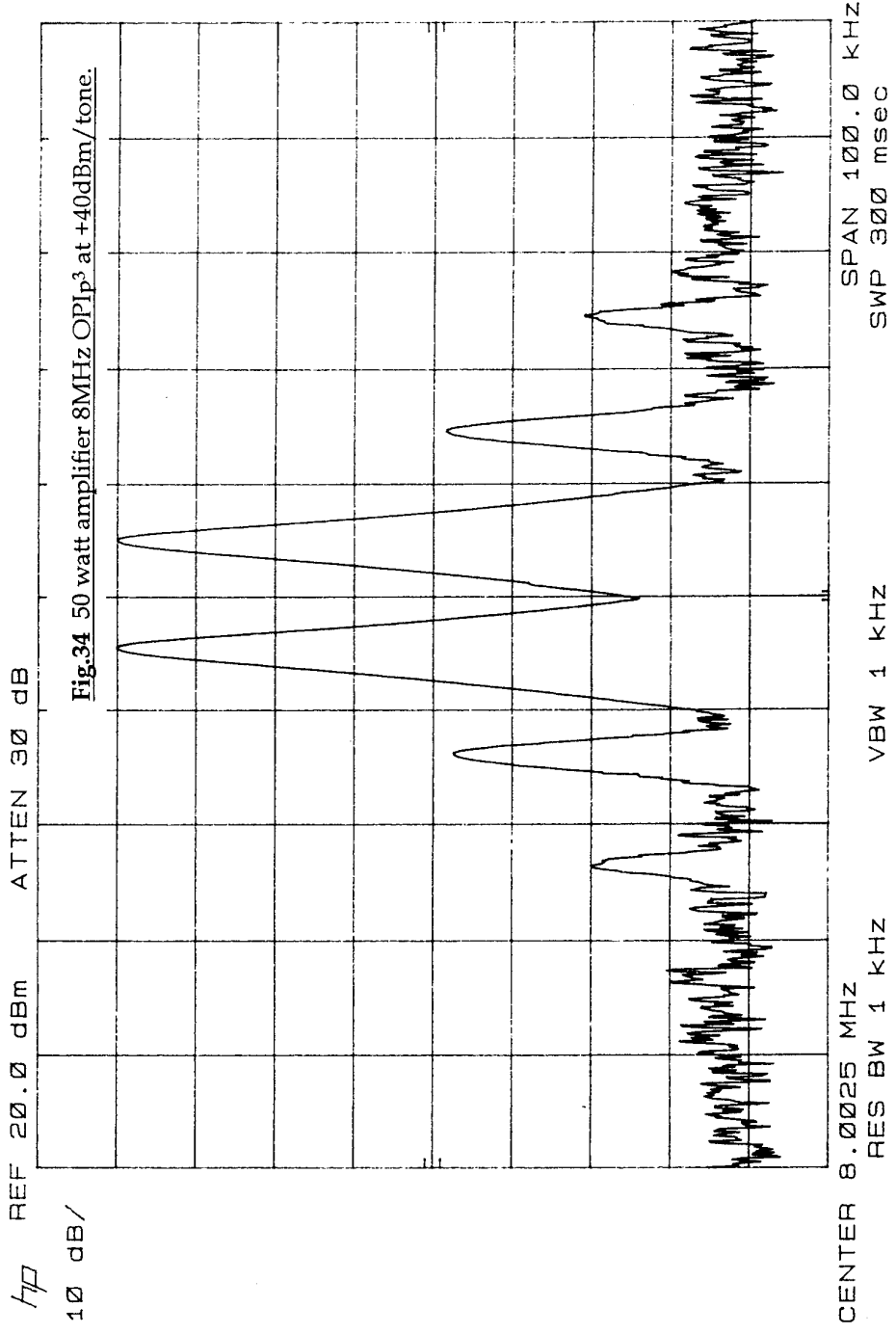


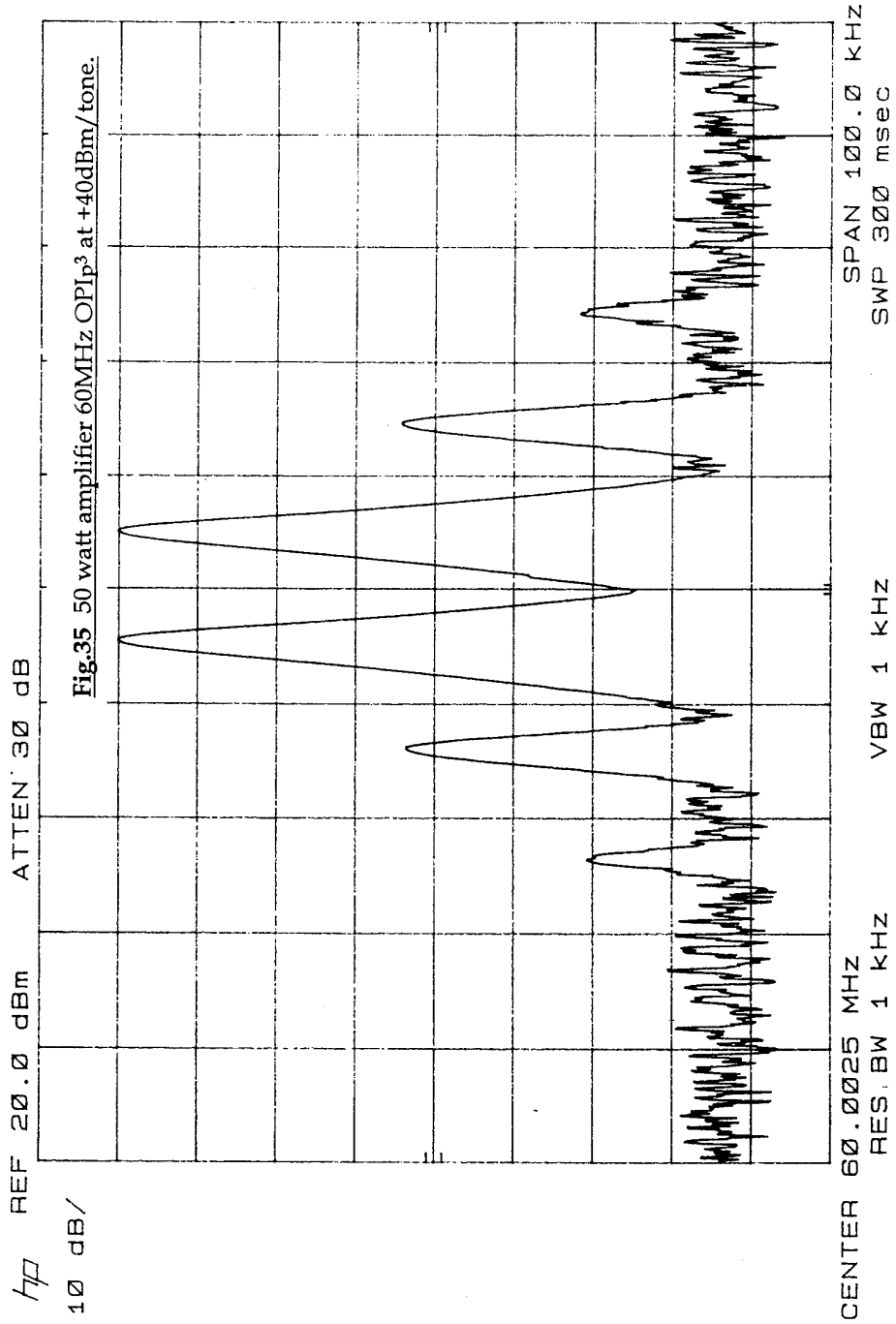


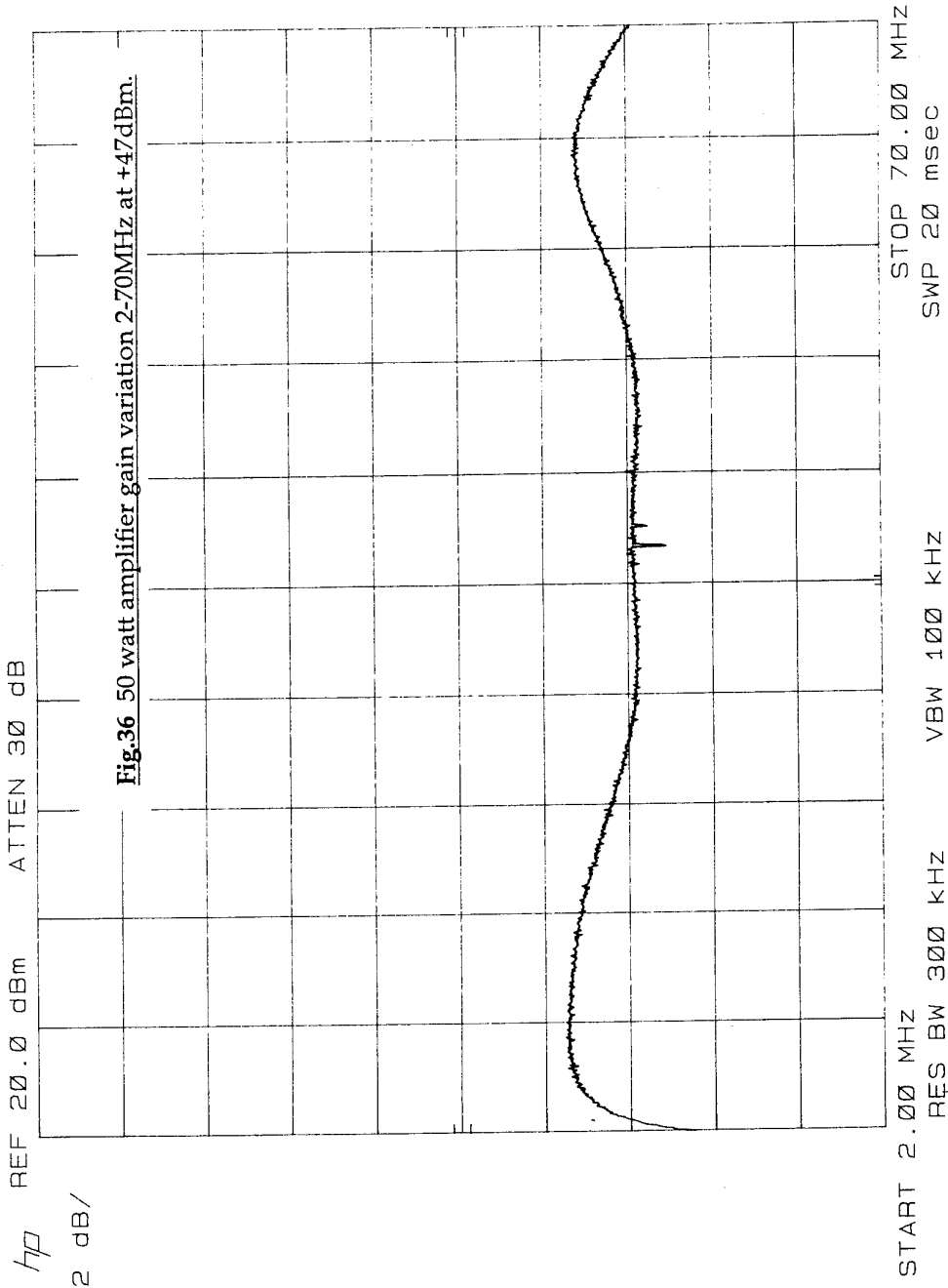












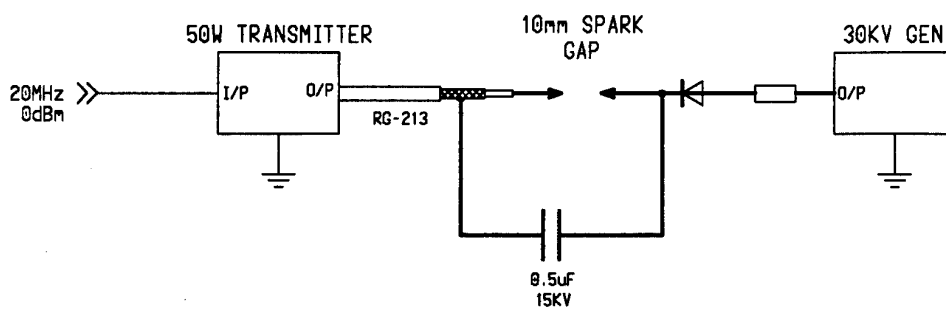


Fig 37

Test setup to simulate large induced differential voltages



**THIS PAGE IS INTENTIONALLY BLANK**

# APPENDIX

Motorola Semiconductor Data Sheets

MRF136

**MOTOROLA**  
**SEMICONDUCTOR**  
**TECHNICAL DATA**

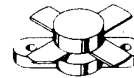
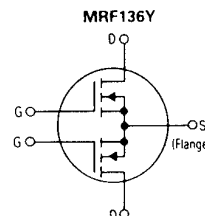
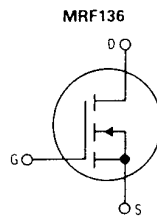
**The RF TMOS Line**  
**RF Power Field-Effect Transistors**  
**N-Channel Enhancement-Mode TMOS**

**MRF136**  
**MRF136Y**

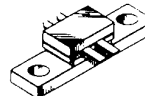
15 W, 30 W 2-400 MHz  
 N-CHANNEL  
 TMOS BROADBAND  
 RF POWER FETs

... designed for wideband large-signal amplifier and oscillator applications in the 2 to 400 MHz range, in either single ended or push-pull configuration.

- Guaranteed 28 Volt, 150 MHz Performance
- **MRF136**  
 Output Power = 15 Watts  
 Narrowband Gain = 16 dB (Typ)  
 Efficiency = 60% (Typical)
- **MRF136Y**  
 Output Power = 30 Watts  
 Broadband Gain = 14 dB (Typ)  
 Efficiency = 54% (Typical)
- Small-Signal and Large-Signal Characterization
- 100% Tested For Load Mismatch At All Phase Angles With 30:1 VSWR
- Space Saving Package For Push-Pull Circuit Applications — MRF136Y
- Excellent Thermal Stability, Ideally Suited For Class A Operation
- Facilitates Manual Gain Control, ALC and Modulation Techniques



MRF136  
 CASE 211-07



MRF136Y  
 CASE 319B-01

**MAXIMUM RATINGS**

Rating	Symbol	Value		Unit
		MRF136	MRF136Y	
Drain-Source Voltage	$V_{DS}$	65	65	Vdc
Drain-Gate Voltage ( $R_{GS} = 1 \text{ M}\Omega$ )	$V_{DGR}$	65	65	Vdc
Gate-Source Voltage	$V_{GS}$	$\pm 40$		Vdc
Drain-Current — Continuous	$I_D$	2.5	5	Adc
Total Device Dissipation (at $T_C = 25^\circ\text{C}$ Derate above $25^\circ\text{C}$ )	$P_D$	55 0.314	100 0.571	Watts W/ $^\circ\text{C}$
Storage Temperature Range	$T_{stg}$	-65 to +150		$^\circ\text{C}$
Operating Junction Temperature	$T_J$	200		$^\circ\text{C}$

**THERMAL CHARACTERISTICS**

Characteristic	Symbol	Max		Unit
		MRF136	MRF136Y	
Thermal Resistance, Junction to Case	$R_{\theta JC}$	3.2	1.75	$^\circ\text{C/W}$

Handling and Packaging — MOS devices are susceptible to damage from electrostatic charge. Reasonable precautions in handling and packaging MOS devices should be observed.

## MRF136, MRF136Y

### ELECTRICAL CHARACTERISTICS ( $T_C = 25^\circ\text{C}$ unless otherwise noted)

Characteristic	Symbol	Min	Typ	Max	Unit
----------------	--------	-----	-----	-----	------

#### OFF CHARACTERISTICS (NOTE 1)

Drain-Source Breakdown Voltage ( $V_{GS} = 0$ , $I_D = 5$ mA)	$V_{(BR)DSS}$	65	—	—	Vdc
Zero-Gate Voltage Drain Current ( $V_{DS} = 28$ V, $V_{GS} = 0$ )	$I_{DSS}$	—	—	2	mA <sub>dc</sub>
Gate-Source Leakage Current ( $V_{GS} = 40$ V, $V_{DS} = 0$ )	$I_{GSS}$	—	—	1	$\mu\text{A}_{dc}$

#### ON CHARACTERISTICS (NOTE 1)

Gate Threshold Voltage ( $V_{DS} = 10$ V, $I_D = 25$ mA)	$V_{GS(th)}$	1	3	6	Vdc
Forward Transconductance ( $V_{DS} = 10$ V, $I_D = 250$ mA)	$g_{fs}$	250	400	—	mmhos

#### DYNAMIC CHARACTERISTICS (NOTE 1)

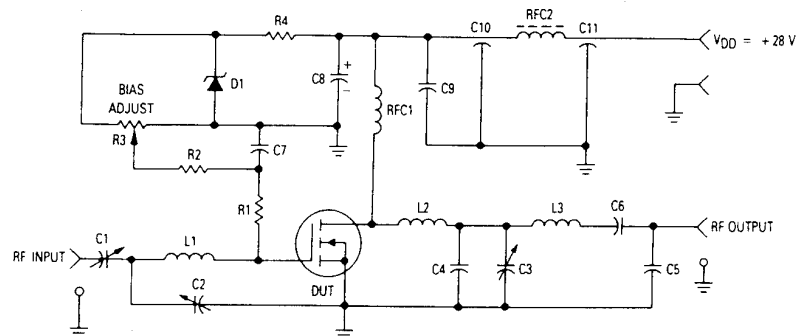
Input Capacitance ( $V_{DS} = 28$ V, $V_{GS} = 0$ , $f = 1$ MHz)	$C_{iss}$	—	24	—	pF
Output Capacitance ( $V_{DS} = 28$ V, $V_{GS} = 0$ , $f = 1$ MHz)	$C_{oss}$	—	27	—	pF
Reverse Transfer Capacitance ( $V_{DS} = 28$ V, $V_{GS} = 0$ , $f = 1$ MHz)	$C_{rss}$	—	5.5	—	pF

#### FUNCTIONAL CHARACTERISTICS (NOTE 2)

Noise Figure ( $V_{DS} = 28$ Vdc, $I_D = 500$ mA, $f = 150$ MHz)	MRF136	NF	—	1	—	dB
Common Source Power Gain (Figure 1) ( $V_{DD} = 28$ Vdc, $P_{out} = 15$ W, $f = 150$ MHz, $I_{DQ} = 25$ mA)	MRF136	$G_{ps}$	13	16	—	dB
Common Source Power Gain (Figure 2) ( $V_{DD} = 28$ Vdc, $P_{out} = 30$ W, $f = 150$ MHz, $I_{DQ} = 100$ mA)	MRF136Y	$G_{ps}$	12	14	—	dB
Drain Efficiency (Figure 1) ( $V_{DD} = 28$ Vdc, $P_{out} = 15$ W, $f = 150$ MHz, $I_{DQ} = 25$ mA)	MRF136	$\eta$	50	60	—	%
Drain Efficiency (Figure 2) ( $V_{DD} = 28$ Vdc, $P_{out} = 30$ W, $f = 150$ MHz, $I_{DQ} = 100$ mA)	MRF136Y	$\eta$	50	54	—	%
Electrical Ruggedness (Figure 1) ( $V_{DD} = 28$ Vdc, $P_{out} = 15$ W, $f = 150$ MHz, $I_{DQ} = 25$ mA, VSWR 30:1 at all Phase Angles)	MRF136	$\psi$	No Degradation in Output Power			
Electrical Ruggedness (Figure 2) ( $V_{DD} = 28$ Vdc, $P_{out} = 30$ W, $f = 150$ MHz, $I_{DQ} = 100$ mA, VSWR 30:1 at all Phase Angles)	MRF136Y	$\psi$	No Degradation in Output Power			

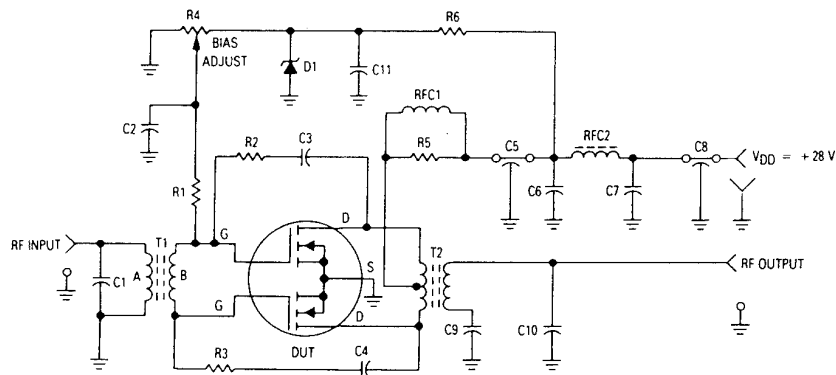
Notes: 1. For MRF136Y, each side measured separately.  
2. For MRF136Y measured in push-pull configuration.

## MRF136, MRF136Y



- C1, C2 — Arco 406, 15–115 pF or Equivalent  
 C3 — Arco 404, 8–60 pF or Equivalent  
 C4 — 43 pF Mini-Unelco or Equivalent  
 C5 — 24 pF Mini-Unelco or Equivalent  
 C6 — 680 pF, 100 Mils Chip  
 C7 — 0.01  $\mu$ F Ceramic  
 C8 — 100  $\mu$ F, 40 V  
 C9 — 0.1  $\mu$ F Ceramic  
 C10, C11 — 680 pF Feedthru  
 D1 — 1N5925A Motorola Zener  
 L1 — 2 Turns, 0.29" ID, #18 AWG, 0.10" Long  
 L2 — 2 Turns, 0.23" ID, #18 AWG, 0.10" Long  
 L3 — 2-1/4 Turns, 0.29" ID, #18 AWG, 0.125" Long  
 RFC1 — 20 Turns, 0.30" ID, #20 AWG Enamel Closewound  
 RFC2 — Ferroxcube VK-200 — 19/4B  
 R1 — 27  $\Omega$ , 1 W Thin Film  
 R2 — 10 k $\Omega$ , 1/4 W  
 R3 — 10 Turns, 10 k $\Omega$   
 R4 — 1.8 k $\Omega$ , 1/2 W  
 Board Material — 0.062" G10, 1 oz. Cu Clad, Double Sided

Figure 1. 150 MHz Test Circuit (MRF136)



- C1 — 5 pF  
 C2, C3, C4, C6, C7, C9, C11 — 0.1  $\mu$ F Ceramic  
 C5, C8 — 680 pF Feedthru  
 C10 — 15 pF  
 D1 — 1N4740 Motorola Zener  
 RFC1 — 17 Turns, #24 AWG Wound on R5  
 RFC2 — Ferroxcube VK-200-19 4B or Equivalent  
 R1 — 10 k $\Omega$ , 1/4 W  
 R2, R3 — 560  $\Omega$ , 1/2 W  
 R4 — 10 Turns, 10 k $\Omega$   
 R5 — 56 k $\Omega$ , 1 W  
 R6 — 1.6 k $\Omega$ , 1/4 W  
 T1 — Primary Winding — 3 Turns #28 Enameled Wire.  
       Secondary Winding — 2 Turns #28 Enameled Wire.  
       Both windings wound through a Fair/Rite Balun 65 core.  
       Part #2865002402.  
 T2 — 1:1 Transformer Wound Bifilar — 2 Turns Twisted Pair  
       #24 Enameled Wire through a Indiana General Balun Q1  
       core. Part #18006-1-Q1. Primary winding center tapped.  
 Board Material — 0.062" G10, 1 oz. Cu Clad, Double Sided

Figure 2. 30–150 MHz Test Circuit (MRF136Y)

# MRF136, MRF136Y

## MRF136

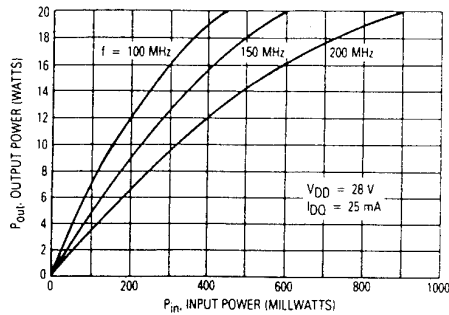


Figure 3. Output Power versus Input Power

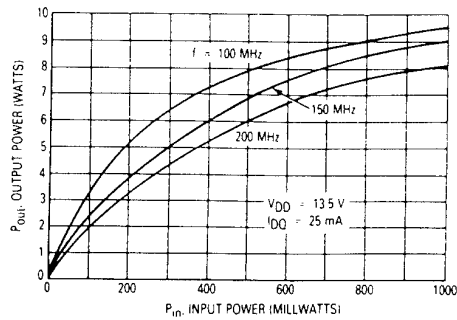


Figure 4. Output Power versus Input Power

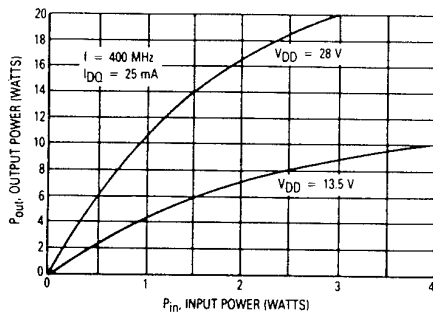


Figure 5. Output Power versus Input Power

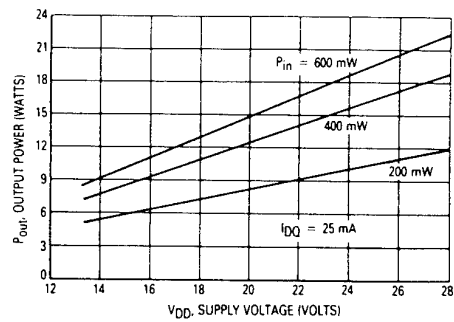


Figure 6. Output Power versus Supply Voltage  
 $f = 100$  MHz

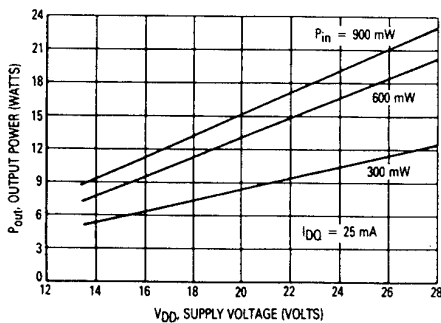


Figure 7. Output Power versus Supply Voltage  
 $f = 150$  MHz

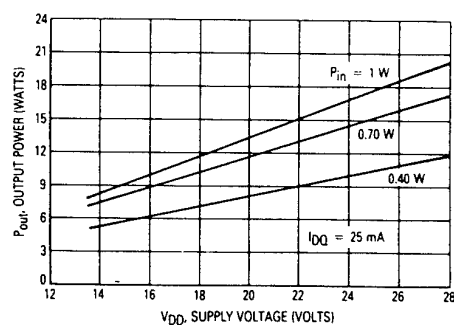


Figure 8. Output Power versus Supply Voltage  
 $f = 200$  MHz

## MRF136, MRF136Y

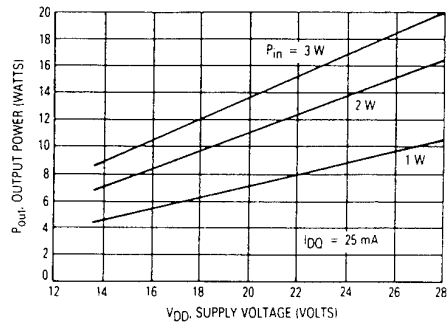


Figure 9. Output Power versus Supply Voltage  
f = 400 MHz  
MRF136

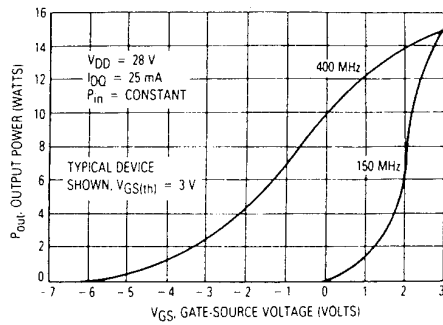


Figure 10. Output Power versus Gate Voltage  
MRF136

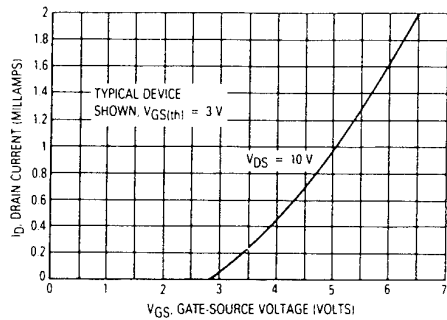


Figure 11. Drain Current versus Gate Voltage  
(Transfer Characteristics)\*  
MRF136/MRF136Y

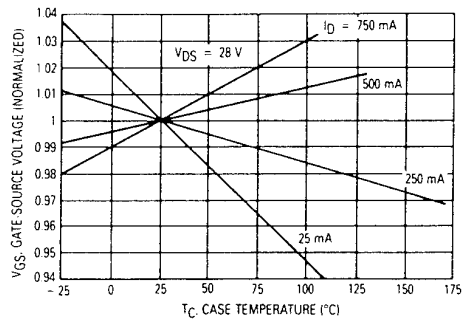


Figure 12. Gate-Source Voltage versus  
Case Temperature\*  
MRF136/MRF136Y

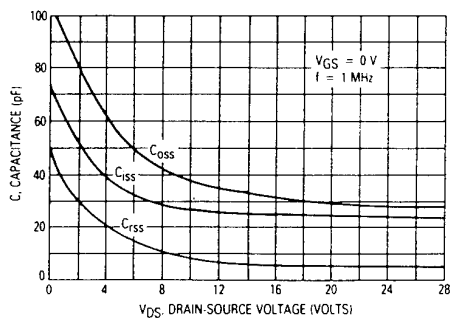


Figure 13. Capacitance versus Drain-Source Voltage\*  
MRF136/MRF136Y

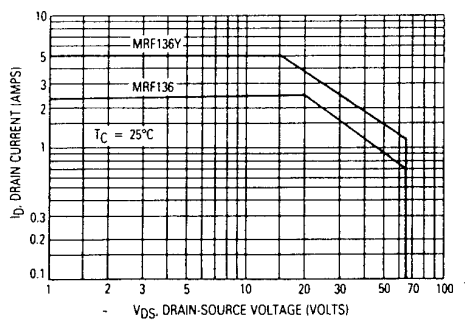


Figure 14. DC Safe Operating Area  
MRF136/MRF136Y

\*Data shown applies to MRF136 and each half of MRF136Y.

## MRF136, MRF136Y

### MRF136Y TYPICAL PERFORMANCE IN BROADBAND TEST CIRCUIT (Refer to Figure 2)

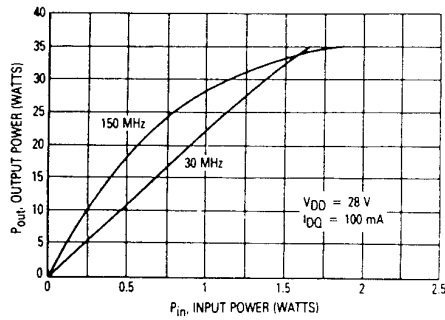


Figure 15. Output Power versus Input Power

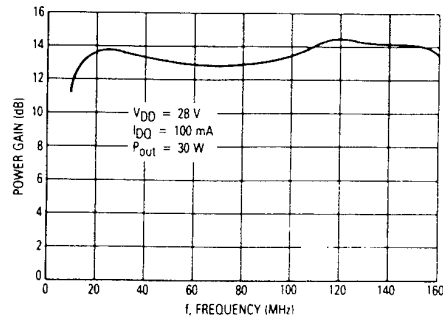


Figure 16. Power Gain versus Frequency

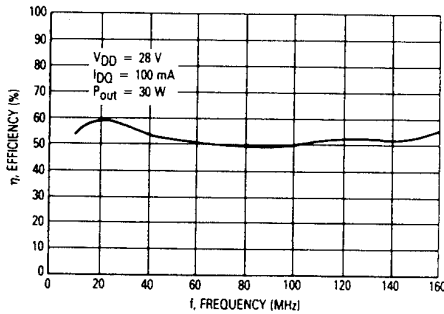


Figure 17. Drain Efficiency versus Frequency

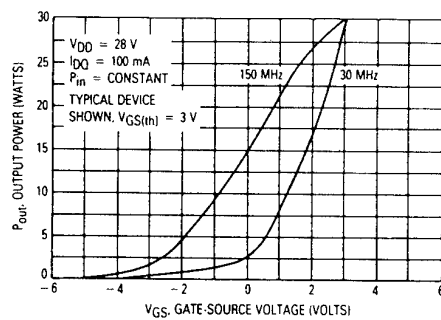


Figure 18. Output Power versus Gate Voltage

### TYPICAL 400 MHz PERFORMANCE

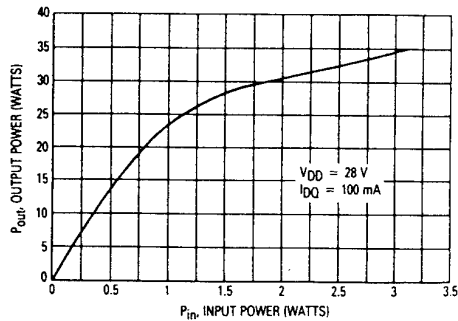


Figure 19. Output Power versus Input Power  
 $f = 400 \text{ MHz}$

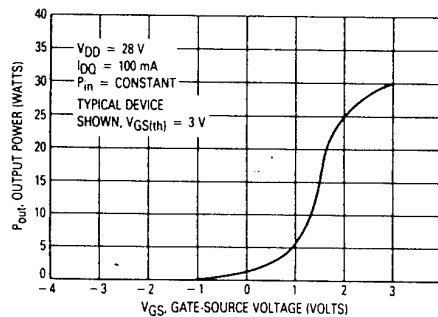


Figure 20. Output Power versus Gate Voltage  
 $f = 400 \text{ MHz}$



# MRF136, MRF136Y

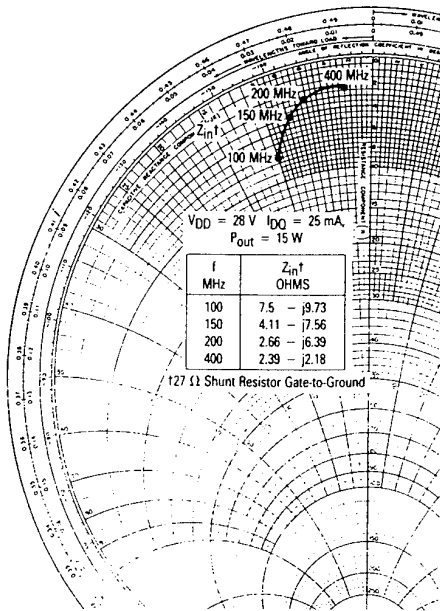


Figure 21. Large-Signal Series Equivalent Input Impedance,  $Z_{in}^{\dagger}$   
MRF136

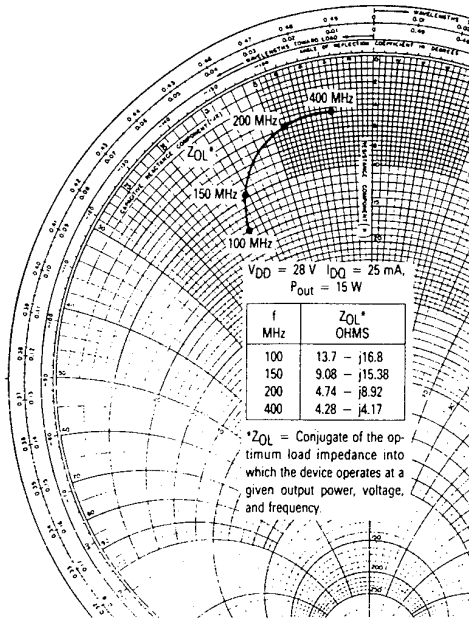


Figure 22. Large-Signal Series Equivalent Output Impedance,  $Z_{OL}^*$   
MRF136

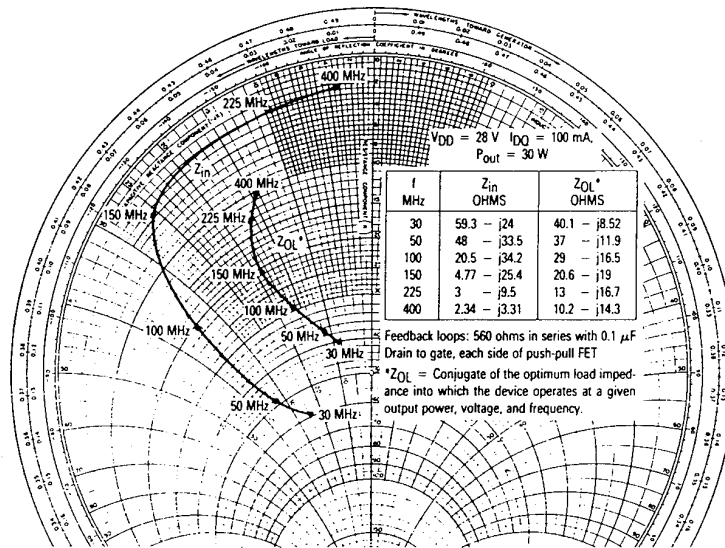


Figure 23. Input and Output Impedance  
MRF136Y

# MRF136, MRF136Y

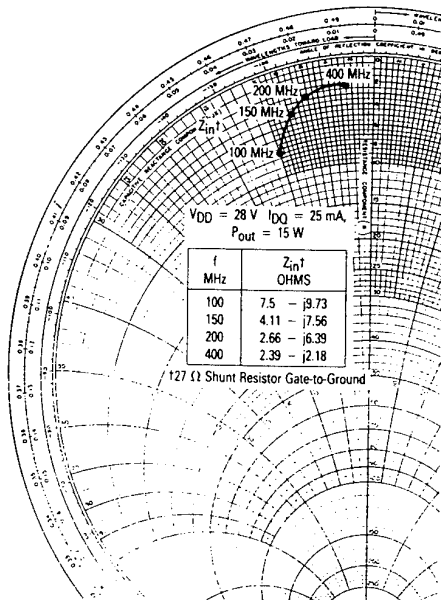


Figure 21. Large-Signal Series Equivalent Input Impedance,  $Z_{in}^{\dagger}$   
MRF136

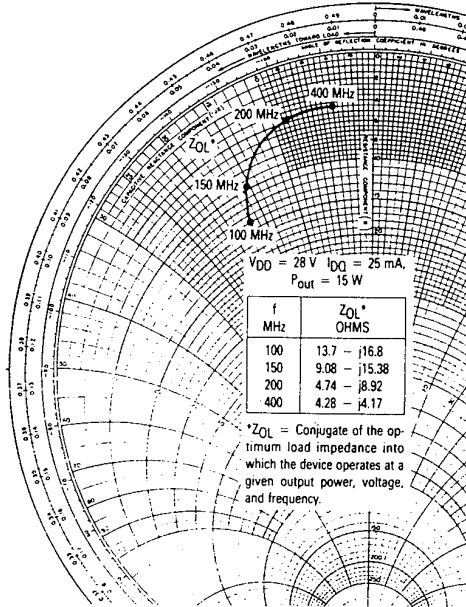


Figure 22. Large-Signal Series Equivalent Output Impedance,  $Z_{OL}^*$   
MRF136

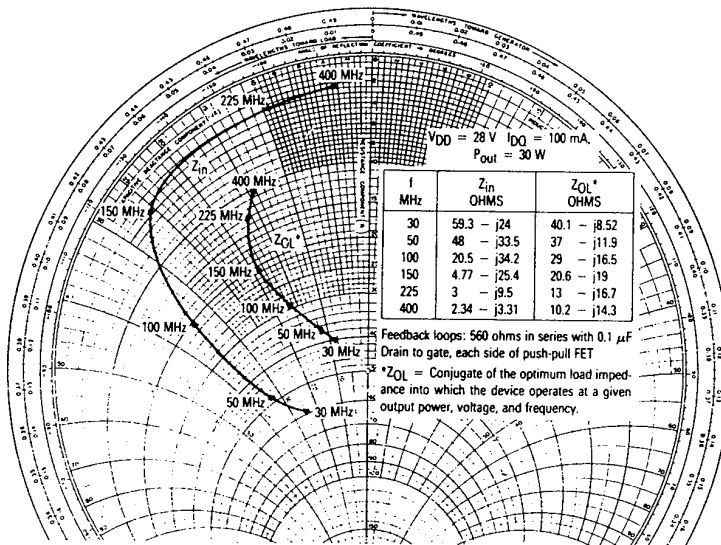


Figure 23. Input and Output Impedance  
MRF136Y

# MRF136, MRF136Y

## MRF136

f (MHz)	S <sub>11</sub>		S <sub>21</sub>		S <sub>12</sub>		S <sub>22</sub>	
	S <sub>11</sub>	∠φ	S <sub>21</sub>	∠φ	S <sub>12</sub>	∠φ	S <sub>22</sub>	∠φ
2.0	0.988	-11	41.19	173	0.006	67	0.729	-12
5.0	0.970	-27	40.07	164	0.014	62	0.720	-31
10	0.923	-52	35.94	149	0.026	54	0.714	-58
20	0.837	-88	27.23	129	0.040	36	0.690	-96
30	0.784	-111	20.75	117	0.046	27	0.684	-118
40	0.751	-125	16.49	108	0.048	22	0.680	-131
50	0.733	-135	13.41	103	0.050	19	0.679	-139
60	0.720	-142	11.43	99	0.050	16	0.678	-145
70	0.709	-147	9.871	96	0.050	14	0.679	-149
80	0.707	-152	8.663	93	0.051	13	0.683	-153
90	0.706	-155	7.784	91	0.051	13	0.682	-155
100	0.708	-157	7.008	88	0.051	13	0.680	-157
110	0.711	-159	6.435	86	0.051	14	0.681	-158
120	0.714	-161	5.899	85	0.051	15	0.682	-159
130	0.717	-163	5.439	82	0.052	16	0.684	-160
140	0.720	-164	5.068	80	0.052	17	0.684	-161
150	0.723	-165	4.709	80	0.052	18	0.686	-161
160	0.727	-166	4.455	78	0.052	18	0.690	-161
170	0.732	-167	4.200	77	0.052	18	0.694	-162
180	0.735	-168	3.967	75	0.052	19	0.699	-162
190	0.738	-169	3.756	74	0.052	19	0.703	-163
200	0.740	-170	3.545	73	0.052	20	0.706	-163
225	0.746	-171	3.140	69	0.053	22	0.717	-163
250	0.742	-172	2.783	67	0.053	25	0.724	-163
275	0.744	-173	2.540	64	0.054	27	0.724	-163
300	0.751	-174	2.323	60	0.055	29	0.736	-163
325	0.757	-175	2.140	58	0.058	32	0.749	-163
350	0.760	-176	1.963	54	0.059	35	0.758	-163
375	0.762	-177	1.838	52	0.062	38	0.768	-163
400	0.774	-179	1.696	50	0.065	41	0.783	-163
425	0.775	-179	1.590	48	0.068	43	0.793	-163
450	0.781	+179	1.493	46	0.071	46	0.805	-163
475	0.787	+177	1.415	43	0.074	47	0.813	-164
500	0.792	+176	1.332	40	0.079	48	0.825	-164
525	0.797	+175	1.259	38	0.083	50	0.831	-164
550	0.801	+175	1.185	37	0.088	51	0.843	-164
575	0.810	+174	1.145	36	0.094	52	0.855	-164
600	0.816	+173	1.091	34	0.101	52	0.869	-165
625	0.818	+171	1.041	32	0.106	53	0.871	-165
650	0.825	+170	0.994	30	0.112	53	0.884	-165
675	0.834	+169	0.962	29	0.119	53	0.890	-165
700	0.837	+168	0.922	27	0.127	53	0.906	-166
725	0.836	+167	0.879	25	0.133	52	0.909	-167
750	0.841	+166	0.838	25	0.140	53	0.917	-167
775	0.844	+165	0.824	24	0.148	52	0.933	-167
800	0.846	+163	0.785	21	0.154	50	0.941	-168

Figure 24. Common Source Scattering Parameters  
V<sub>DS</sub> = 28 V, I<sub>D</sub> = 0.5 A

# MRF136, MRF136Y

## MRF136

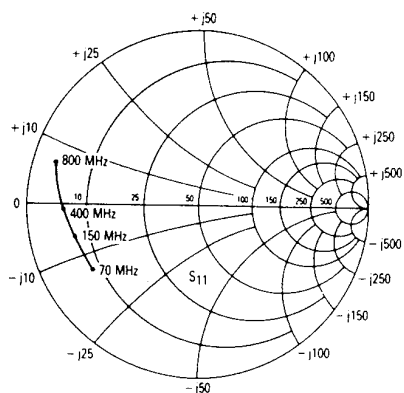


Figure 25.  $S_{11}$ , Input Reflection Coefficient versus Frequency  
 $V_{DS} = 28 \text{ V}$   $I_D = 0.5 \text{ A}$

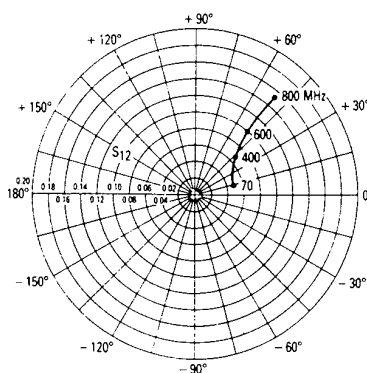


Figure 26.  $S_{12}$ , Reverse Transmission Coefficient versus Frequency  
 $V_{DS} = 28 \text{ V}$   $I_D = 0.5 \text{ A}$

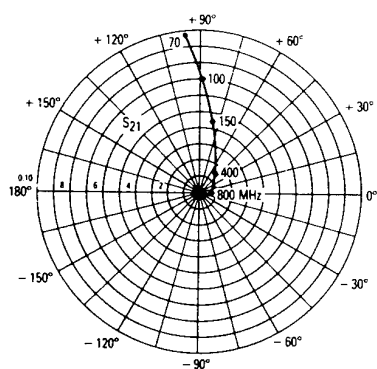


Figure 27.  $S_{21}$ , Forward Transmission Coefficient versus Frequency  
 $V_{DS} = 28 \text{ V}$   $I_D = 0.5 \text{ A}$

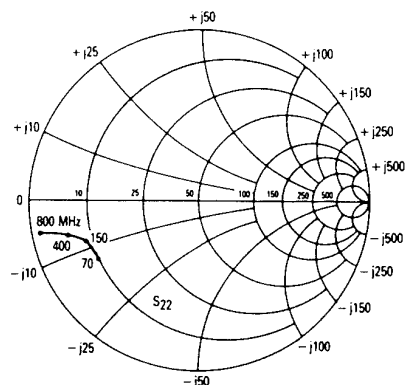


Figure 28.  $S_{22}$ , Output Reflection Coefficient versus Frequency  
 $V_{DS} = 28 \text{ V}$   $I_D = 0.5 \text{ A}$

## MRF136, MRF136Y

### DESIGN CONSIDERATIONS

The MRF136 and MRF136Y are TMOS RF power N-Channel enhancement mode field-effect transistors (FETs) designed especially for HF and VHF power amplifier applications. Motorola TMOS FETs feature planar design for optimum manufacturability.

Motorola Application Note AN211A, FETs in Theory and Practice, is suggested reading for those not familiar with the construction and characteristics of FETs.

The major advantages of TMOS RF power FETs include high gain, low noise, simple bias systems, relative immunity from thermal runaway, and the ability to withstand severely mismatched loads without suffering damage. Power output can be varied over a wide range with a low power dc control signal, thus facilitating manual gain control, ALC and modulation.

#### DC BIAS

The MRF136 and MRF136Y are enhancement mode FETs and, therefore, do not conduct when drain voltage is applied without gate bias. A positive gate voltage causes drain current to flow (see Figure 11). RF power FETs require forward bias for optimum gain and power output. A Class AB condition with quiescent drain current ( $I_{DQ}$ ) in the 25–100 mA range is sufficient for many applications. For special requirements such as linear amplification,  $I_{DQ}$  may have to be adjusted to optimize the critical parameters.

The MOS gate is a dc open circuit. Since the gate bias circuit does not have to deliver any current to the FET, a simple resistive divider arrangement may sometimes suffice for this function. Special applications may require more elaborate gate bias systems.

#### GAIN CONTROL

Power output of the MRF136 and MRF136Y may be controlled from rated values down to the milliwatt region (>20 dB reduction in power output with constant input power) by varying the dc gate voltage. This feature, not available in bipolar RF power devices, facilitates the incorporation of manual gain control, AGC/ALC, and mod-

ulation schemes into system designs. A full range of power output control may require dc gate voltage excursions into the negative region.

#### AMPLIFIER DESIGN

Impedance matching networks similar to those used with bipolar transistors are suitable for the MRF136 and MRF136Y. See Motorola Application Note AN721, Impedance Matching Networks Applied to RF Power Transistors. Both small signal scattering parameters (MRF136 only) and large signal impedance parameters are provided. Large signal impedances should be used for network designs wherever possible. While the s parameters will not produce an exact design solution for high power operation, they do yield a good first approximation. This is particularly useful at frequencies outside those presented in the large signal impedance plots.

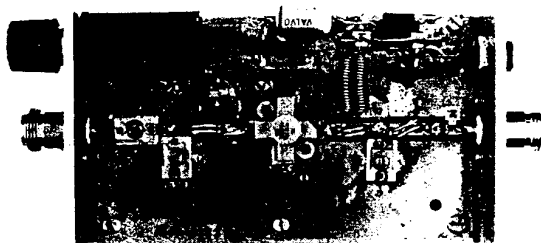
RF power FETs are triode devices and are therefore not unilateral. This, coupled with their very high gain, yields a device capable of self oscillation. Stability may be achieved using techniques such as drain loading, input shunt resistive loading, or feedback. S parameter stability analysis can provide useful information in the selection of loading and/or feedback to insure stable operation. The MRF136 was characterized with a 27 ohm input shunt loading resistor, while the MRF136Y was characterized with a resistive feedback loop around each of its two active devices.

For further discussion of RF amplifier stability and the use of two port parameters in RF amplifier design, see Motorola Application Note AN215A on page 6-204 in the RF Device Data (DL110 Rev 1).

#### LOW NOISE OPERATION

Input resistive loading will degrade noise performance, and noise figure may vary significantly with gate driving impedance. A low loss input matching network with its gate impedance optimized for lowest noise is recommended.

Figure 29. MRF136  
Test Circuit



**THIS PAGE IS INTENTIONALLY BLANK**

# A Robust 2-70MHz Linear Power Amplifier

W. Martinsen

(DSTO - TR - 0217)

## DISTRIBUTION LIST

Chief Defence Scientist and members of the	
DSTO Central Office Executive	1 shared copy
Assistant Secretary Scientific Analysis	1 copy
Director, Aeronautical & Maritime Research Laboratory	1 copy
Counsellor, Defence Science, London	Doc Control sheet
Counsellor, Defence Science, Washington	Doc Control sheet
Senior Defence Scientific Adviser	1 copy
Scientific Adviser - Polcom	1 copy
Navy Scientific Adviser (NSA)	1 copy
Scientific Adviser, Army (SA-A)	1 copy
Air Force Scientific Adviser (AFSA)	1 copy
Defence Central Library - Technical Reports Centre	1 copy
Manager Document Exchange Centre (MDEC) (for retention)	1 copy
Additional copies which are to be sent through MDEC	
DIS for distribution:	
Defence Research Information Centre, United Kingdom	2 copies
National Technical Information Centre. United States	2 copies
Director Scientific Information Services, Canada	1 copy
Ministry of Defence, New Zealand	1 copy
National Library of Australia	1 copy
Defence Science and Technology Organisation Salisbury,	
Research Library	2 copies
Library Defence Signals Directorate Canberra	1 copy
AGPS	1 copy
British Library Document Supply Centre	1 copy
Parliamentary Library of South Australia	1 copy
The State Library of South Australia	1 copy
Chief Communication Division, ESRL/CD/230Labs	1 copy
Dr. Ian Fuss, ESRL/CD/203Labs	1 copy
Dr. Warren Marwood, ESRL/CD/DSP/203Labs	1 copy
Dr. Russell H. Clarke, ESRL/CD/DSPG/200Labs	1 copy
W. M. Martinsen, ESRL/CD/DSP/203Labs	6 copies
Peter Wilinski, ESRL/CD/DSP/203Labs	1 copy
Angus Massie, ESRL/CD/DSP/203Labs	1 copy
Rick C. Grivell, ESRL/CD/DSPG/200Labs	1 copy
Nick Burrowes, ESRL/HFRD/HFRE/200Labs	1 copy
Keith Gooley, ESRL/HFRD/RTS/200Labs	1 copy
John Arnold, ESRL/CD/SC/203Labs	1 copy
Ian Leach, ESRL/CD/SC/203Labs	1 copy
The Radio Center,	
Building 108, Ditchmen Ave., Archierfield Airport, Brisbane, Qld.	1 copy

Codan Pty. Ltd.,  
81 Graves St., Newton, Adelaide, S.A.

1 copy

**Spares**

Defence Science and Technology Organisation Salisbury,  
Research Library

6 copies



**Department of Defence**  
**DOCUMENT CONTROL DATA SHEET**

1. Page Classification UNCLASSIFIED
2. Privacy Marking/Caveat (of document) N/A

3a. AR Number AR-009-345	3b. Laboratory Number DSTO-TR-0217	3c. Type of Report DSTO TECHNICAL REPORT	4. Task Number ADL 94/215	
5. Document Date JULY 1995	6. Cost Code 837782	7. Security Classification UNCLASSIFIED	8. No of Pages	96
10. Title  A Robust 2-70MHz Linear Power Amplifier		* <table border="1" style="display: inline-table; vertical-align: middle;">U</table> <table border="1" style="display: inline-table; vertical-align: middle;">U</table> <table border="1" style="display: inline-table; vertical-align: middle;">U</table> Document      Title      Abstract  S (Secret) C (Conf) R (Rest) U (Unclas)  * For UNCLASSIFIED docs with a secondary distribution LIMITATION, use (L) in document box.	9. No of Refs	13
11. Author(s)  Mr W. M. Martinsen		12. Downgrading/Delimiting Instructions  N/A		
13a. Corporate Author and Address  Electronics & Surveillance Research Laboratory PO Box 1500, Salisbury SA 5108		14. Officer/Position responsible for  Security: .....N/A.....  Downgrading: .....N/A.....  Approval for Release: ....CCD.....		
13b. Task Sponsor DGFD(L)				
15. Secondary Release Statement of this Document  APPROVED FOR PUBLIC RELEASE				
16a. Deliberate Announcement  NO LIMITATION				
16b. Casual Announcement (for citation in other documents)  <div style="display: flex; justify-content: space-around;"> <span><input checked="" type="checkbox"/> No Limitation</span> <span><input type="checkbox"/> Ref. by Author, Doc No. and date only</span> </div>				
17. DEFTEST Descriptors Power amplifiers Reliability.			18. DISCAT Subject Codes	
19. Abstract  Spatial Processing Group DSTOS currently has oblique ionosonde transmitters deployed in a variety of remote, often unmanned, locations in tropical, arid inland, and polar regions, and equipment reliability is of the utmost importance. The commercial H.F. power amplifiers initially installed proved unreliable in the field, and motivated the development of a more robust unit. 10 Watt and 50 Watt designs are presented with their measured characteristics, and a detailed discussion of important design criteria.				